Characterization of EBV nuclear protein 3 (EBNA3) genome binding and gene regulation in EBV transformed lymphoblastoid cell lines (LCLs)

By

Anqi Wang

A dissertation submitted in partial fulfillment of

the requirements for the degree of

Doctor of Philosophy

(Cellular and Molecular Biology)

At the

UNIVERSITY OF WISCONSIN−MADISON

2016

Date of final oral examination: 1/7/2016

The dissertation is approved by the following members of the Final Oral Committee:

Eric Johannsen, Assitant Professor, Medicine and Oncology
Bill Sugden, Professor, Oncology
Norman Drinkwater, Professor, Oncology
Rob Kalejta, Professor, Molecular Virology and Oncology
Wei Xu, Professor, Oncology

Characterization of EBV nuclear protein 3 (EBNA3) genome binding and gene regulation in EBV transformed lymphoblastoid cell lines (LCLs)

Anqi Wang

Under the supervision of Professor Eric Johannsen

at the University of Wisconsin-Madison

Latent infection of B lymphocytes by Epstein-Barr virus (EBV) *in vitro* results in their immortalization into lymphoblastoid cell lines (LCLs); this latency program is controlled by the EBNA2 viral transcriptional activator that targets promoters via RBPJ, a DNA binding protein in the Notch signaling pathway. Three other EBNA3 proteins (EBNA3A, EBNA3B, and EBNA3C) interact with RBPJ to regulate cell gene expression. The mechanism by which EBNAs regulate different genes via RBPJ remains unclear. Our ChIP-seq analysis of the EBNA3 proteins analyzed in concert with prior EBNA2 and RBPJ data demonstrate that EBNA3A, EBNA3B and EBNA3C bind to distinct, partially overlapping genomic locations. Although RBPJ interaction is critical for EBNA3A and EBNA3C growth effects, only 30-40% of EBNA3 bound sites co-localize with RBPJ. Using LCLs conditional for EBNA3A or EBNA3C activity, we demonstrate that EBNA2 binding at sites near genes regulated by EBNA3A or EBNA3C is specifically regulated by the respective EBNA3. To investigate EBNA3 binding specificity, we identified sequences and transcription factors enriched at EBNA3A, EBNA3B, and EBNA3C bound sites. This

confirmed the prior observation that IRF4 is enriched at EBNA3A and EBNA3C bound sites and revealed IRF4 enrichment at EBNA3B bound sites. Using the IRF4 negative BJAB cell, we demonstrate that IRF4 is essential for EBNA3C, but not EBNA3A or EBNA3B binding to specific sites. These results support a model in which EBNA2 and EBNA3s compete for distinct subsets of RBPJ sites to regulate cell genes and where EBNA3 subset specificity is determined by interactions with other cell transcription factors. Finally, we examined changes in the H3K27me3 mark that is believed to mediate EBNA3 repression of cell genes. Surprisingly, we observed no correlation between changes in this mark with EBNA3A or EBNA3C binding upon EBNA3A or EBNA3C inactivation. Furthermore, EBNA3 bound sites were characterized by activating (H3K4me3 and H3K9ac) histone marks. This suggests that EBNA3 proteins may exert their transcriptional effects through indirect mechanisms. We performed H3K27me3 ChIP-seq analysis in the presence and absence of EBNA3C activity to determine the exact locations that undergo this mark change in response to EBNA3C activity. Our study represents the first genome-wide characterization of EBNA3A, EBNA3B and EBNA3C binding in LCLs; as well as the first genome-wide characterization of H3K27me3 pattern in response to EBNA3C activity. Moreover, our results suggest a mechanism by which EBNA3 proteins regulate distinct, but partially overlapping, sets of cell genes and provide a basis for understanding their role in lymphomagenesis.

ACKNOWLEDGEMENTS

First and foremast, I would like to express my deepest gratitude to my advisor Eric Johannsen. I wouldn't have finished this thesis project without your guidance, support and patience. Your enthusiasm, critical thinking and immense knowledge make you a great role model that I always look up to.

I would like to thank my thesis committee Dr. Bill Sugden, Dr. Norman Drinkwater, Dr. Rob Kalejta, and Dr. Wei Xu. Thank you for your guidance and advice on both my research and career development in the past five years.

I would like to thank my collaborators Dr. Sunduz Keles and Rene Welch for their help on the bioinformatics analysis. I also would like to thank the Kenney lab and the Mertz Lab for the discussions during out joint group meetings and the advice on my project.

I would like to thank my lab mates Reza Djavadian, Mark Eichelberg, and Ahmed Ali. It has been a great pleasure to work with you guys.

I would like to thank my dear friends in Madison: Zhangli Su, Hao Zeng, Xingmin Zhang, Ronghui Li, Xiaomeng Lu, Fei Meng, Yan Wang, Fengbin Wang, Shan Jiang, Xin Chen, Wenjing Ma, Zibo Zhao, and Ya-Fang Chiu. You guys have made my life in a foreign

country no longer feel lonely. I have had so much laughter and joy having you guys around throughout the years in Madison. I hope our friendship will last for a lifetime.

I would like to thank my parents who I love more than anything in the world. I wouldn't have come to the US to pursue my Ph.D in the first place without your support. Even if we have been separated by the Pacific Ocean for five years, I always feel your endless love.

Finally, I would like to thank my husband Yuxuan Wang. Thank you for always being there for me through happiness and tears. You have taught me so many things and helped me become a better person. I couldn't imagine a life without you. I am excited to continue our journey no matter where it takes us.

TABLE OF CONTENTS

List of tables

List of figures

List of abbreviations

4HT	4-hydroxytamoxifen
A	Alanine
ADAM28	Disintegrin and metalloproteinase domain-containing protein 28
ADAMDEC1	ADAM-like, decysin 1
AICE	AP1/IRF4 composite element
AIDS	Acquired immunodeficiency syndrome
ALOXE3	Arachidonate lipoxygenase 3
ALPK2	Alpha-kinase 2
AP1	Activator protein 1
AR	Androgen receptor
ARHGAP25	Rho GTPase activating protein 25
ATF2	Activating transcription factor 2
BACH2	BTB and CNC homolog 2
BART	BamHI-A rightward transcript
BATF	B-cell-activating transcription factor
BAX	BCL2-associated X protein
BCL2	B-Cell CLL/Lymphoma 2
BCL211A	BCL2-like 11
BIM	Bcl-2 interacting mediator of cell death
BL	Burkitt lymphoma
Blimp1	B-Lymphocyte-induced maturation protein 1

BLK	B lymphocyte kinase
bp	Base pair
℃	Degrees centigrade
C20orf24	Chromosome 20 open reading frame 24
CACNB4	Calcium channel, voltage-dependent, beta 4 subunit
CAS9	CRISPR associated protein 9
CCDC80	Coiled-coil domain containing 80
CD40	Cluster of differentiation factor 40
CDH1	Cadherin 1
CDK1	Cyclin-dependent kinase 1
CDK2	Cyclin-dependent kinase 2
CDKN2A	Cyclin-dependent kinase inhibitor 2A
cDNA	Complementary DNA
CGI	CpG-island
ChIP-seq	Chromatin immunoprecipitation followed by sequencing
CHK2	Checkpoint kinase 2
CRISPR	Clustered regularly interspaced short palindromic repeat
Chr	Chromosome
cm	Centimeter
Cp	BamHI restriction fragment C promoter
CTBP	C-terminal binding protein
CTCF	CCCTC-binding factor

CTLA4	Cytotoxic T-lymphocyte-associated protein 4
CXCR5	C-X-C chemokine receptor type 5
CXCL9	Chemokine (C-X-C Motif) ligand 9
CXCL10	Chemokine (C-X-C Motif) ligand 10
DHS	DNase I hypersensitive sites
DLBCL	Diffuse large B cell lymphomas
DMEM	Dulbecco's modified eagle's medium
DNA	Deoxyribonucleic acid
DNase	Deoxyribonuclease
EBER	Epstein-Barr encoded RNA
EBNA	Epstein-Barr nuclear antigen
EBNA-LP	Epstein-Barr virus nuclear antigen leader protein
EBV	Epstein-Barr virus
EDTA	Ethylenediaminetetraacetic acid
Eμ	Enhancer mu
EED	Embryonic ectoderm development
EICE	ETS/IRF4 composite element
EIF2AK3	Eukaryotic translation initiation factor 2-alpha kinase 3
ENCODE	Encyclopedia of DNA elements
ERK	Extracellular signal-regulated kinases
EZH2	Enhancer of zeste 2
F	Phenylalanine

FBS	Fetal bovine serum
FDR	False discovery rate
FOXM1	Forkhead box protein M1
FOXO3	Forkhead box protein O3
FR	Family of Repeats
G_1/G_0	Gap 1/Gap 0
Gag-Pol	Group antigen/polymerase (viral core, reverse transcriptase, integrase)
GAPDH	Glyceraldehyde-3-phosphate dehydrogenase
GC	Gastric carcinoma
GSG2	Germ cell specific gene 2
GST	Glutathione S-transferase
H19	An imprinted maternally expressed non-coding transcript
H3K4me1	Histone 3 lysine 4 monomethylation
H3K4me2	Histone 3 lysine 4 dimethylation
H3K4me3	Histone 3 lysine 4 trimethylation
H3K9ac	Histone 3 lysine 9 acetylation
H3K9me3	Histone 3 lysine 9 trimethylation
H3K27ac	Histone 3 lysine 27 acetylation
H3K27me3	Histone 3 lysine 27 trimethylation
H3K36me3	Histone 3 lysine 36 trimethylation
HDAC	Histone deacetylase 7
HEIH	Highly expressed in hepatocellular carcinoma long non-coding RNA

HEPES	N-2-hydroxyethylpiperazine-N`-2-ethanesulfonic acid
HIV	Human immunodeficiency virus
HL	Hodgkin lymphoma
HNRPLL	Heterogeneous nuclear ribonucleoprotein L-like
HOX	Homeobox
HOTAIR	HOX transcript antisense RNA
HPV	Human papilloma virus
ICN	Intracellular domain of Notch
Ig	Immunoglobulin
IgH	Immunoglobulin heavy locus
IL7R	Interleukin 7 receptor
ING4	Inhibitor of growth protein 4
ING5	Inhibitor of growth protein 5
IP	Immunoprecipitation
ITGB4	Integrin beta 4
IRF4	Interferon regulatory factor 4
JAK1	Janus kinase 1
JAK/STAT	Janus kinase/signal transducer and activator of transcription
JARID1C	Jumonji/ARID domain-containing protein 1C
JMJD3	Jumonji domain containing 3
Kb	Kilobase pairs
KCl	Potassium chloride

KDM5C	Lysine (K)-specific demethylase 5C
KDM6A	Lysine (K)-specific demethylase 6A
KDM6B	Lysine (K)-specific demethylase 6B
KO	Knock out
LCL	Lymphoblastoid cell line
LMP	Latent membrane protein
LC/MS/MS	Liquid chromatography–tandem mass spectrometry
LncRNA	Long non-coding RNA
Lid	Protein little imaginal disks
M	Mitosis
MACC1	Metastasis associated in colon cancer 1
MAML	Mastermind-like 1
MAPK	Mitogen-activated protein kinases
MDM2	Mouse double minute 2 homolog
MEF	Mouse embryonic fibroblast
MEME	Multiple EM for Motif Elicitation
METTL13	Methyltransferase Like 13
MHC	Major histocompatibility complex
MMLV	Moloney murine leukemia virus
MOSAiCS	MOdel-based one and two Sample Analysis and inference for ChIP-seq
µg	Microgram
µL	Microliter

μm	Micrometer
μM	Micromolar
miRNA	Micro-ribonucleic acid
mL	Milliliter
mM	Millimolar
MYC	Myelocytomatosis viral oncogene homolog
NaCl	Sodium chloride
NCoR	Nuclear receptor co-repressor
NFATC2	Nuclear factor of activated T-cells 2
NF-κB	Nuclear factor kappa B
NFIC	Nuclear factor I/C
NLS	Nuclear localization signal
NOXA	NADPH oxidase activator 1
ng	Nanogram
nm	Nanometer
NPC	Nasopharyngeal carcinoma
NRF1	Nuclear respiratory factor-1
NTD	N-terminal domain of RBPJ
OriP	Origin of latent plasmid replication of EBV
P	Proline
P14ARF	CDKN2A alternate open reading frame
P16INK4a	Inhibitor of cyclin-dependent kinase 4A

P300	E1A binding protein p300
PARP9	Poly ADP-ribose polymerase 9
PAX5	Paired box 5
PBS	Phosphate-buffered saline
PcG	Polycomb-group proteins
PCR	Polymerase chain reaction
PIP5K1B	Phosphatidylinositol-4-phosphate 5-kinase, Type I, Beta
POU2F1	POU Class 2 homeobox 1
PPIA	Peptidyl-prolyl isomerase A
PRDM1	PR domain containing 1
PTLD	Post-transplant lymphoproliferative disorder
PTMA	Prothymosin, Alpha
PU.1	PU-box binding protein; aka SPI1
PUMA	p53 upregulated modulator of apoptosis
qPCR	Quantitative polymerase chain reaction
QSK	Serine/threonine-protein kinase
RAPH1	Ras association and pleckstrin homology domains 1
RB	Retinoblastoma protein
RbAp46/48	Retinoblastoma-binding protein p46
RBPJ	Recombination signal binding protein for immunoglobulin kappa J region
REF	Rat embryonic fibroblastic cells
RNA	Ribonucleic acid

RNase	Ribonuclease
ROCK1	Rho-associated, coiled-coil-containing protein kinase 1
RPMI 1640	Roswell park memorial institute formulation 1640
RT-PCR	Reverse transcription polymerase chain reaction
RUNX3	Runt-related transcription factor 3
S	Synthesis
SAM	Sequence Alignment Map
SDS	Sodium dodecyl sulfate
SDS-PAGE	SDS-polyacrylamide gel electrophoresis
SEM	Stardard error of the mean
SHQ1	H/ACA ribonucleoprotein assembly factor
shRNA	Short hairpin ribonucleic acid
SV40	Simian virus 40
SP1	Specificity protein 1
SPI1	Spleen focus forming virus (SFFV) proviral integration oncogene
Su(H)	Suppressor of hairless
SUZ12	Suppressor of zeste 12
SYTL3	Synaptotagmin-like 3
T	Threonine
TAD	Topological association domain
TCF12	Transcription factor 12
TFII-I	General transcription factor II-I

TMEM109	Transmembrane protein 109
TOX	Thymocyte selection-associated high mobility group box
TP53I3	Tumor protein p53 inducible protein 3
TRIB2	Tribbles pseudokinase 2
TSS	Transcription start site
U	Unit
UBC	Ubiquitin C
USP12/46	Ubiquitin specific peptidase 12/46
UTX	Ubiquitously transcribed X chromosome tetratricopeptide repeat protein
v/v	Volume/Volume
Wp-BL	Wp-restricted Burkitt lymphoma (endemic)
w/v	Weight per volume
WDR20/48	WD repeat domain 20/48
Wnt	Wingless-type MMTV integration site family
W	Tryptophan
XIST	X-inactive specific transcript
YY1	Ying Yang 1
ZEB1/2	Zinc finger E-box binding homeobox 1
ZNF217	Zinc finger protein 217

CHAPTER I:

INTRODUCTION

EBV and its associated malignancies

Epstein-Barr virus (EBV), a member of the gamma-herpes virus subfamily, is a highly successful human pathogen, infecting 90-95% of the adult human population (1). It is the first human tumor virus discovered, having been isolated from Burkitt lymphoma cells in 1964 by Epstein and colleagues (2). EBV is primarily transmitted via saliva and in healthy immunocompetent individuals it establishes a life-long latent infection in B-lymphocytes (3, 4). EBV transformation of B lymphocytes *in vitro* is an important model system for understanding oncogenesis. This propensity to transform cells is usually controlled by an intact immune response, making EBV cancers rare in immunocompetent individuals. Nevertheless, EBV's high seroprevalance makes it a major human carcinogen (5, 6). Epidemiological studies estimate the global burden of mortality from EBV-attributed malignancies to be equal to 1.8% of all cancer deaths (7). To date, EBV has been causally linked to Burkitt lymphoma (BL), Hodgkin lymphoma (HL), gastric (GC) and nasopharyngeal (NPC) carcinomas, and post-transplant lymphoproliferative disorder (PTLD) (8). There is currently no licensed EBV vaccine and no available antiviral therapy with demonstrated efficacy in treating EBV-associated cancers.

EBV transformed lymphoblastoid cell lines (LCLs)

Much of what we know about EBV's role in malignant transformation of cells derives from studies of its ability to transform B lymphocytes into indefinitely proliferating lymphoblastoid cell lines (LCLs) *in vitro* (2, 9). This transformation capacity of EBV has been widely used to establish 'normal' human B cell lines for genetic, epigenetic and

tumorigenesis studies. For example, the ENCODE (**ENC**yclopedia **O**f **D**NA **E**lements) project and the HapMap (haplotype map) project relied heavily on LCLs to study functional human genomics and genetics, respectively (10, 11). After several decades of study, we have gained tremendous knowledge about the general strategies used by EBV to drive resting B cells from quiescence into the active proliferation state, to promote survival of infected cells, to evade immune surveillance, and to regulate the switch from latent infection to viral replication (12). However, fundamental questions about how EBV gene products manipulate B lymphocyte development to establish lifelong infection of its host remain.

EBV latent gene products

In LCLs and EBV associated cancers, EBV does not replicate and gene expression is restricted to so-called "latency genes". EBV latency genes encode 6 nuclear proteins (EBNAs), 3 membrane proteins (LMPs) and non-coding RNAs (EBERs and microRNAs) (8). Expression of this full complement of latency genes is referred to as latency III, though some EBV associated tumors express more restricted subsets of genes termed latency I and II (Table I.1).

EBV latent membrane proteins are multi-pass membrane proteins that lack extracellular domains, but signal constitutively through their cytoplasmic tails. LMP1 induces B cell proliferation by mimicking activated CD40 signaling, activating the NF-κB pathway as well as JAK/STAT, ERK/MAPK, IRF and Wnt (13-19). LMP2A is a B cell receptor (BCR) mimic (20). Therefore, EBV latent membrane proteins mimic two signals that are critical for B cell development and function. LMP2A appears to provide survival

and developmental signal to B cells, and in some cases LMP2A can activate viral lytic replication (21-23). LMP2B is a splice variant of LMP2A that lacks the cytotoplasmic signaling tail. LMP2B co-localizes with LMP1 and LMP2A in the cytoplasmic membrane and several studies have suggested that LMP2B can enhance LMP1 signaling and negatively regulate LMP2A function (24, 25).

EBV also encodes about 22 microRNAs derived from the non-coding BamHI A Rightward Transcripts (BART). Because the fully transforming B95.8 laboratory strain of EBV contains a deletion that eliminates 17 of 22 BART microRNAs, it was not clear whether these played a significant role in EBV oncogensis (26). However, it has long been known that the BARTs are highly expressed in many cancers, particularly NPC, and accumulating evidence suggested they exert important oncogenic effects *in vivo*. BARTs have been implicated in inhibition of apoptosis by regulating genes in apoptosis pathway, such as Caspase 3, PUMA and BIM. BARTs are also involved in immune evasion by modulating host cytokine networks (27-31). A second type of EBV non-coding RNAs (EBERs) is the most abundant EBV RNAs in latently infected cells. They are transcribed by RNA polymerase III and localize to the nucleus (32, 33). Several studies have suggested a role for EBERs in EBV associated cancer; however, EBV deleted for EBERs showed similar transformation efficiency and LCLs growth rate compared with wild type EBV (34-39). Thus, the exact role of EBERs in EBV biology is still mysterious.

EBV nuclear proteins play a crucial role in EBV mediated transformation. EBNA1 is a DNA binding protein that ensures that the EBV episome is licensed for replication by the cellular machinery and, via bridging interactions with the EBV genome

and host chromosomes, ensures partitioning to daughter cells (40-42). Because EBNA1 is expressed in all EBV associated cancers, there has been considerable interest in determining if it has a direct oncogenic effect (reviewed in (43)). Though many potentially important mechanisms have been proposed for EBNA1 oncogenic effects, studies in animal models have been equivocal (44-47).

EBNA2 is a strong transcriptional activator that up-regulates the other EBV latent gene products required for LCL growth, as well as cell oncoproteins such as c-MYC (48-51). EBNA-LP is co-expressed with EBNA2 soon after EBV infection in B cells from the Wp-initiated transcripts. Multiple isoforms of EBNA-LP with different numbers of W-repeat domains are produced during the early stage of Wp activation (52-54). EBNA-LP is thought to act as a co-activator of EBNA2 to potentiate its effects on cell and EBV promoters (55-58). Genetic studies support a role for EBNA-LP in EBV mediated transformation (59), but have yet to establish if co-activation explains this requirement.

EBNA3 protein family

Expressed only during latency III and in Wp restricted BL cells, EBNA3A, EBNA3B and EBNA3C comprise a protein family with no known homologues outside the primate lymphocryptoviruses (60-62). The EBNA3 proteins are approximately 1000 amino acids in size and share a similar exon structure. They are encoded in tandem in the EBV genome and exhibit approximately 40% homology of their N-terminal 300aa, suggesting they arose from triplication of a single ancestral gene (63, 64). Each EBNA3 protein contains multiple nuclear localization signals (NLS) and demonstrates an exclusively

nuclear distribution. They also associate tightly with chromatin and/or the nuclear matrix, but do not bind directly to DNA (65-70) (Figure I.1). An early indication that the EBNA3 proteins were transcription factors was the demonstration that specific EBNA3 domains could mediate transcriptional repression or activation in heterologous reporter assay systems (71-73).

Genetic studies using recombinant viruses indicated that EBNA3A and EBNA3C are essential for *in vitro* transformation of B cells into LCLs and maintain their continuous proliferation. By contrast, EBNA3B is dispensable for LCL formation and growth (74-77). However, in a mouse model of EBV lymphomagenesis, EBNA3B deleted EBV lead to development of aggressive diffuse large B cell lymphoma (DLBCL) not seen with wild type virus (78). These studies suggest that EBNA3B may be a tumor suppressor gene that is important *in vivo* for attenuating the oncogenic potential of EBV and ensuring long-term survival of infected host.

EBNA3s, EBNA2 and RBPJ

Shortly after EBNA2 was identified as an essential transactivator of viral and cellular genes during B cell transformation, it was found not to bind DNA by itself, but instead be targeted to EBNA2 responsive promoters by a cellular DNA sequence-specific transcription factor called RBPJ (Recombination Signal Binding Protein for Immunoglobulin Kappa J Region, also called RBP-Jκ, KBF2, CBF1 or CSL) (79-81). RBPJ is ubiquitously expressed and highly conserved during evolution. In *Drosophila*, it is known as Suppressor of Hairless Su(H). RBPJ/Su(H) is involved in the Notch signaling pathway,

which plays an essential role in cell fate decisions in all metazoan organisms (82). Upon Notch ligandation, the cytoplasmic tail of the Notch receptor is cleaved and intracellular Notch (ICN) is released. ICN translocates to the nucleus, where it interacts with RBPJ and replaces the co-repressor complexes which ultimately lead to downstream gene activation (83) (Figure I.3). Since EBNA2 could also interact with RBPJ to modulate gene expression, EBNA2 may be viewed as a functional homologue of ICN. In contrast, EBNA2 activation is ligand independent (49, 80, 84-87). Despite the functional similarities between ICN and EBNA2, ICN cannot fully substitute for EBNA2 to maintain LCL growth. Unlike EBNA2, ICN does not induce LMP1 or c-MYC expression and that may explain the inability of ICN to maintain proliferation of immortalized B cells (88-92).

Remarkably, all of the EBNA3 proteins (EBNA3A, EBNA3B, and EBNA3C) were also found to bind to RBPJ. However, unlike EBNA2 which binds to RBPJ beta-trefoil domain via its "Notch-like" WΦP motif, EBNA3s bind to the RBPJ N-terminal domain (NTD) through their highly conserved "homology domains" (93-97). Immunoprecipitation experiments demonstrated that EBNA2, EBNA3A, EBNA3B, and EBNA3C all form distinct RBPJ complexes in LCLs (98). By gel shift assays, the EBNA3 proteins compete with EBNA2 for RBPJ binding (99). Furthermore, in transient reporter assays, each EBNA3 protein can inhibit EBNA2 mediated activation of viral LMP2A and Cp promoters (100-102). This suggested that one role of the EBNA3s may act as functional antagonists of EBNA2, preventing uncontrolled up-regulation of the EBNA (Cp) promoter by EBNA2. This hypothesis was also supported by the observation that EBNA3A over-expression dissociated EBNA2 from RBPJ, down-regulated c-MYC and Cyclin D2 expression, and

lead to G0/G1 cell cycle arrest (76, 103). Interestingly, in the context of the LMP1 promoter, EBNA3C potentiates EBNA2 transactivation (104-107), suggesting a complex interplay exists among these RBPJ targeting EBNA proteins.

An observation that reinforced the importance of RBPJ in EBV biology is that EBNA3A and EBNA3C mutants defective for RBPJ interaction are null for LCL proliferation and survival *in vitro* (77, 108, 109). However, it remains unclear if EBNA3 interactions with RBPJ are important for limiting EBNA2 access to RBPJ, for targeting EBNA3 proteins to DNA, or both. In some assays EBNA3s destabilize RBPJ interaction with DNA and it has been suggested that the EBNA3 interaction with RBPJ serves only to limit EBNA2 access to RBPJ (93, 99, 101). However, this shared mechanism does not explain the unique requirement that both EBNA3A and EBNA3C must interact with RBPJ to maintain LCLs in a transformed state.

ChIP-seq (chromatin immunoprecipitation followed by high-throughput sequencing) studies have become a powerful tool to map transcription factor protein binding on a genome-wide scale. Several groups have published ChIP-seq studies for EBNA2, EBNA3A, EBNA3C and RBPJ localization in BLs and LCLs. An EBNA3C ChIP-seq study done by Jiang *et al.* showed that most EBNA2 sites coincided with RBPJ whereas 84% of EBNA3C sites were without significant RBPJ co-binding (110). They also claimed that the interaction of EBNA3C with RBPJ is not important for EBNA3C targeting; instead, the cellular TFs IRF4, BATF, SPI1 and RUNX3 play a central role. An EBNA3A ChIP-seq study done by Schmidt *et al.* reported that EBNA3A also showed minor concordance with RBPJ binding. They suggested that RBPJ may be unimportant for EBNA3A targeting to

DNA and instead claimed that EBNA3A is tethered to DNA through interactions with BATF-containing protein complexes (111). By contrast, a study done by Harth-Hertle *et al.* demonstrated RBPJ interaction did play a critical role in EBNA3A repression of the *CXCL9* and *CXCL10* genes by allowing it to displace EBNA2 (112). McClellan *et al.* showed that, in MutuIII cells, 38% of EBNA2 bound sites are co-bound by one EBNA3 protein. They also claimed that 80% of EBNA3 proteins targeted genes were also targeted by EBNA2 (113). However, no functional data was offered to support this assertion and the role of RBPJ in mediating EBNA3 binding was not explored. Because these prior studies have either focused on single EBNA proteins or studied them in non-LCL contexts, we conducted a complete survey of EBNA3 binding in LCLs and analyzed the data together with EBNA2 and RBPJ ChIP-seq datasets. We observed that only 30-40% of EBNA3A, EBNA3B and EBNA3C bound sites are also bound by RBPJ. Furthermore, we found that sites exhibiting EBNA3/RBPJ co-localization were largely EBNA2 co-bound. This suggests that EBNA3-RBPJ interactions may primarily serve to limit EBNA2 binding and may be site specific. In Chapter III, I will discuss detailed studies which demonstrate that these EBNA3 proteins regulate EBNA2 binding to distinct RBPJ sites in LCLs.

EBNA3 gene regulation in BLs and LCLs

Gene profiling studies done in BLs and LCLs using EBNA3 knockout, conditional or mutant viruses have demonstrated the host transcriptome is extensively regulated by EBNA3 expression (114-118). Using BL31 cells infected with EBV BACmids deleted for one or more EBNA3 genes, White et al. found over 1000 genes to be regulated by EBNA3s

(116) (Figure I.2A). Remarkably, a third of these genes are regulated by more than one EBNA3, indicating an extensive overlap of regulatory target among EBNA3 proteins. Microarray studies conducted in LCLs conditional for EBNA3A or EBNA3C activity showed that 52 of 287 genes regulated by EBNA3A regulated are also regulated by EBNA3C (114, 119) (Figure I.2B). The molecular mechanisms by which EBNA3s uniquely regulate some genes while cooperatively regulating others remain poorly understood.

EBNA3 interacting proteins

EBNA3 proteins have been reported to interact with many cellular proteins. Frequently these interactions were defined by the ability to bind to EBNA3 proteins in over-expression pull-down assays and/or yeast two-hybrid screens. EBNA3A and EBNA3C have been reported to associate with cell transcriptional co-activators such as prothymosin alpha (PTMA) and the p300 histone acetyltransferase (120, 121). EBNA3A and EBNA3C are also reported to interact with transcriptional repressors including histone deacetylases (HDACs) HDAC-1 and HDAC-2, the E1A C-terminal binding protein (CtBP), NCoR and Sin3A (110, 115, 122-124). Several studies indicated that EBNA3C can physically interact with a variety of cellular factors involved in the regulation of cell cycle progression, including SCF^{SKP2}, RB, E2F1, Cyclin A, Cyclin E, Cyclin D1, Cyclin D3, CHK2 and Aurora kinase B; as well as factors involved in apoptosis, including p53, MDM2, ING4 and ING5 (125-134). Despite an extensive literature on putative EBNA3 interacting proteins, it remains to be fully determined which of these interactions are functionally important during B cell transformation *in vitro* or during B cell lymphomagenesis *in vivo.*

To date, the most studied EBNA3 interacting protein is RBPJ which is absolutely required for EBNA3A and EBNA3C mediated growth effects (as detailed in the previous section). A second protein, the E1a C-terminal binding protein (CtBP) has also been shown to be required for EBNA3A and EBNA3C mediated p16INK4a repression, and is important, but less important than RBPJ for LCL growth. A recent study from our lab attempted to define other physiologic binding partners of EBNA3 proteins by purifying endogenous EBNA3A, EBNA3B, and EBNA3C complexes in LCLs and determining their protein composition by LC/MS/MS (98). This revealed that EBNA3 complexes contain a surprisingly limited repertoire of cell proteins: RBPJ, CtBP and the USP12/USP46 DUB complex with its chaperones WDR20 and WDR48. Although the role of the DUB complex is unknown, like RBPJ and CtBP, it was shown to bind to EBNA3 domains required for LCL growth.

EBNA3s and cell cycle regulation

The initial observation that EBNA3A and EBNA3C cooperate with oncogenic mutant Ras (Ha-Ras) in the transformation of primary rat embryo fibroblasts (REFs) indicated that EBNA3A and EBNA3C might possess anti-senescence activity, since Ha-Ras alone induces exit from the cell cycle to a state called “premature senescence” (135, 136). Additional evidence that EBNA3A and EBNA3C can disrupt the cell cycle includes that, in both rodent and human cells, constitutive over-expression of EBN3A or EBNA3C could induce a prolonged G0/G1 cell cycle arrest or aberrant cell division resulting in multi-nucleation, polyploidy and eventually cell death (76, 103, 137). Many of these effects

have been attributed to EBNA3s ability to interact with the cell cycle regulators as indicated in the previous section.

The most direct and compelling evidence that EBNA3A and EBNA3C play a key role in regulating cell cycle entry came from a study using LCLs established with recombinant EBV encoding conditional EBNA3A or EBNA3C (138). In this study, inactivation of either EBNA3A or EBNA3C activity resulted in accumulation of the *CDKN2A* gene products p16INK4a and p14ARF. This occurred at the mRNA and protein levels and was accompanied by a dramatic reduction in proliferation and, with time, cell death. Moreover, siRNA knockdown of *CDKN2A* gene products restores growth despite EBNA3A or EBNA3C inactivation. The fact that EBNA3A and EBNA3C are able to regulate p16INK4a transcript levels also reinforces the notion that they exert their transforming effects by acting as transcription factors. Subsequent experiments demonstrated that B lymphocyts from individuals with a 19 bp germ line deletion in the *CDKN2A* gene that disrupts p16INK4a (Leiden cells) could be transformed by EBV genomes lacking EBNA3C (118, 139). Contrary to earlier studies, EBV genomes deleted for EBNA3A have been found to transform B lymphocytes from healthy donors, albeit at reduced efficiency compared to wild type EBV (114). Collectively these studies suggest that EBNA3A and EBNA3C can repress the *CDKN2A* gene products, EBNA3C plays the more important role, and that repression of p16INK4a is sufficient to explain the requirement for EBNA3C in LCL transformation. The molecular details of how EBNA3A and EBNA3C repress cell genes, including p16INK4a, are discussed in the next section.

EBNA3s mediate epigenetic gene silencing

The critical role played by EBNA3C, and to a lesser extent, EBNA3A in LCL outgrowth has been linked to their ability to cooperatively repress the *CDKN2A* gene that encodes two tumor suppressors: p16INK4a and p14ARF (138). The *CDKN2A* gene, located on human chromosome 9p21, is among the most frequently mutated genes in human cancer. p16INK4a and p14ARF share exons 2 and 3 of *CDKN2A* gene, but remarkably, are encoded in different reading frames determined by their unique exons 1-alpha and 1-beta, respectively. The p16INK4a and p14ARF proteins have no amino acid similarity and regulate distinct tumor suppressor pathways. p16INK4a is a Cyclin-dependent kinase (CDK) inhibitor that acts on the Cyclin D-dependent kinases CDK4 and CDK6 to abolish their binding to D-type Cyclins. Therefore, repression of p16INK4a leads to activation of CDK4/6-mediated phosphorylation of the retinoblastoma protein (RB). On the other hand, increased p16INK4a expression causes a G1 cell cycle arrest and senescence (reviewed in (140)). p14ARF regulates p53 by inactivating MDM2, which is an E3 ubiquitin ligase that targets p53 for degradation, thus stabilizing and activating p53. This can lead to cell cycle arrest by inducing the p53-dependent CDK regulator p21WAF1or apoptosis by inducing p53-dependent pro-apoptotic factors including BAX and NOXA (141, 142).

Using LCLs conditional for EBNA3C activity, Maruo et al. demonstrated that p16INK4a up-regulation upon EBNA3C inactivation was not accompanied by changes in histone marks associated with active transcription (138). Instead, levels of the repressive H3K27me3 histone mark were found to decrease across the *CDKN2A* locus particularly at the *INK4a* TSS. Furthermore, returning the LCLs to conditions permissive for EBNA3C

activity resulted in re-establishment of the H3K27me3 histone mark at the *CDKN2A* locus and repressed p16INK4a expression. Analysis of LCLs established with EBNA3A knockout and LCLs conditional for EBNA3A activity revealed that EBNA3A also plays a role in maintaining the H3K27me3 modification and the repressed state of p16INK4a (115, 138). Neither EBNA3A nor EBNA3C can replace the other in this process. Therefore, EBNA3A and EBNA3C cooperatively repress p16INK4a and inactivation of either protein causes LCLs to stop proliferating (Figure I.4). Furthermore, EBV genomes expressing EBNA3A or EBNA3C mutants that lack CtBP binding, have been used to show that interaction with this co-repressor is necessary for the efficient deposition of H3K27me3 at *CDKN2A* and for repression of p16INK4a expression. However, why both EBNA3A and EBNA3C are required for p16INK4a repression and what specific role each EBNA3 protein plays in this process is poorly understood.

Another important tumor suppressor inactivated by the cooperative effects of EBNA3A and EBNA3C is BIM (Bcl2-interacting mediator). BIM is a pro-apoptotic member of the BH3-only family of BCL2-like proteins and is encoded by the *BCL2L11*gene. BIM binds with high affinity to BCL2 (and other pro-survival family members) and thereby acts as a potent initiator of apoptosis. BIM is a particularly important regulator of cell survival during lymphocyte development (143, 144). The relevance of BIM in EBV lymphomagenesis was first suspected based on studies of the *Eμ-MYC* transgenic mouse model. In these mice, expression of the *MYC* gene is driven by the mu heavy chain enhancer, mimicking the effects of the translocation present in classical Burkitt lympomas. In the *Eμ-MYC* transgenic model, Burkitt-like lympoma development was consistently associated

with loss of *BIM* (145). Hemann and colleagues showed that MYC could activate BIM expression in EBV negative BL cells (146). Thus, high level MYC expression results in a pro-apoptotic response unless accompanied by loss of p53, p14ARF or BIM (147, 148). MYC is also strongly induced early after EBV infection of primary human B cells; suggesting that EBV must target one of these pro-apoptotic genes as well. A role for the EBNA3 proteins in this anti-apoptotic effect was first suggested by the observation that Wp-restricted BLs, which express the EBNA3 proteins are more resistant to apoptosis in vitro than latency I BLs, which do not. Subsequent work demonstrated that EBNA3A and EBNA3C cooperatively repress BIM expression (149-152). The mechanism of EBNA3A and EBNA3C repression of BIM is similar to the way of p16INK4a repression: through the deposition of the H3K27me3 signature on chromatin proximal to the transcription start site for *BIM* locus (153, 154). Again, the precise mechanism of how EBNA3A and EBNAC cooperatively mediate H3K27me3 changes at the *BIM* gene locus remains to be elucidated.

In both vertebrate and invertebrate cells, H3K27me3 is the major histone modification associated with facultative repression and is mediated by the Polycomb repressive complex 2 (PRC2). PRC2 is a multi-protein complex with the key components including the SET domain H3 methyltransferase protein EZH2, SUZ12 and RbAp46/48 which mediate nucleosome binding, and EED which is required for full methyltransferase activity of EZH2 (Figure I.5). Polycomb group (PcG) proteins were first discovered in *Drosophila melanogaster* as the products of genes that are required to prevent inappropriate expression of homeotic (*HOX*) genes. In *Drosophila*, PRC2 is recruited to target genes by binding to the Polycomb response elements (PREs). However, there are no such PREs

discovered in mammalian cells to date. Thus, the precise mechanism of RPC2 targeting is less understood in vertebrate animals. Several factors have been proposed to play a role in PRC2 targeting, including CpG dinucleotide enrichment, CTCF, YY1, and long non-coding RNA (lncRNA) (reviewed in (155)). In the case of EBNA3 mediated H3K27me3 deposition at the *CDKN2A* and *BIM* loci, a simple model has been proposed by the Allday group in which EBNA3A and EBNA3C physically interact with PRC2 components and recruit them to sites near genes targeted for repression (154). However, our detailed examination of several of the predictions of this model have found it wanting as I will discuss in Chapter IV.

The level of H3K27me3 modification in cells is also determined by specific histone demethylases: KDM6A (UTX) and KDM6B (JMJD3). KDM6B has been shown to remove H3K27me3 marks from the *INK4a* promoter during *Ras/Raf* oncogene induced cellular senescence (156, 157), whereas KDM6A has been implicated in the removal of H3K27me3 marks from the promoters of several genes encoding RB binding proteins (158). Human papillomavirus (HPV) E7 oncoprotein induces KDM6B and thereby globally decreases H3K27me3 levels, which results in the up-regulation of p16INK4a that characterizes HPV positive cervical cancers (159). EBV LMP1 is also reported to up-regulate KDM6B in germinal center B cells and is over-expressed in Hodgkin Lymphoma (160). How PRC2 and KDM6A/6B are involved in EBNA3A and EBNA3C mediated H3K27me3 changes at *CDKN2A* and *BIM* loci and whether EBNA3s regulate PRC2 targeting to mediate the site specific changes in H3K27me3 levels are important unresolved questions.

Summary

EBV latent gene products cause many human cancers and drive the transformation of B lymphocytes into immortalized lymphoblastoid cell lines *in vitro.* EBV encoded nuclear antigens (EBNAs) and membrane proteins promote lymphomas by constitutive activation of pathways important for B lymphocyte growth and survival. An important unresolved question is how four different EBNAs (2, 3A, 3B, and 3C) exert unique effects via RBPJ, a transcription factor in the Notch signaling pathway. To investigate this we mapped the genome-wide binding distribution of RBPJ and the RBPJ-interacting EBNA proteins in LCLs. Chapter III details how each EBNA binds to distinct but partially overlapping set of genomic sites. Remarkably, EBNA3A and EBNA3C specifically regulate EBNA2's access to different RBPJ sites, providing a mechanism by which each EBNA can regulate distinct cell genes. In Chapter III, I described our efforts to identify other cell factors that determine EBNA3 binding specificity. These revealed that IRF4, an essential regulator of B cell differentiation, is a critical determinant of EBNA3C (but not EBNA3A or EBNA3B) binding specificity.

EBNA3A and EBNA3C have been shown to cooperatively regulate tumor suppressor p16INK4a and BIM. They do so by depositing the repressive histone modification H3K27me3 along the TSS of these two genes. However, the precise mechanism by which EBNA3s mediate the epigenetic silencing effect is unclear. In Chapter IV, I described my work on examining this issue and how my findings challenge the current model that EBNA3s directly recruit PRC2 to EBNA3 repressed sites.

Table I.1

Latency Type	EBERs	EBNA1	EBNA2/LP	EBNA3s	LMP1	LMP2s	BARTs	Malignancies
I	+	+	−	−	−	−*	+	BL, GC
Wp-restricted	+	+	−	+	−	−	+	Wp-restricted BL
II	+	+	−	+	+	+	+	HL, NPC, NK/T
III	+	+	+	+	+	+	+	PTLD, IM

Table I.1: EBV gene expression in 3 latency types and their associated malignancies.

*LMP2A is expressed in about half of EBV-associated GC. BL, Burkitt lymphoma; GC, gastric cancer; HL, Hodgkin lymphoma; NPC, nasopharyngeal carcinoma; PTLD, post-transplant lymphoproliferative disorders; IM: Infectious mononucleosis, BART, BamHI A fragment Rightward Transcripts – serve as precursors for the majority of EBV encoded microRNAs.

Figure I.1

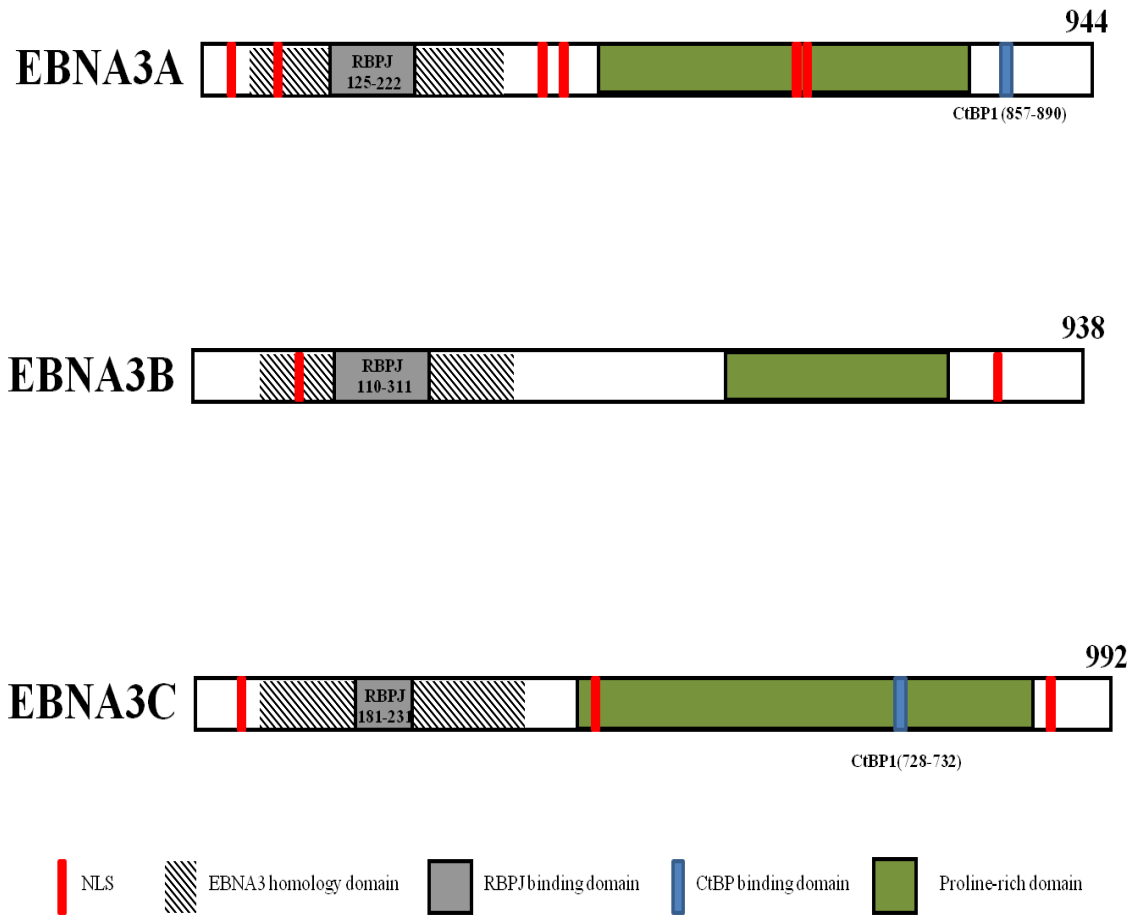

Figure I.1 Schematic representation of the EBNA3 protein family. EBNA3A (944aa), EBNA3B (938aa) and EBNA3C (992aa) domains and structural motifs are shown by the filled grey, green, blue and striped rectangles as indicated. The locations of nuclear localization signals (NLS) that have been demonstrated in each protein are represented by red lines. These schematics are not drawn accurately to scale.

Fgure I.2A

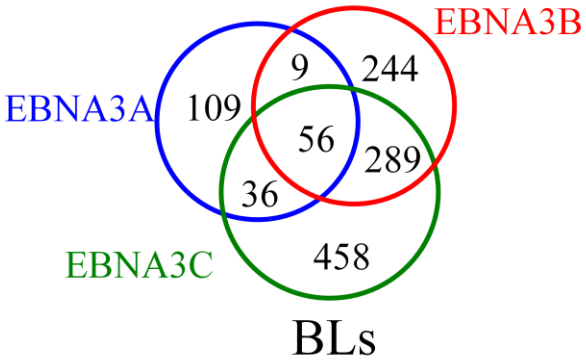

Figure I.2B

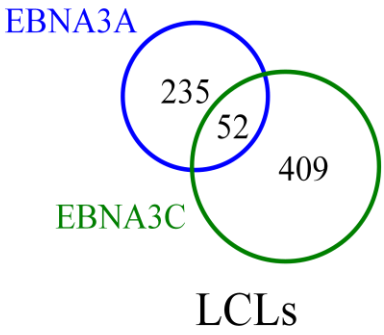

Figure I.2 Overlap of genes differentially regulated by EBNA3s in BL31 cells and LCLs. Venn diagram showing the number of genes regulated by each EBNA3 protein by microarray analysis. A) EBNA3A, EBNA3B and EBNA3C regulated genes in knockout virus-infected BL31 cell lines (p-value < 0.001 and fold change>2). B) EBNA3A (p-value<0.01) and EBNA3C (FDR < 0.01 and fold change>1.5) regulated genes in LCLs.

Figure I.3

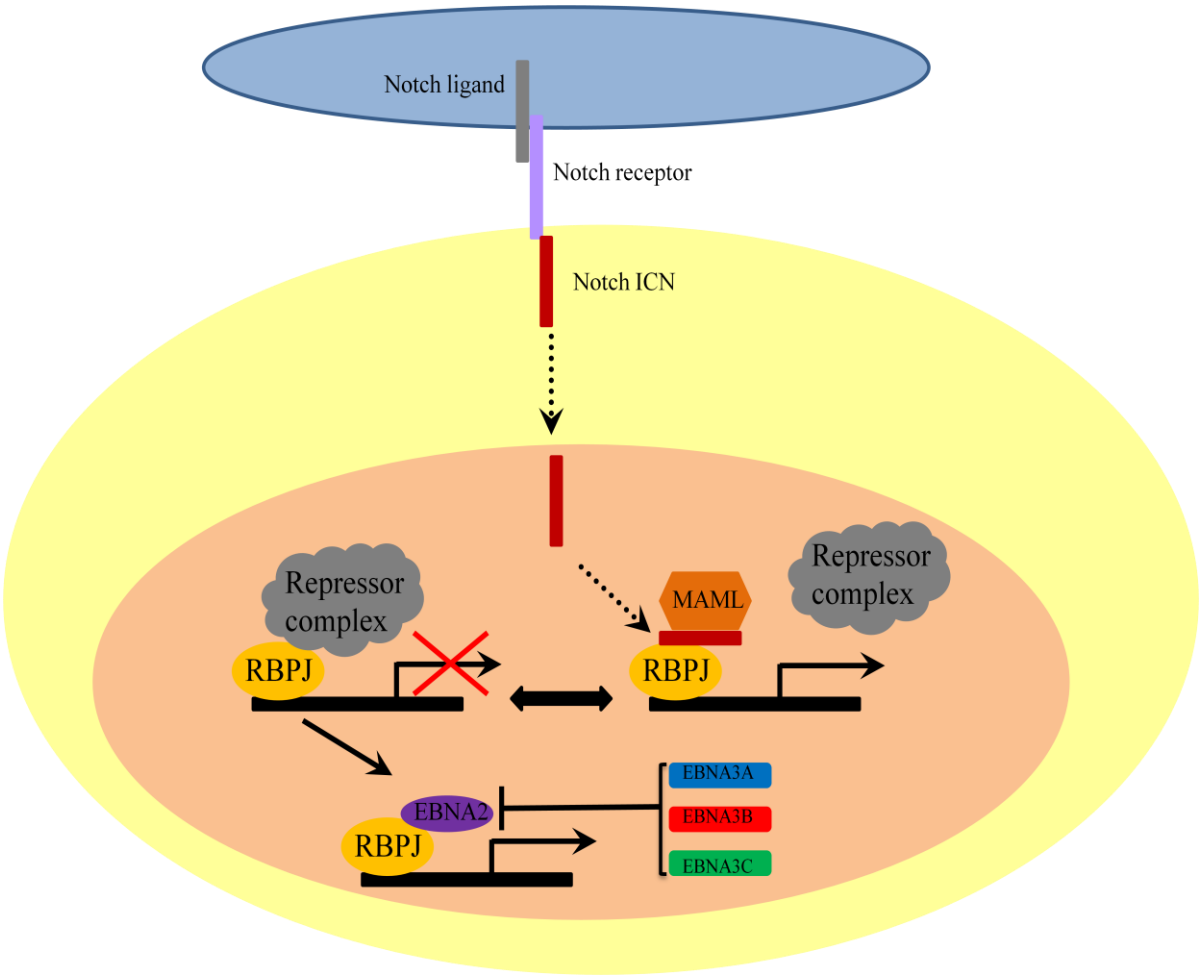
Notch ligand
Notch receptor
Notch ICN
Repressor complex
RBPJ
MAML
Repressor complex
RBPJ
EBNA2
RBPJ
EBNA3A
EBNA3B
EBNA3C

Figure I.3 Schematic representation of the Notch signaling pathway disrupted by EBNA proteins. The Notch receptor exists at the cell surface consisting of a large ectodomain and a membrane-tethered intracellular domain. Notch ligand interacts with Notch receptor on an adjacent cell (lower cell, shown in yellow) induces two cleavages that free the Notch intracellular domain (ICN) from the cell membrane. ICN translocates to the nucleus, where it forms a complex with the RBPJ protein, displacing a repressor complex from the RBPJ protein. Components of an activation complex, such as MAML1is recruited to the ICN-RBPJ complex, leading to the transcriptional activation of Notch target genes. EBNA2 is a strong transactivator that targets RBPJ in a ligand independent manner to activate EBNA2 responsive promoters. EBNA3A, EBNA3B and EBNA3C all interact with RBPJ which likely limits EBNA2 access and thereby abolish EBNA2 activation of target genes.

Figure I.4

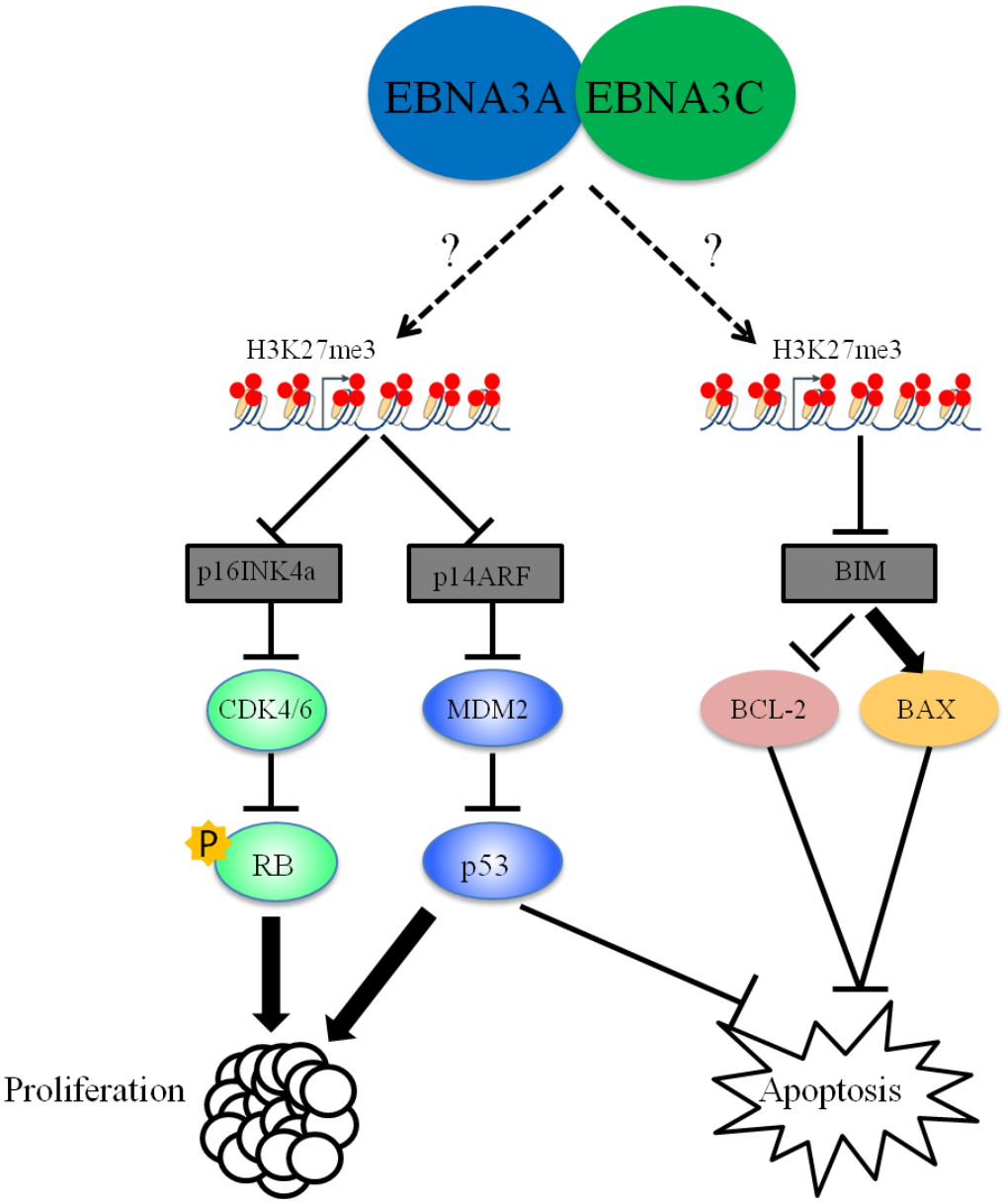
EBNA3A
EBNA3C
?
?
H3K27me3
H3K27me3
p16INK4a
p14ARF
BIM
CDK4/6
MDM2
BCL-2
BAX
P
RB
p53
Proliferation
Apoptosis

Figure I.4 Schematic representation of EBNA3A and EBNA3C regulation of p16INK4a, p14ARF and BIM. EBNA3A and EBNA3C jointly mediate the repression of the two closely related tumor suppressor p16INK4a / p14ARF (encoded by *CDKN2A*) and pro-apoptotic protein BIM. In both cases, repression of transcription is associated with the deposition of H3K27me3 repressive mark on the *CDKN2A* and *BIM* loci, however the exact mechanism by which EBNA3A and EBNA3C mediate this histone modification is unclear. p16INK4a inhibits CDK4/6 activity which leads to the hypophosphorylation of RB and cell cycle arrest. The p14ARF protein regulates p53 activity by inhibiting MDM2-mediated degradation of p53, allowing p53 to induce cell cycle arrest and apoptosis. By repressing p16INK4a and p14ARF, EBNA3A and EBNA3C cooperatively drive cell proliferation. On the other hand, BIM inhibits anti-apoptotic BCL-2 family members and directly activates pro-apoptotic proteins such as BAX, which causes Caspase dependent apoptosis. Repression of BIM by EBNA3A and EBNA3C inhibits apoptosis in LCLs and Wp restricted BLs, promoting their survival.

Figure I.5

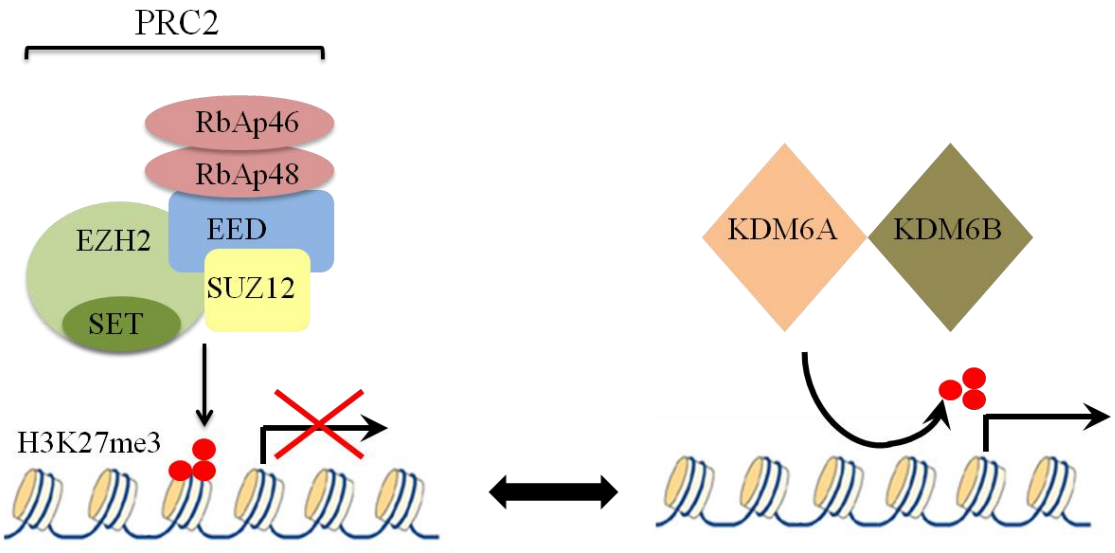

Figure I.5 Schematic representation of Transcriptional regulation through H3K27me3. Transcriptional repression regulated by the polycomb repressive complex 2 (PRC2) which include EED, SUZ12, RbAp46/48 and EZH2 that catalyze H3K27 di- and tri-methylation via its SET domain. This in turn leads to transcriptional repression. KDM6A and KDM6B are histone demethylase that mediate the removal of methyl groups from H3K27me3 leads to transcriptional activation.

CHAPTER II:

MATERIALS AND METHODS

Plasmids

pCEP-EBNA3A-F-HA, pCEP-EBNA3B-F-HA and pCEP-EBNA3C-F-HA plasmids were constructed by re-cloning the EBNA3 C-terminal flag-HA fusions used to make EBV recombinants into pCEP-EBNA3A, 3B, and 3C, respectively. pVxy-puro-IRF4 (161), a kind gift of Dr. Lixin Rui, UW-Madison, expresses the human *IRF4* gene, contains a PGK promoter driven puromycin resistance gene, and was fully sequenced prior to use. pCEP-EBNA3CF144A-F-HA plasmid contains phenylalanine to alanine mutation at amino acid 144 of EBNA3C protein sequence.

Cell lines

LCLs expressing EBNA3A-HT (E3A-HT), EBNA3C-HT (E3C-HT), EBNA3A-F-HA, EBNA3B-F-HA, or EBNA3C-F-HA has been previously described (76, 98, 109). BJAB is an EBV-negative BL cell line (162). B cell lines were maintained in RPMI 1640 medium supplemented with 10% fetal bovine serum, streptomycin, and penicillin; for E3A-HT and E3C-HT LCLs, the permissive condition included addition of 400 nM 4-hydroxytamoxifen (Sigma). 293T is a human cell line transformed by adenovirus 5 and SV40 large T antigen (163) was cultured in Dulbecco's modified Eagle's (Gibco) medium supplemented with 10% fetal bovine serum, streptomycin and penicillin. Stable cell lines were generated by first introducing pCEP-EBNA3A-F-HA, pCEP-EBNA3B-F-HA or pCEP-EBNA3C-F-HA plasmids into BJAB cells followed by hygromycin selection (600ug/ml). Hygromycin resistant clones were then infected with a retrovirus expressing IRF4 or empty vector control followed by puromycin selection (0.4ug/ml). Hygromycin and

puromycin resistant clones were screened by western blot for expression of the appropriate transgenes and maintained in RPMI 1640 medium supplemented with 10% fetal bovine serum, streptomycin, penicillin, 300ug/ml hygromycin and 0.2ug/ml puromycin. E3C-HT p16INK4a/p14ARF KO is a cell line derived from E3C-HT LCL which contains a deletion in exon 2 of *INK4a* and *ARF* locus, thus could not express functional p16INK4a and p14ARF proteins. This cell line was made by Dr. Makoto Ohashi in our lab using CRISPR-CAS9 technique.

Antibodies

The following antibodies were used for ChIP-qPCR and western blot: Anti-HA-tag mAb-Magnetic beads (M132-9; MBL), anti-EBNA2 PE2 and anti-EBNA3C A10 mouse monoclonal antibodies (164), anti-EBNA3A antibody (F115P, Exalpha Biologicals), anti-RBPJ rabbit polyclonal sera (79), anti-HA.11 (16B12, Covance), anti-IRF4 antibody (SC-6059), and anti-alpha-tubulin (B-5-1-2, Sigma), anti-trimethyl-histone H3K27 (17–622; Millipore), anti-histone 3(Abcam, AB1791-100UG), anti-EZH2 antibody. The HA-probe Antibody F-7 (sc-7392; Santa Cruz) was used for ChIP-seq.

Cloning

1. pCEP-EBNA3C-FHA: i) 10 ug pCEP-E3C plasmid was first digest with XbaI for 2 hours (B3 +BSA) at 37 ℃, then added SalI and incubated overnight. Gel purified desired fragment (#1) which was 8875 base pairs (other fragments were: 3554bp, 1096bp, and 6bp). ii) 10 ug pCEP-E3C plasmid was digested with BsiWI first at 55 ℃ for 2 hours

(B3 + BSA), then cooled to 37 ℃, then added SalI enzyme and incubated overnight. Gel purified desired fragment (#2) which was 2952bp (other fragments were 8881 bp and 1698 bp). iii) 10ug pSG5-E3C-f-HA (E3C-TAP) plasmid was with BsiWI first at 55 ℃ for 2 hours (B3 + BSA), then cooled to 37 ℃, then added SalI/SpeI enzyme and incubated overnight. (SpeI is only needed to make the desired fragment easier to excise). Gel purified desired fragment (#3) which was 1757bp (other fragments were 3964bp, 1065, and 791bp). iv) The three fragments above were combined in an equal molar ratio with total DNA added were adjusted to be 17uL, then added 2uL of T4 DNA ligase buffer and 1 uL of T4 DNA ligase, incubate at 16 ℃ overnight. In addition, a control ligation with only fragment #3 in the ligation reaction was done. v) 2ul of ligation reaction was used to transform DH5alpha competent *E.coli* cells and the transformation was spread onto LB plates with ampicillin antibiotics selection of resistant clones. vi) The resistant clones was confirmed by DNA sequencing and then transected into 293T cells and blot for HA tagged EBNA3C expression.

2. pCEP-EBNA3CF144A-FHA: i) PCR amplify pSG5-flag-EBNA3C plasmid DNA using forward primer EBNA3C_F144A which contain two nucleotides mutation compared to wild type sequence and reverse primer E3C-C407 (primer sequences shown in Table II.1). PCR reaction was done in 50ul total volume which contains 100ng template DNA, 1ul 10mM dNTP mix, 1ul 10uM forward primer, 1ul 10uM reverse primer, 1ul Phusion DNA polymerase, 5ul 10X Phusion DNA polymerase buffer, and nuclease-free water. The cycle condition was 98 ℃ for 2 minutes, followed by 29 cycles of 98 ℃ for 30 seconds, 58 ℃ for 30 seconds, 72 ℃ for 1 minutes. Final extension was 72 ℃ for 10

minutes. The PCR product size was 1280 bp (#1). ii) Gel purified the PCR fragment and digested with AfeI/SpeI (B4 + BSA) at 37 ℃ for 2 hours. Gel purified desired fragment which was 725 bp (the other fragment was 560 bp). iii) 10ug of pSG5-flag-EBNA3C was digested with AfeI/SpeI (B4 + BSA) at 37 ℃ for 2 hours. Gel purified desired fragment (#2) which was 6809bp (the other fragment was716bp). iv) Ligated the fragment #1 and #2 in molar ratio of 3:1, with total DNA added were adjusted to be 17uL, then added 2uL of T4 DNA ligase buffer and 1 uL of T4 DNA ligase, incubate at 16 ℃ overnight. In addition, a control ligation with only fragment #2 in the ligation reaction was done. v) 2ul of ligation reaction was used to transform DH5alpha competent *E.coli* cells and the transformation was spread onto LB plates with ampicillin antibiotics selection of resistant clones. vi) The resistant clones was confirmed by DNA sequencing and then transected into 293T cells and blot for HA tagged EBNA3C expression.

Transfection

$2x10^6$ BJAB cells were harvested during log-phase growth, wash with phosphate buffered saline (PBS), resuspended in 100ul of buffer V (Lonza) and transferred in a 2cm cuvette after addition of 2ug of appropriate plasmid DNA. Program M-013 of Amaxa Nucleofector (Lonza) was used, and cells were resuspended in RPMI1640 supplemented with 10% fetal bovine serum, streptomycin and penicillin after transfection and cultured in 6-well plate. 293T cells were transfected using Effectene (Qiagen) in 10cm culture dish with retroviral packing plasmids as previously described (165).

Western blot analysis

Total cell lysates and immunoprecipitated proteins were separated by sodium dodecyl sulfate (SDS)-polyacrylamide gel electrophoresis, transferred onto nitrocellulose membrane, and blotted with appropriate antibodies. After extensive washing, the membrane was probed with horseradish peroxidase conjugated secondary antibodies (Jackson Immuno Research). The membrane was washed again after 1 hour incubation, and developed with chemiluminescence reagent (Perkin Elmer).

Chromatin-immunoprecipitation and quantitative PCR (ChIP-qPCR) assays

$2x10^7$ cells were cross-linked in 1% (w/v) formaldehyde (Sigma) for 5 min at room temperature and the cross-linking reaction stopped by addition of glycine to a final concentration of 0.125M. Cells were washed twice with cold PBS and lysed in 1 ml of lysis buffer (50 mM Tris-HCl [pH 8.1], 10 mM EDTA, 1% [w/v] SDS, 1 mM PMSF, 1 μg/ml leupeptin, 20 μg/ml aprotinin) for 30 min on ice before extensive sonication using a Qsonica LLC Q700 sonicator to an average fragment size of 200-500 bp. After extract clearing by centrifugation, supernatants were diluted 1:10 in dilution buffer (16.7 mM Tris-HCl [pH 8.1], 1.2 mM EDTA, 167 mM NaCl, 1.1% [v/v] Triton X-100, 0.01% [w/v] SDS, 1 mM PMSF, 1 μg/ml leupeptin, 20 μg/ml aprotinin). About 10% of the chromatin lysate was reserved for qPCR and not subjected to any further manipulation. 1ml of diluted chromatin lysates were incubated with ChIP antibodies with rotation at 4℃ overnight. 15ul Protein A/G magnetic beads were added to each 1ml chromatin lysate and incubated for 1 hour at 4℃ with rotation. After incubation, Protein A/G magnetic beads were pelleted with a

magnetic separation rack and then washed once with cold low salt wash buffer (20 mM Tris-HCl [pH8.1], 2 mM EDTA, 150 mM NaCl, 1% [v/v] Triton X-100, 0.1% [w/v] SDS), once with high salt wash buffer (identical to low salt wash buffer, except 500 mM NaCl), once with LiCl wash buffer (10 mM Tris-HCl [pH8.1], 1 mM EDTA, 0.25 M LiCl, 1% [v/v] NP40, 1% Deoxycholic acid), and finally twice with TE buffer (10 mM Tris-HCl [pH8.1], 1 mM EDTA). Samples were then resuspended in 150 µl of elution buffer (0.1 M $NaHCO_3$, 1% [w/v] SDS) and rotated for 20 min at room temperature. Two elutions of protein-DNA complexes were performed and pooled. NaCl and Proteinase K were added to each ChIP DNA sample and input to a final concentration of 200 mM and 100ug/ml respectively. ChIP DNA samples were then reverse cross-linked at 65 ℃ for 4 hours. DNA was purified using the QIAquick PCR purification kit (28706; Qiagen) and quantified with the iTaq™ universal SYBR Green supermix (1725121;Bio-Rad) using a BioRad CFX96 system. Purified inputs DNA were used in real-time PCR reactions for standardization. For ChIP-seq, the above procedure was scaled approximately 10 fold as previously described (166). Sequence reads were aligned to the human hg19 genome using Bowtie (http://bowtie-bio.sourceforge.net/index.shtml) to produce SAM files for further analysis.

Retroviral transduction

Retrovirus were generated by co-transfecting 293T cells in a 60-90% confluent 10 cm dish with 4 µg of a plasmid encoding MMLV Gag-Pol, 3 µg of a plasmid encoding the vesicular stomatitis virus G protein, 4 µg of a plasmid encoding human IRF4 protein(pVxy-puro-IRF4) or empty vector using Effectene transfection reagent (Qiagen).

Twenty-four hours after transfection, the culture medium was replaced with Dulbecco's modified Eagle medium supplemented with 10% fetal bovine serum and 50 mM HEPES. On days three after transfection, the media was collected and filtered through a 0.45 μm pore size filter after spinning. 10^6 BJAB cells were resuspended in 1ml of RPMI supplemented with 10% fetal bovine serum and mixed with 1ml of retrovirus in a 12-well plate. 24 hours later, the old culture medium was replaced. 48 hours later, the transduced BJAB cells were selected by puromycin (0.4ug/ml) in 96-well plate.

RNA isolation and Reverse Transcription Quantitative PCR

Total cell RNA was isolated from $5x10^6$ EBNA3CHT cells using GeneJet RNA purification kit (Thermo Scientific), following the manufacturer's protocols. RNA was treated with RQ1 RNase-Free DNase (Promega) to digest any residual cellular DNA following the manufacturer's protocols. Then 1ug RNA was mixed with random haxamer in a total volume of 5 μL, incubated at 70 ℃ for 5 minutes, and then immediatedly chill in ice-water for at least 5 minutes. The reverse transcription reaction was done by adding ImProm-II 5x reaction buffer, $MgCl_2$, dNTP mix, Recombinant RNasin Ribonuclease Inhibitor and ImProm-II Reverse Transcriptase (Promega) in a total volume of 15ul. The RT reaction was done using a thermocycler at 25 ℃ for 5 minutes, then at 42 ℃ for an hour and at 70 ℃ for 15 minutes. The cDNA product was then used for Quantitative PCR to measure the level of individual transcripts with corresponding primers.

Peak calling

Peak calling in the ChIP-seq samples was performed using MOSAiCS (MOdel-based one and two Sample Analysis and inference for ChIP-seq Data) (167) controlling the false discovery rate (FDR) at 0.05. We ran MOSAiCS in two sample mode where it estimated the distribution of the background read counts from input data and the distribution of the reads counts in peak regions with a two component Negative Binomial mixture model. MOSAiCS is available at http://www.bioconductor.org/packages/release/bioc/html/mosaics.html.

Peak co-localization

To perform downstream analysis of the peak lists, we first generated a union peak set by merging peaks that overlap in the EBNA2, EBNA3A, EBNA3B, EBNA3C, and RBPJ peak lists. Then we built the incidence matrix by using the union peak set and the peak lists. Each entry of the incidence matrix was set to 1 when a peak in the list was used to construct the region and 0 otherwise. Additionally, we overlapped the union peak set with 76 GM12878 ChIP-seq peak sets and DNase I hypersensitive sites (DHS) reported by the ENCODE project for further analysis (data from https://www.encodeproject.org).

Histone profile plots

The average histone modification profiles were calculated using Segvis (https://github.com/keleslab/Segvis) for each 4 kb window centered at the EBNA protein peak summits that overlap DHS. For each coordinate in the window, we calculated the signal as the number of extended reads within a 151 bp window. These signals were then

averaged to generate a smooth aggregation profile. Each profile was normalized to 1 million reads and the profiles for a given peak set were averaged coordinate-wise. The histone modification ChIP-seq datasets were downloaded from the ENCODE portal (https://www.encodeproject.org).

Chromatin states classification

Chromatin states were assigned to EBNA protein peaks by clustering the maximum normalized histone signal values in 250 bp around the peak summit using the partition around medoids algorithm of the cluster package in R (https://cran.r-project.org/web/packages/cluster/index.html).

Motif and gene enrichment analysis

Motif analysis was performed using the MEME-ChIP (168) tool from MEME suite [http://meme.sdsc.edu]. Input data consisted of 500 bp genomic sequences centered around the peak summits from the top 500 peaks (ranked by the posterior probabilities of binding from MOSAiCS) that overlapped DHS. TFs targeting the discovered motifs were determined by comparing the motifs with annotated motifs in the JASPAR and TRANSFAC databases using the TOMTOM tool of MEME suite.

Data deposition

The ChIP-seq data reported in this paper has been deposited in the GEO database 205 under accession number GSE76166.

Table II.1

Gene	Primer sequence	
HDAC7	P1:CGAACCTGTCACTCCCAGAC	P2:CCCATTCCAAGGAGCCTAGC
EIF2AK3	P1:CTTCCGGACGCAATTACCAATGAG	P2:GTAGGAAAGGTATTCCGGGAACTG
METTL13	P1:AAAGCGTTTAGGTGTCTGCGACG	P2:TCAGCTAGTCATTGGTCGCTGCTT
C20orf24	P1:ACCGTTCTACCAAGATTGTCCCTC	P2:AAGCCATCCGAGTGAAACAGCGA
IL6R	P1:CAGTTGAGTCTGTGGGAACTC	P2:CCTGTTCCTCTTGCTCCTAATG
QSK	P1:GCTGTAGCAGGCAATACTCTCTTG	P2:GCAGCTGACTTTACATTGGGCAGA
HNRPLL	P1:GAACTGGGAAACCAAAAGAGCGGT	P2:GATGGCTTCCAGACTGTGGT
NFATC2	P1:CGCACAGCAGCCCAAATTAC	P2:ACCTGTCACCCCAATTAGCAG
ALOXE3	P1:CCGGATAGCTCAGTCGGTAG	P2:GCGGTACCCAAAAGCAAAGA
POU2F1	P1:TCTGGCGGCAGGAGAAA	P2:TGGCCCTTCGGTAGCTAAA
PIP5K1B	P1:AATGGGAATCCTAGGTCCCTGACT	P2:AGCTCCAGGTCTAGCTCCATCTTC
CTLA4	P1:CGTTGCAATAACATGGGGCAG	P2:GCATTCTGCCCAGCCTAATCT
CXCR5	P1:CACCACCCAGAAGACATGAA	P2:GCAAGGTGCTCTGGAAACTA
CCDC80	P1:TCTACCTCATGCTGCCCAAACTGT	P2:TTACCTCCTCTGTGGCTGCATTTG
ARHGAP25	P1:AGACAAGGGTAGTGGATGTTGCCT	P2:AGCATCACAGTAGCCACAGAACCT
JAK1	P1:TTCCTGCTTTGCACTTCAGCTCAG	P2:TGCTTCCCTCCCAAATACACCTCA
SHQ1	P1:GGTTTCATTTCCTCTGCCCAAACC	P2:GTCCTCTGTGATCAATTGTGGGCT
ROCK1	P1:ACCTAACAGAGTACAACCTGTC	P2:CCTCCTGAGAGTGCTTCTGTC
SYTL3	P1:ATCCTGGTGACTGCAGCCCCTT	P2:CCAGCGGAGGCCCTGCTATAC
BLK	P1:AAGGCACATGGAAGGAGAGCTGAA	P2:ACTAGACCCTAGCTCTGAAACGCC
BACH2	P1:AGCAGTAGTAGCAGTAGTAGCA	P2:ACCCAAACAGTGGTTCATAGAG
CDH1	P1:CAAAGGGAAACCCTGTCTCTAC	P2:TCCTGGACTCAAGGGATCTAC
CACNB4	P1:GTGGATGTCTTAGCAGTGATGA	P2:CTAGTGTGGATTGGCTCTGAAT
GSG2	P1:TTGCCCTGGTACAGGATAGT	P2:CCTGCTTGGTTTCATTGGTTTC
TMEM109	P1:AGCCACATTGGCCTTTCA	P2:ACATTGGAGGGTTTGAGACAG
SUB1	P1:GCAAAGAAGGGCAAGTCAAAG	P2:GCATCCTGTCCAATCTCATAGG
FOXO3	P1:GAAGCACGCATGTGCATTTA	P2:TTATGCACACATGACTAGGAGAC
ALPK2	P1:CTAGGAGTAAGCCCAACATAGTG	P2:CAGAGGGTCAGAGAAGCTAAAG
PARP9	P1:TGTCTGGCACCTTCTGTTAAG	P2:ACTGCCTTGAGGCAATTCA
TRIB2	P1:CATCTTGGCGACCATGGTATAG	P2:ACAAGGCATGCTATCTCTTTCA
PPIA	P1:GGGCCGAACGTGGTATAA	P2:CCATGGCTAATAGTACACGGTTT
INK4a	P1:CCCCTTGCCTGGAAAGATAC	P2:AGCCCCTCCTCTTTCTTCCT
BIM	P1:CGAGCGGGAAAAAAGGTTTGGTTCA	P2:TAGGCTCCCACTTCCTTCTCCCAGT
RAPH1	P1:CTCGTGCCTCGCCTTTCCTCC	P2:TGGGGCAGCACTGGGATTTTCC
MACC1	P1:TTGTGGTTCCTGGGCCTTAG	P2:ACCGAAGAGCAACACACCAA
TP53I3	P1:TGCGGCAGAGCAGGACAACG	P2:TTACTCCTGGCCCGGCTCCC

Table II.1: Primer pairs used for ChIP-qPCR in this study.

For the indicated genomic loci sequences of the forward and reverse primers are listed. PPIA primers are from a study by McClellan et al (117).

Table II.2

Gene	Primer sequence	
GAPDH	P1:TGAAGGTCGGAGTCAACGGATTG	P2:GCCATGGAATTTGCCATGCCATGGGTGG
EZH2 V1	P1:AGAATGGAAACAGCGAAGGA	P2:CTGCTGTAGGGGAGACCAAG
EZH2 V2	P1:GGGACTAGGGAGGTGGAAGA	P2:CCACATTCTCTATCCCCGTG
KDM6A	P1:CGCTTTCGGTGATGAGGAA	P2:TGAAATCTCACGAACCCAAAGA
KDM6B	P1:AAATCCAACTGCGCCACT	P2:TGTCTCCGCCTCAGTAACA

Table II.2: Primer pairs used for RT-qPCR in this study.

For the indicated genomic loci sequences of the forward and reverse primers are listed.

CHAPTER III:

EBNA3 PROTEINS REGULATE EBNA2 BINDING TO DISTINCT RBPJ GENOMIC SITES

*A significant portion of this chapter is derived from my first author paper published on Journal of Virology with the same title. My contributions to this work include evaluation of the ChIP-Seq dataset, performed MEME motif analysis, all ChIP-qPCR assay, Western blot experiment and established BJAB-E3s-IRF4 cell lines. Sunduz Keles, Rene Welch and Tram Ta performed bioinformatics analysis for ChIP-Seq. Eric Johannsen and I designed research and wrote the manuscript.

Introduction

Epstein-Barr virus (EBV) is a herpesvirus that infects over 90% of the population by adulthood. Primary EBV infection usually presents as a non-specific illness in early childhood, but often manifests as infectious mononucleosis in adolescents (169). Thereafter, EBV establishes lifelong latent infection in B lymphocytes and periodically reactivates and is shed in saliva. Rarely, EBV latent infection results in malignancy, including Burkitt and Hodkgin lymphoma, lymphoproliferative disease, nasopharygeal carcinoma and gastric cancer. Much of our knowledge of the transforming effects of EBV latent genes derives from the study of EBV latent infection of B lymphocytes *in vitro* which results in their growth transformation into lymphoblastoid cell lines (LCLs). Extensive investigation of the effects of EBV latent genes in LCLs has demonstrated that they constitutively activate growth and survival signals essential for normal B cell development, including the CD40 and B cell receptors (reviewed in (170)).

EBV nuclear antigens (EBNAs) are proteins expressed during latent infection that extensively target the Notch signaling pathway. EBNA2 is a strong transcriptional activator that is targeted to promoters through an interaction with the RBPJ DNA binding protein that normally mediates intracellular Notch (ICN) binding (79, 85). EBNA2 up-regulates the other EBV latent gene products as well as cell oncogenes such as c-MYC, required for LCL growth (49-51, 87). EBNA2 effects are substantially similar, but not identical to those of ICN (89, 91, 92, 171). Unlike ICN, EBNA2 activation is constitutive and ligand independent. Remarkably, three other EBV nuclear proteins, EBNA3A, EBNA3B, and EBNA3C associate with RBPJ in LCLs. The EBNA3 proteins bind RBPJ through their

highly homologous N-terminal regions and are thought to have arisen from the triplication of a single ancestral gene (93, 94). Although EBNA3s bind an RBPJ domain that is distinct from the EBNA2/ICN binding site, they nevertheless, limit EBNA2 activation by competing for RBPJ binding (95, 97, 99, 103). In LCLs and Burkitt lymphoma tumor cells the EBNA3 proteins have been shown to regulate distinct, but extensively overlapping sets of cell genes (114, 116, 118, 119, 138, 148, 172, 173). EBNA3 proteins have been implicated in the pathogenesis of Burkitt lymphoma and in attenuating an anti-proliferative DNA damage response during EBV transformation of primary B lymphocytes (148, 154, 174, 175). Moreover, EBNA3A and EBNA3C repression of the *CDKN2A* encoded tumor suppressors p16INK4a and p14ARF is essential for LCL growth, requires interaction with RBPJ, and is associated with increased H3K27me3 modification at the *CDKN2A* promoter (96, 108, 109, 118, 138).

Despite significant advances in our understanding of the role of EBNA3 proteins in LCL growth, the basis for their different effects via RBPJ remains an area of active investigation. The selectivity in gene regulation suggests that EBNA3 proteins either target different RBPJ bound sites or exert different effects at the same sites. Chromatin immunoprecipitation experiments have led to a rapid advance in our understanding of this problem. McClellan et al. demonstrated that EBNA3 proteins bound to sites distinct from EBNA2 in the Mutu III Burkitt lymphoma cell line, but due to cross-reactivity among some EBNA3 antibodies, they could only distinguish between EBNA3A, EBNA3B, and EBNA3C at specific EBNA3 bound sites by ChIP-qPCR (113). To overcome this limitation, we derived LCLs which express a single EBNA3 protein with a C-terminal flag-HA tag (98).

Using our EBNA3C-flag-HA LCLs, Jiang et al. reported that EBNA3C co-localized to BATF/IRF4/SPI1/RUNX3 sites and observed that EBNA3C binding signals were stronger at IRF4 co-bound sites than sites without IRF4 binding. Remarkably, EBNA3A bound sites were also found to be enriched for many of the same factors, although ChIP-re-ChIP experiments supported a critical role for BATF in EBNA3A binding (110). To extend these results, we performed new ChIP-seq experiments from the EBNA3A-flag-HA, EBNA3B-flag-HA, and EBNA3C-flag-HA LCLs, analyzed them concurrently, and in this chapter I will report the first comprehensive analysis of EBNA3 binding in LCLs. More importantly, I am going to address the long standing mystery of how EBNA3s regulate EBNA2 function *in vivo* and what cellular factors determine EBNA3 binding specificity.

Results

Genome-wide binding analysis of EBNA3 proteins in LCLs.

In order to identify EBNA3A, EBNA3B, and EBNA3C bound sites in LCLs, we performed chromatin immunoprecipitation with deep sequencing (ChIP-seq) experiments using three LCLs: EBNA3A-F-HA, EBNA3B-F-HA and EBNA3C-F-HA that are transformed with recombinant EBV genomes in which one of the EBNA3 proteins has a Flag-HA epitope fused to its C-terminus as previously described (98). This approach allowed each EBNA3 protein to be precipitated with an anti-HA monoclonal antibody, minimizing the possibility that observed differences were attributable to differences among antibodies used in EBNA3A, EBNA3B, or EBNA3C ChIP.

ChIP samples were used to prepare libraries for Illumina sequencing, and the raw reads were aligned to the human hg19 genome using Bowtie (http://bowtie-bio.sourceforge.net/index.shtml) (176). Genomic sites bound by each EBNA3 were identified as peaks in ChIP-seq data set relative to input DNA using MOSAiCS (167). For comparison, we performed an RBPJ ChIP-seq from one of the cell lines (EBNA3C-F-HA LCL) and reanalyzed previously published EBNA2 and RBPJ ChIP-seq datasets (166) using the same bioinformatics pipeline. This identified a total of 1640 EBNA3A, 3033 EBNA3B, 3588 EBNA3C, 8592 EBNA2, and 9938 RBPJ bound sites. In total, we identified 6791 distinct genomic sites bound by EBNA3 proteins in LCLs (Table III.1). Although this estimate is comparable to that reported for EBNA3 binding in Mutu III cells (113), only 1466 (21%) of these sites are in common (Figure III.1). This limited overlap may reflect true differences between EBNA3 binding in LCLs and BL cells or be

due to technical differences such as undersampling or the use of different antibodies in the ChIP-seq procedure. To facilitate identification of transcription factors that may mediate EBNA3 binding to the human genome we exploited the observation that the vast majority of cell transcription factor binding sites lie within the DNase I hypersensitivity sites (DHS) (177) and defined subsets of EBNA3 binding sites that overlapped DHS sites in the GM12878 LCL (178) for additional analysis. In total we identified 1064 EBNA3A, 2648 EBNA3B, 1802 EBNA3C, 7772 EBNA2, and 8294 RBPJ binding sites within DHS (Figure III.2 and Table III.1).

We further validated the specificity of our ChIP-seq peak calling by examining 20 genomic loci bound by one or more EBNA3s. For these experiments, we performed replicate ChIPs using EBNA3-F-HA LCLs and wild type LCLs and assessed enrichment relative to input by qPCR for each bound site using specific primers (Table II.1). EBNA3 binding sites were classified as EBNA3A only (*HDAC7, EIF2AK3* and *METTL13*), EBNA3B only (*IL6R* and *C20ORF24*), EBNA3C only (*HNRPLL, QSK, ALOXE3* and *NFATC2*), EBNA3A and 3B (*POU2F1, PIP5K1B* and *CTLA4*), EBNA3B and 3C (*JAK1* and *SHQ1*), EBNA3A and 3C (*CXCR5, CCDC80* and *ARHGAP25*), EBNA3A, 3B, 3C (*BLK, ROCK1* and *SYTL3*), based on ChIP-seq results. We considered a peak as validated if there were statistically significant enrichment in HA ChIP from the respective EBNA3-FHA LCL relative to that observed in the wild type (untagged) LCL by a two sample t-test. Using this approach, we confirmed 10 of 12 EBNA3A, 9 of 10 EBNA3B, and 9 of 12 EBNA3C bound sites identified by ChIP-seq (Figure III.3). In addition, we found evidence of EBNA3B binding at 3 sites (*EIF2AK3, QSK* and *ALOXE3*) by ChIP-qPCR that were not

observed by ChIP-seq. Based on these results, we estimated the overall sensitivity and specificity of our EBNA3 ChIP-seq experiments relative to ChIP-qPCR to be 92% and 83% respectively.

EBNA3 bound sites are over-represented at promoter and enhancer elements.

We constructed average histone profile plots for ±2 kb regions centered on EBNA3 peak summits for the activation marks H3K9ac, H3K27ac, H3K4me1, H3K4me2, and H3K4me3 and the repressive marks H3K27me3 and H3K9me3, and transcribed region associated mark H3K36me3 using ENCODE histone ChIP-seq datasets (179). For each EBNA3 protein, the signals from acetylation marks (H3K9Ac and H3K27Ac) were strong as were mono, di, and tri- methylation of H3K4 (Figure III. 4A). For all EBNA3s, repressive marks characteristic of facultative (H3K27me3) and constitutive (H3K9me3) heterochromatin were very low, despite the prior observation that H3K27me3 levels are increased at EBNA3A and EBNA3C repressed genes such as *CDKN2A* and *BCL2L11* (*BIM*). We also annotated EBNA3 bound peaks according to their locations within the epigenetic landscape (180). Results for EBNA3B were typical: 8% of EBNA3B sites reside within active promoters defined by high H3K4me3 and H3K9ac, 12% within weak and poised promoters characterized by high H3K4me3 and low H3K27ac or high H3K27me3, 33% within strong enhancers with high H3K4me1 and high H3K27ac, 25% within weak enhancers with intermediate H3K4me1 and little H3K27ac, 22% were found in heterochromatin regions characterized by the absence of these histone marks (Figure III. 4B). Thus, the EBNA3 proteins, despite their roles in the repression of multiple cell genes

(114, 116, 118, 119, 138, 148, 172), bind predominantly at genomic sites bearing marks of transcriptionally active chromatin.

Overlap among EBNA3A, EBNA3B, EBNA3C, EBNA2 and RBPJ sites in LCLs

Because the EBNA3 proteins cooperatively regulate many cell genes and because EBNA2, EBNA3A, and EBNA3C must interact with the RBPJ transcription factor to transform B lymphocytes, we wanted to examine the extent of overlap among EBNA3A, EBNA3B, EBNA3C, and EBNA2 bound sites. Significant overlap between EBNA3A and EBNA3C has been noted previously (110). Our experiments estimate this overlap to be about 26% of EBNA3A peaks are EBNA3C co-bound, and reveal that this overlap extends to EBNA3B bound sites. For EBNA3B, 21% are shared with EBNA3A, 22% with EBNA3C, and 37% with EBNA2. Thus, in LCLs there is substantial overlap among EBNA2, EBNA3A, EBNA3B, and EBNA3C bound sites, mirroring the overlap observed in the cell genes regulated by these EBNAs.

Although EBNA3 proteins are extensively complexed with RBPJ in LCLs (98, 181), we found that 66% of EBNA3A, 57% of EBNA3B, and 56% of EBNA3C bound sites lack RBPJ binding (Figure III.5). RBPJ independent binding has been noted in prior EBNA3A and EBNA3C ChIP-seq experiments (111, 113). This does not appear to be a technical artifact of the RBPJ ChIP-seq as we did not observe enrichment for RBPJ cognate binding sequences (e.,g., GTGGGAA – see further discussion below) at EBNA3A, EBNA3B, or EBNA3C bound sites as might occur if the RBPJ ChIP was impaired by EBNA3 co-binding. The EBNA3A, EBNA3B, or EBNA3C bound sites that do co-localize with RBPJ are frequently co-bound by EBNA2 as well, suggesting that EBNA3 binding at

RBPJ sites may primarily serve to limit EBNA2 binding (Figure III.5, compare 21-34% co-bound by both with 9-16% RBPJ only). We further observed that 27% of EBNA2/RBPJ/EBNA3 bound sites exhibit binding by more than one EBNA3.

EBNA3A and EBNA3C regulate EBNA2 binding at different RBPJ sites in the genome

Despite this extensive RBPJ-independent EBNA3 binding, multiple lines of evidence argue that RBPJ interaction is central to EBNA3A and EBNA3C mediated gene regulation and LCL growth (96, 108, 109, 112). Further, these effects are specific: EBNA3A over-expression cannot compensate for EBNA3C loss and vice versa (76, 109). The extensive overlap between EBNA2 and RBPJ suggests that each EBNA3 may regulate EBNA2's access to RBPJ at distinct genomic locations. To examine this possibility directly, we determined EBNA2 occupancy at several EBNA3C/RBPJ co-bound sites, in the presence or absence of EBNA3C activity using the EBNA3C-HT LCL. EBNA2, EBNA3C and RBPJ ChIPs were performed in EBNA3C-HT LCLs supplied with 4HT (4HT+) or cultured in medium after withdrawal of 4HT for two weeks (4HT-). We used qPCR to examine genomic loci bound by EBNA3C near genes known to be repressed by EBNA3C expression (116, 118), including BACH2, JAK1, and CXCR5 (Figure III.6A). As expected, the EBNA3C binding signal was present at each of the three EBNA3C bound sites (*BACH2*, *JAK1*, and *CXCR5*) in EBNA3C-HT cells grown in the presence of 4HT and markedly declined upon 4HT withdrawal. Although EBNA3C has been observed to reduce RBPJ binding to DNA in gel shift assays, we did not observe any reduction in the RBPJ binding signal due to EBNA3C co-binding under physiologic conditions. By contrast, EBNA3C inactivation had a dramatic effect on EBNA2 occupancy at these RBPJ bound sites. At each

location, EBNA2 levels were low in the presence of EBNA3C, but increased significantly in the non-permissive EBNA3C condition. As controls, we also examined RBPJ and EBNA2 binding at two sites near EBNA3A regulated genes (*HDAC7* and *CDH1*) that are bound by EBNA3A, but not EBNA3C (114, 116). At these control sites, no significant change in RBPJ occupancy or increase in EBNA2 binding was observed upon EBNA3C inactivation by 4HT withdrawal. These results suggest that EBNA3C does not compete with EBNA2 for global access to RBPJ, but rather competes in a manner that is highly site specific. It is noteworthy that in the presence of active EBNA3C, EBNA2 binding was not detectible above background at the *BACH2, JAK1,* and *CXCR5* sites and that EBNA2 peaks were not observed at these sites by ChIP-seq (i.e., in cells with EBNA3C expression). Thus, not only is EBNA3C able to reduce EBNA2 binding at specific sites to undetectable levels, but EBNA2/EBNA3C co-localization by static ChIP experiments (e.g., Figures III.2 and III.6A), likely underestimates the extent of competition for RBPJ bound sites.

We next examined the specificity of EBNA3A competition with EBNA2 using the EBNA3A-HT LCLs cultured in the presence of 4HT or after 2 weeks of 4HT withdrawal. At EBNA3A bound and regulated genes (*HDAC7* and *CDH1*), we observed decreased EBNA3A ChIP signal upon 4HT withdrawal (Figure III.6B, top panel, right side). These sites lack EBNA2 binding by ChIP-seq, but EBNA2 binding dramatically increased at these locations upon EBNA3A inactivation. By contrast, EBNA3A exerted no effect on RBPJ binding signal. As controls, we examined EBNA3A, EBNA2, and RBPJ binding at the EBNA3C bound and regulated loci (*BACH2, JAK1* and *CXCR5*). At the *BACH2* and *JAK1* sites, no EBNA3A binding was observed, and EBNA3A inactivation had no

discernable effect on EBNA2 or RBPJ binding (Figure III.6B, left side). Notably, *CXCR5* is not EBNA3A regulated, despite being EBNA3A bound (Figure III.6B, top panel; see also Figure III.3). At this *CXCR5* site, we observed a decrease in EBNA3A binding upon 4HT withdrawal, but no corresponding increase in EBNA2 binding. The inability of EBNA3A to affect EBNA2 binding at the *CXCR5* site potentially explains why *CXCR5* is only regulated by EBNA3C, despite being bound by both EBNA3A and EBNA3C (Figure III.3). Thus EBNA3A also appears to compete with EBNA2 for occupancy of specific RBPJ sites in the genome, but not for global access to RBPJ. These results are consistent with a prior report that EBNA3A can regulate EBNA2 binding to the *CXCL9/10* promoter (112), but our results further demonstrate that EBNA3A only limits EBNA2 binding to a subset of RBPJ bound sites where EBNA3A/RBPJ co-binding occurs. Further, as with EBNA3C, the absence of EBNA2 at an EBNA3A/RBPJ co-bound site does not exclude the possibility that EBNA3A regulates EBNA2 binding at that locus.

EBNA3 binding sites co-localize with multiple cell transcription factors

In an effort to identify transcription factors that contribute to EBNA3 binding specificity, we determined cell transcription factor co-occupancy at EBNA3A, EBNA3B, and EBNA3C bound sites using ENCODE transcription factor ChIP-seq data from GM12878 LCLs. RUNX3 (83%), EBF1 (70%), PAX5 (66%), NFIC (63%), ATF2 (60%), BATF (57%), p300 (56%), POU2F2 (54%), FOXM1 (54%), BCL11A (53%), TCF12 (51%), SP1 (50%), and IRF4 (49%) represented the transcription factors with the highest co-localization for EBNA3B (Figure III.7B). Many of the same transcription factors are enriched at EBNA3A (Figure III.7A) and EBNA3C sites (Figure III.7C and (110, 111, 117)).

Because ChIP-seq data is available for only a limited number of transcription factors, we also determined the sequence motifs enriched at EBNA3 bound sites using MEME-ChIP (168). EBNA3B bound sites were enriched for motifs potentially corresponding to ETS, PKNOX2, AP1, KLF4, and RUNX binding sites (Figure III.7D). Notably, we did not observe enrichment for the RBPJ binding motif at EBNA3B bound sites. The RBPJ motif is also not enriched at EBNA3A or EBNA3C bound sites, even though it can be readily detected at EBNA2 bound sites (166, 171).

Our observation that transcription factor and motif enrichment at EBNA3B sites are remarkably similar to those present at EBNA3A and EBNA3C sites is consistent with prior results demonstrating similarity between EBNA3A and EBNA3C bound sites themselves. These results are perhaps not surprising given that many of these sites are bound by more than one EBNA3 and hence many of the same *cis*-acting sites are being reanalyzed for each EBNA3. To overcome this, we repeated our motif analyzes restricting our attention to sites that do not exhibit co-binding with EBNA2 or the other EBNA3s. We initially sought to determine if any shared binding motifs determined a preference for EBNA3 compared to EBNA2 (Figure III.8A). Uniquely bound EBNA2 and EBNA3 sites still shared many common motifs including PU.1 and RUNX; however, enrichment for AP1, NRF1, and IRF4 motifs was specifically observed at EBNA3 bound sites that lacked EBNA2 binding. We extended this approach to sites uniquely bound by only EBNA3A, EBNA3B, or EBNA3C (Figure III.8B). Results for IRF4 were particularly striking as enrichment for IRF4 binding sites and to the IRF4 containing EICE and AICE composite elements was only observed at EBNA3C unique sites. This observation and previous reports

that EBAN3C binding signals are stronger at IRF4 co-bound sites than at EBNA3C sites without IRF4 binding (110), suggested that IRF4 may be especially important for EBNA3C binding. IRF4 enrichment at other EBNA3 bound sites may be a consequence of overlapping binding among the EBNA3s.

IRF4 is essential for EBNA3C binding specificity

We sought to determine the extent to which IRF4 expression contributes to binding of each of the EBNA3 proteins. Establishing the significance of IRF4/EBNA3C co-localization presented a challenge since IRF4 knockdown in LCLs promotes apoptosis and decreases proliferation (182). To circumvent this problem, we stably expressed flagHA tagged EBNA3 proteins in the BJAB lymphoma cell line, which lacks IRF4 expression (Figure III.9). The resulting BJAB-E3A-FH, BJAB-E3B-FH, BJAB-E3C-FH lines expressed epitope tagged EBNA3A, EBNA3B, and EBNA3C proteins at levels comparable to those of LCLs (Figure III.10). Consistent with LMP1 being the principle inducer of IRF4 during latency III gene expression, none of the EBNA3 proteins resulted in detectable IRF4 expression. Each BJAB-EBNA3-FH line was then converted to stable IRF4 expression by retroviral transduction, which resulted in IRF4 levels comparable to that observed in our LCLs (Figure III.10). Using these BJAB stable cell lines, we examined the dependence of EBNA3A, EBNA3B, and EBNA3C binding on IRF4. We initially examined 8 sites that exhibited EBNA3C/IRF4 co-binding in LCLs, including four EICE (*CACNB4*, *GSG2*, *TMEM109*, and *SUB1*) and four AICE (*FOXO3*, *ALPK2*, *TRIB2*, and *PARP9*) sites. In the absence of IRF4 expression, weak EBNA3C binding was observed at some of these locations, particularly *FOXO3*; however, with IRF4 expression, EBNA3C binding was

markedly increased at all AICE and 3 of 4 EICE sites (Figure III.11A). By contrast, IRF4 expression did not result in detectible EBNA3A or EBNA3B binding at any of these sites. Importantly, the one EICE site where EBNA3C binding was absent (*GSG2*), also lacked IRF4 binding by ChIP-qPCR (Figure III.11A, lower panel). Although the reasons for the lack of binding of IRF4 at the *GSG2* are unclear, this probably accounts for absence of EBNA3C binding at this site and further reinforces the notion that IRF4 plays a critical role in targeting EBNA3C to chromatin.

In order to confirm that these AICE and EICE containing sites represented authentic EBNA3C binding sites, we performed additional HA ChIPs in the EBNA3C-F-HA LCL. As shown in Figure III.11B, EBNA3C binding was observed at all eight of these sites, including the *GSG2* site, but not at a site near the *PPIA* gene which has been used in previous EBNA3 ChIP studies as a negative control (117). We additionally confirmed IRF4 binding at each of these sites by ChIP, albeit at low levels at the *GSG2*, *ALPK2*, and *TRIB2* sites which were nevertheless significantly above the PPIA control site ($p < 0.004$, two sample t-test).

Banerjee S *et. al.* had previously mapped the domain of EBNA3C that is required for interacting with IRF4 (183). In this study, they initially performed GST-pulldown assays using in-vitro translated, full length, and truncated EBNA3C mutant fragments followed by co-incubation with bacterially expressed and purified GST-IRF4, in which they identified amino acid 130–159 residues of EBNA3C as showing the highest binding affinity for IRF4. They further showed that mutating Phenylalanine 144 to Alanine (F144A) of EBNA3C dramatically reduced its interaction with IRF4. Given this result, we determined to

investigate whether EBNA3C_F144A mutant would have any binding defect at the AICE and EICE sites in our BJAB with IRF4 expression. In order to do this experiment, we first cloned the pCEP-EBNA3CF144A-FHA plasmid which contains the Phenylalanine 144 to Alanine (F144A) mutation of EBNA3C. Then we transfected this expression plasmid into BJAB cells stably expressing IRF4, and selected stable cell line with hygromycin. The stable BJAB cell line expresses the mutant version of EBNA3C that is deficient for IRF4 binding at the level comparable to wild type EBNA3C as in BJAB EBNA3C-F-HA cell line, showing by HA western blot (figure III.12).

Using these BJAB cell lines, we performed HA ChIP-qPCR to examine wild type EBNA3C versus EBNA3C_F144A mutant binding at EICE (*CACNB4, GSG2, TMEM109,* and *SUB1*) and four AICE (*FOXO3, ALPK2, TRIB2,* and *PARP9*) sites in the presence of IRF4. We also examined three sites that are bound by EBNAC but not IRF4 as controls (*BACH2, RAPH1, TP53I3*). As shown in Figure III.13, there was a significant decrease of EBNA3C mutant binding to all four EICE and AICE sites compared with wild type EBNA3C. However, at the three control sites where IRF4 were not co-bound with EBNA3C, the binding of EBNA3C_F144A mutant were largely unaltered compared to wild type EBNA3C. Taken together, these results demonstrated that EBNA3C interaction with IRF4 is likely to be responsible for the specificity of EBNA3C binding to EICE and AICE sites.

To more thoroughly evaluate the dependence of EBNA3A and EBNA3B binding on IRF4 we did additional ChIP experiments using the BJAB-E3A-FH and BJAB-E3B-FH cells. We first considered 4 sites that are co-bound by EBNA3A and IRF4 in LCLs (*CDH1, HDAC7, BLK,* and *CCDC80*). In the absence of IRF4 expression, there was detectible

binding above the control PPIA site at each of these four locations (Figure III.14A). However, we observed no detectible change in EBNA3A binding with IRF4 co-expression. Additional ChIP-qPCR experiments confirmed IRF4 binding at each site (Figure III.14A, bottom panel). Using the BJAB-E3B-FH cells we examined binding to four EBNA3B/IRF4 co-bound sites (*CTLA4*, *SHQ1*, *BLK*, and *SYTL3*). Similar to our results for EBNA3A, binding was above the *PPIA* control site at each location, but there was no observed increase in EBNA3B binding with IRF4 co-expression. We confirmed IRF4 binding was detectible at each site by ChIP-qPCR (Figure III.14B, bottom panel). Taken together, our data provided direct evidence that IRF4 specifically contributes to EBNA3C binding. By contrast, despite significant overlap between IRF4 and EBNA3A or EBNA3B binding sites, we find no evidence that IRF4 contributes to EBNA3A or EBNA3B binding at any IRF4 co-bound site examined in this study.

Discussion

In this chapter we report a comprehensive survey of the genome-wide binding of EBNA3 proteins in LCLs. We believe our approach offers several advantages over prior studies, including distinguishing among EBNA3A, EBNA3B, and EBNA3C binding on a genome-wide basis. In addition, using the same epitope tag to ChIP each EBNA3 protein avoids confounding effects of differences in antibody sensitivity and specificity when different sera are used for each EBNA3. Furthermore, as our BJAB/IRF4 experiments highlight, EBNA3 binding is a function of the cell's transcription factor milieu. Thus, the best opportunity to understand the role of EBNA3 proteins in the transformation of resting B lymphocytes into LCLs is afforded by binding data obtained from LCLs. These results have revealed important mechanistic insights into the role of EBNA3s in LCL gene regulation. We find that EBNA3A, EBNA3B, and EBNA3C bind to distinct, partially overlapping genome sites, a phenomenon that almost certainly underlies their ability to regulate partially overlapping gene subsets. Second, we demonstrate that EBNA3A and EBNA3C can regulate EBNA2 binding at unique RBPJ co-bound sites. Importantly, we provide direct evidence that IRF4 is a critical determinant of EBNA3C binding, but does not affect EBNA3A or EBNA3B binding in BJAB cells. This represents a significant advance in our understanding of the mechanism by which EBNA3C regulates cell gene expression, but also supports a more general model where differences in EBNA3 binding specificity are conferred by interactions with cell transcription factors other than RBPJ.

The precise role played by RBPJ in EBNA3 function remains controversial despite extensive study. Since the initial discovery that EBNA3s, like EBNA2, target RBPJ,

numerous studies have confirmed that EBNA3s are highly associated with RBPJ in LCLs (94, 103, 181). Each EBNA3 forms a distinct RBPJ complex (98), though there is some evidence to suggest that these may interact with each other (154, 184). Despite this high degree of association, our ChIP-seq results and those of others reveal that only a minority of EBNA3 bound sites are co-bound by RBPJ. This limited overlap and the observation that EBNA3s can disrupt RBPJ binding to DNA by EMSA have led to the interpretation that the RBPJ interaction is not involved in EBNA3 binding to chromatin (99, 110). Several lines of evidence suggest this is not the case. In a detailed study of EBNA3A regulation of the *CXCL9/CXCL10* locus, RBPJ expression was demonstrated to be critical for EBNA3A binding to this bidirectional promoter (112). Further, EBNA3A and EBNA3C mutants defective for RBPJ interaction are unable to regulate the *CDKN2A* gene or support LCL growth. Thus, a model where RBPJ is recruited to DNA by EBNA3s (and not vice versa) seems improbable since neither EBNA3A nor EBNA3C can compensate for the loss of the other in *CDKN2A* regulation (96, 108, 109). Finally, data presented in Figure III.6 of this chapter demonstrate that EBNA3A or EBNA3C inactivation produces a dramatic change in EBNA2 binding at multiple genomic sites, without significant effect on RBPJ binding. This result, and the specificity with which EBNA3A and EBNA3C regulate RBPJ bound sites, suggests that EBNA3s are targeted to distinct RBPJ sites via interactions with RBPJ and other cell transcription factors. In this model, the requirement for both EBNA3A and EBNA3C to interact with RBPJ to perform unique roles in *CDKN2A* co-regulation is readily explained if they target two distinct RBPJ sites.

Our observation that EBNA3-EBNA2 competition occurs at RBPJ sites where there

is no apparent EBNA2 binding in LCLs has important implications. This finding underscores the ability of EBNA3 proteins to successfully compete for RBPJ bound sites despite the weaker correlation between EBNA3s and RBPJ binding compared to EBNA2. Whether EBNA3 competition for RBPJ affects the ability of Notch to signal in LCLs is an important, unresolved question. In addition, our results imply that the degree to which EBNA3 and EBNA2 compete for genomic sites is underestimated by static ChIP-seq experiments. Thus, gene repression due to binding at EBNA3 “only” sites may still be attributable to impaired (abrogated) EBNA2 binding. This phenomenon may explain the recent discovery that the increased transforming effects of EBNA2 from type I EBV compared to type II EBV are due to increased binding of EBNA2 at ETS/IRF4 sites (171). The "novel" binding sites observed with type I EBNA2 may actually be due to an enhanced ability to compete with EBNA3C for binding at ETS/IRF4 sites. Given the strong transcriptional activation properties of EBNA2, effective competition for RBPJ by EBNA3s should almost always result in repression of target cell genes. At non-RBPJ sites, EBNA3s likely target chromatin via the same factors that determine RBPJ subset specificity. Since competition for EBNA2 binding is infrequent at these sites, EBNA3 binding may cause either activation or repression, depending on chromatin context (Figure III.15).

The finding that IRF4 expression is a critical mediator of EBNA3C binding to specific genome sites represents an important advance in our understanding of EBNA3 binding specificity. Although IRF4/EBNA3C co-binding has been previously reported, the significance of this correlation remained to be demonstrated. Indeed, other transcription factors, including RUNX3 and ATF2 were more strongly correlated with EBNA3C bound

sites. Moreover, EBNA3A and EBNA3B bound sites are also enriched for IRF4 binding (Figures III.7A/7B and (173)). However, some lines of evidence suggested that the IRF4 interaction might be more important for EBNA3C, including the increased EBNA3C binding signals at IRF4 sites compared to non-IRF4 sites and the ability of EBNA3C to bind directly to IRF4 and promote its stabilization (110, 183). When we restricted our analysis to sites uniquely bound by EBNA3A or EBNA3B or EBNA3C, we only observed enrichment for the IRF4 binding motif in the EBNA3C subset. Using an IRF4 negative BJAB cell line, we provide experimental evidence that IRF4 is determinative of EBNA3C binding. In the absence of IRF4 expression, we observed little to no EBNA3C binding signal at genomic sites normally co-bound by EBNA3C and IRF4 in LCLs. Upon IRF4 expression at levels comparable to that seen in LCLs, EBNA3C binding was readily detected. This occurs at both AP1/IRF4 and ETS/IRF4 composite elements (AICEs and EICEs, respectively). By contrast, at sites co-bound by EBNA3A/IRF4 or EBNA3B/IRF4 in LCLs, we observed no increase in EBNA3A or EBNA3B binding, respectively upon IRF4 expression. It is important to note that EBNA3C binding was only observed by ChIP-seq at two of the EBNA3B/IRF4 sites (*SHQ1* and *STYL3*) and none of the EBNA3A/IRF4 sites. Thus, IRF4 binding alone does not appear sufficient to confer EBNA3C binding to chromatin. Nevertheless, these results provide strong evidence that IRF4 is a critical mediator of EBNA3C binding specificity. Furthermore, this finding lends implicit support for the model that other cell transcription factors underlie EBNA3A and EBNA3B binding specificity.

The dependence of EBNA3C on IRF4 is further demonstration of EBV targeting of intrinsic B lymphocyte growth and survival pathways. IRF4 suppression of

BCL6 and PAX5 is critical event for B lymphocyte exit from germinal center reactions (185, 186). Further increases in IRF4 expression upregulate PRDM1 (Blimp1) and XBP1 expression, promoting differentiation into antibody secreting plasma cells. Although we do not currently know the extent to which EBNA3C effects depend on IRF4, transcriptional profiling studies suggest that they co-regulate many transcription factors responsible for B cell fate, including repression of PAX5, BACH2, NFATC1, SPIB, EBF1, and IL7R and activation of PRDM1 (BLIMP1), AICDA and IL6R (116, 118, 187). This suggests that many key EBNA3C transcriptional effects are dependent on IRF4 and/or EBNA3C accentuates the IRF4 program. In addition to its role in follicular B cell differentiation, IRF4 has also been found to play a role in marginal zone B cell development (188). Marginal zone B cells are unique among B cell subsets in their dependence on Notch signaling and respond rapidly to blood borne pathogens (189, 190). Interestingly, IRF4 null mice exhibited both increased NOTCH2 expression and enhanced ICN activation in response to CD40 and BCR signaling (188). Although the mechanism of this latter effect is incompletely defined, it suggests that EBNA3C targeting of IRF4 may have been selected for, in part, to limit ICN-like effects due to EBNA2. Given the central role of Notch signaling and especially RBPJ in EBNA3 effects, cell transcription factors that modulate Notch signaling in B cells are attractive candidates for transcription factors that, like IRF4, determine EBNA3 specificity.

Table III.1

	Total Reads	Human	Called peaks	DHS filter
EBNA3A	59,941,027	8,832,593 (15%)	1640	1064
EBNA3B	71,646,718	6,989,005 (10%)	3033	2648
EBNA3C	105,734,958	8,639,412 (8 %)	3588	1802
*EBNA2	12,947,095	4,883,146 (34%)	8592	7772
RBPJ Rep1	125,720,183	4,577,382 (36%)	4225	3329
*RBPJ Rep2	13,382,267	7,284,453 (54%)	8348	7526
RBPJ total			9938	8294

Table III.1: Summary of ChIP-seq read alignment and peak calling.

For each ChIP-seq experiment, total reads, total reads aligned to human genome, and number of called peaks are indicated. Two of these datasets (indicated with an *) have been previously reported (166), but are reanalyzed here for comparison. The peaks called from initial data processing are further filtered based on their overlapping with the DNase hypersensitivity site (DHS) reported from ENCODE project.

Figure III.1

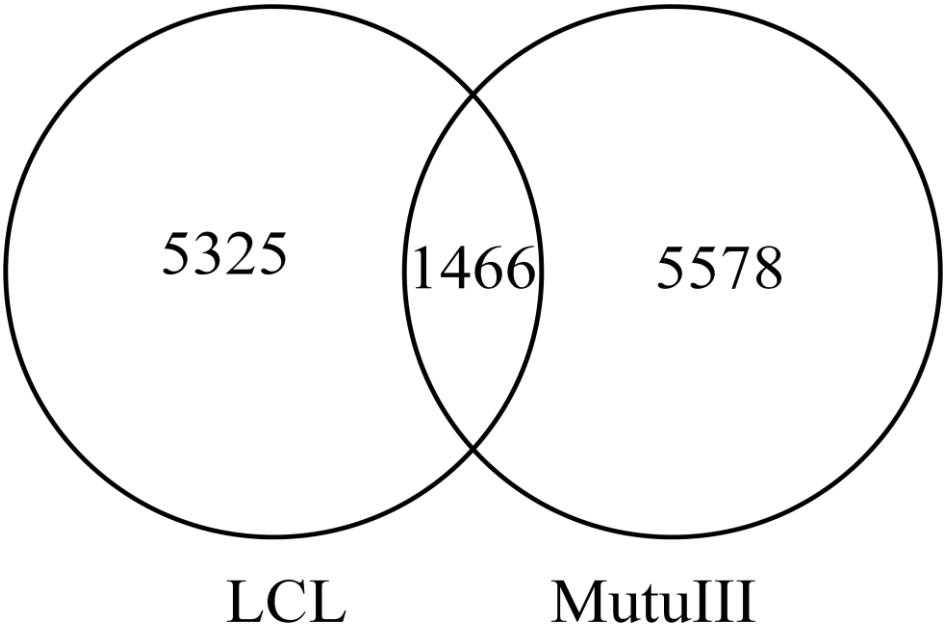

Figure III.1: Overlap of EBNA3 binding peaks with previously published data.

A total number of 6791 EBNA3A, EBNA3B and EBNA3C bound sites (pooled sites from three ChIP-seq datasets) identified by our ChIP-seq experiments (LCL) is indicated in the left circle. A total number of 7044 EBNA3 proteins bound sites from previous published data (113) is indicated in the right circle (MutuIII). 1466 bound sites overlap between our data and previously published data, which is defined by sharing one or more 200 bp bin.

Figure III.2

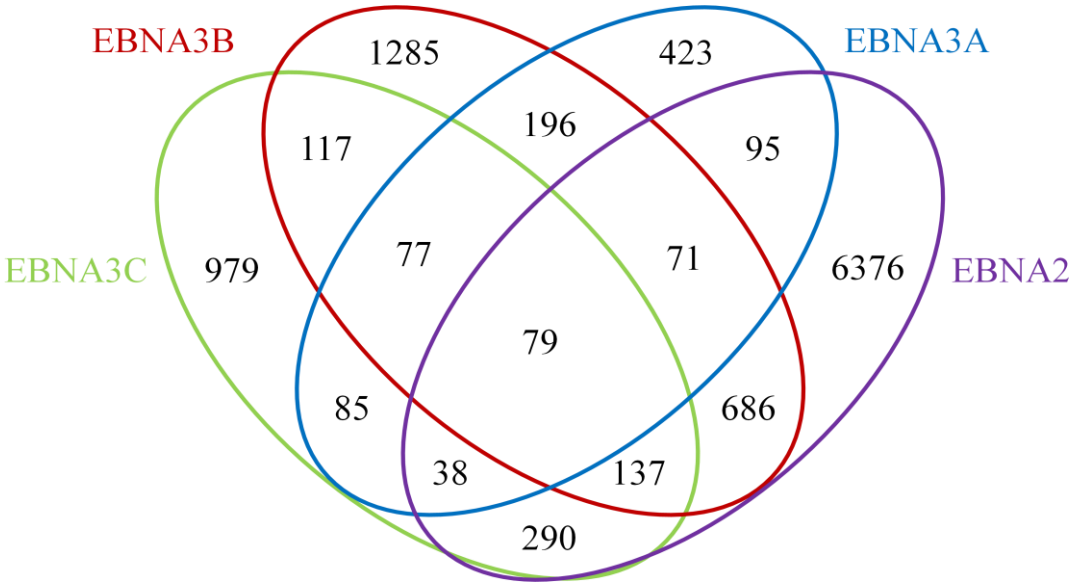

Figure III.2: Venn diagram showing co-localization of EBNA3A, EBNA3B, EBNA3C and EBNA2 binding sites in LCLs. Sites on the human genome bound by EBV EBNA proteins were identified from ChIP-seq data as peaks relative to input using MOSAiCS. Numbers of bound sites and their extent of overlap are indicated for EBNA2 (purple circle), EBNA3A (blue circle), EBNA3B (red circle) and EBNA3C (green circle).

Figure III.3

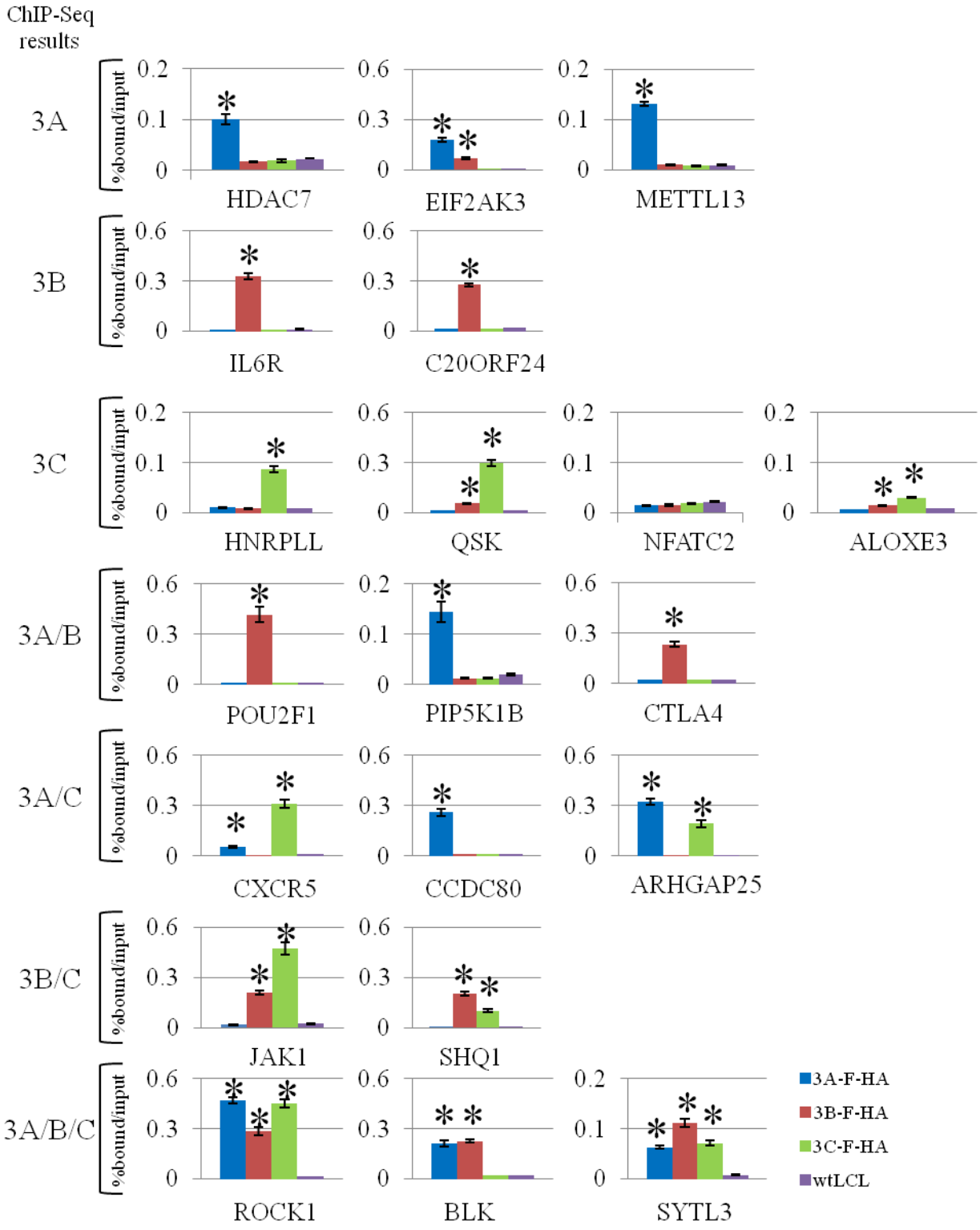
ChIP-Seq results
3A
3B
3C
3A/B
3A/C
3B/C
3A/B/C
%bound/input
HDAC7
EIF2AK3
METTL13
IL6R
C20ORF24
HNRPLL
QSK
NFATC2
ALOXE3
POU2F1
PIP5K1B
CTLA4
CXCR5
CCDC80
ARHGAP25
JAK1
SHQ1
ROCK1
BLK
SYTL3
3A-F-HA
3B-F-HA
3C-F-HA
wtLCL

Figure III.3: ChIP-qPCR validation of EBNA3 binding sites in LCLs identified by ChIP-seq. Bar plots showing enrichment genomic DNA from ChIP of EBNA3A, EBNA3B, or EBNA3C relative to input. Each EBNA3 was specificaly ChIPed using HA antibody with either the EBNA3A-F-HA, EBNA3B- F-HA, EBNA3C-F-HA LCL and wild type (untagged) LCLs as a negative control. Genomic loci were chosen based on the peak patterns observed by ChIP-seq and included EBNA3A only peaks (*HDAC7*,*EIF2AK3* and *METTL13*), EBNA3B only peaks *(IL6R* and *C20ORF24*), EBNA3C only peaks (*HNRPLL, QSK, NFATC2* and *ALOXE3*), EBNA3A and EBNA3B co-bound peaks (*POU2F1, PIP5K1B* and *CTLA4*), EBNA3A and EBNA3C co-bound peaks (*CXCR5, CCDC80* and *ARHGAP25*), EBNA3B and EBNA3C co-bound peaks (*JAK1* and *SHQ1*), EBNA3A, EBNA3B and EBNA3C co-bound peaks (*ROCK1, BLK* and *SYTL3*). All qPCR signals are reported as percentage of ChIPed DNA relative to input DNA. Results are shown as mean ± SEM of three independent experiments. Asterisk indicates a p-value < 0.05 by two sample t-test.

Figure III.4

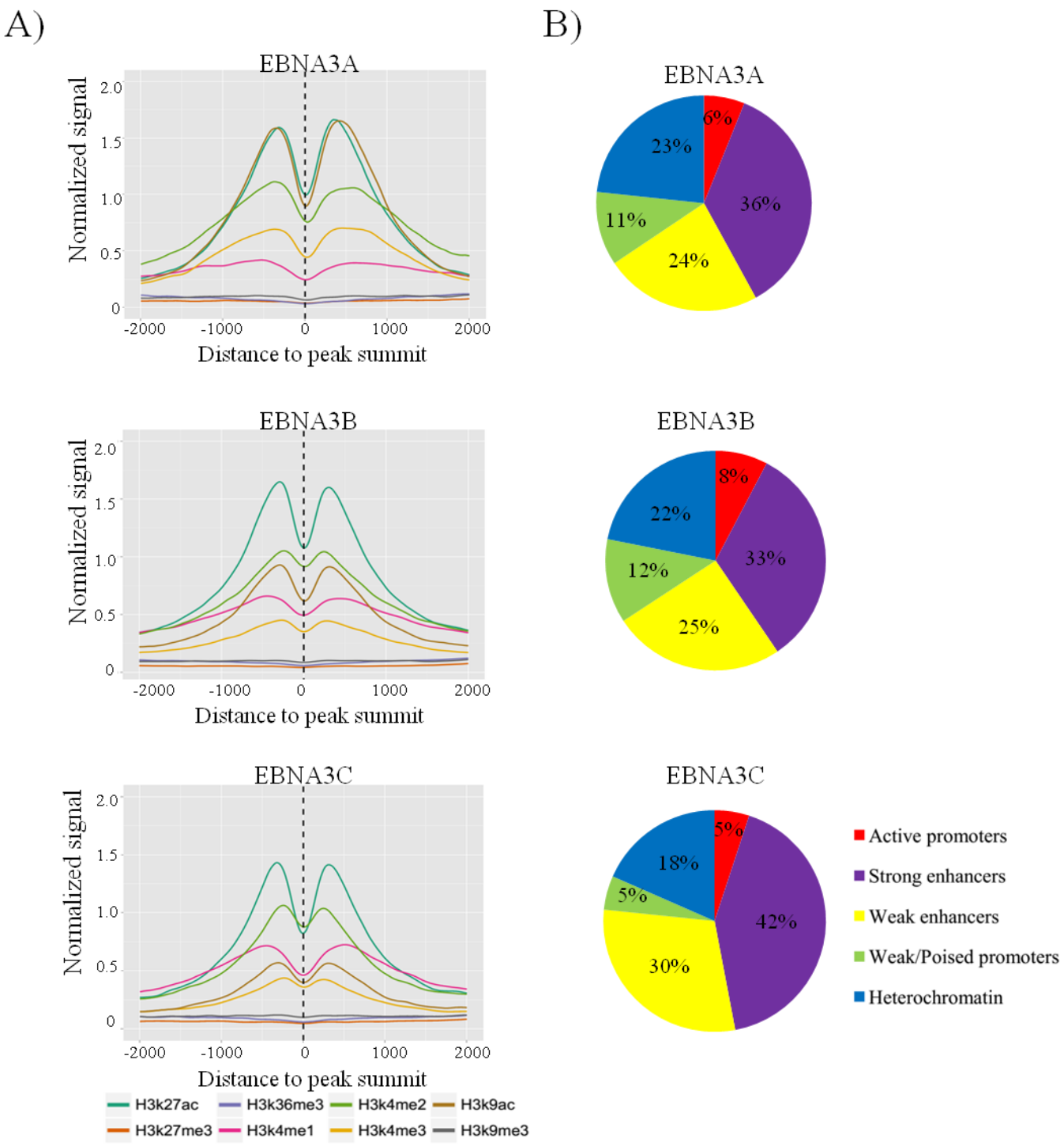
A)
B)
EBNA3A
Normalized signal
2.0
1.5
1.0
0.5
0
-2000
-1000
0
1000
2000
Distance to peak summit
EBNA3B
Normalized signal
Distance to peak summit
EBNA3C
Normalized signal
Distance to peak summit
H3k27ac
H3k36me3
H3k4me2
H3k9ac
H3k27me3
H3k4me1
H3k4me3
H3k9me3
EBNA3A
6%
36%
24%
11%
23%
EBNA3B
8%
33%
25%
12%
22%
EBNA3C
5%
42%
30%
5%
18%
Active promoters
Strong enhancers
Weak enhancers
Weak/Poised promoters
Heterochromatin

Figure III.4: Characterization of EBNA3 bound sites. A) Average histone profile plots for EBNA3A, EBNA3B, and EBNA3C bound sites. The average density of ChIP-seq reads for the indicated histone modifications are plotted for ±2 kb window around the summits of the indicated EBNA3 bound sites. Normalized signal strength of each histone modification was derived from ChIP-seq datasets from GM12878 LCLs downloaded from the ENCODE database and is reported in reads per kilobase per million mapped reads (RPKM) for each curve. B) Pie chart showing the proportion of EBNA3A, EBNA3B, or EBNA3C bound sites located within different functional chromatin domains as defined by Ernst, et al. (180)

Figure III.5

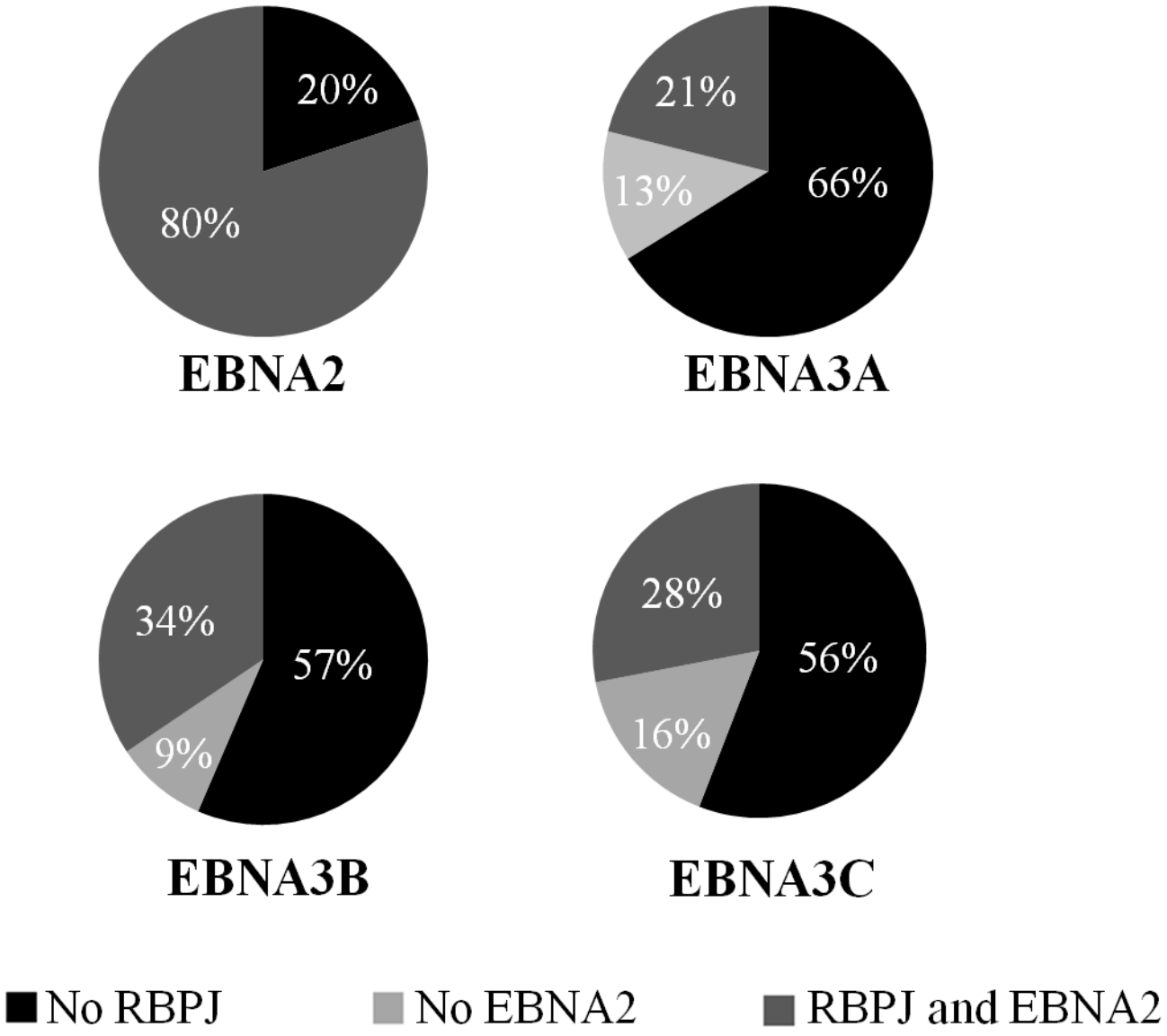

Figure III.5: The extent of RBPJ co-localization with EBNA proteins. Pie chart summarizing extent of EBNA2 and RBPJ, and EBNA3 co-binding in LCLs. For EBNA3 charts, percent of peaks exhibiting RBPJ and EBNA2 co-binding (dark gray) as well as RBPJ co-binding without EBNA2 (light gray) is indicated.

Figure III.6A

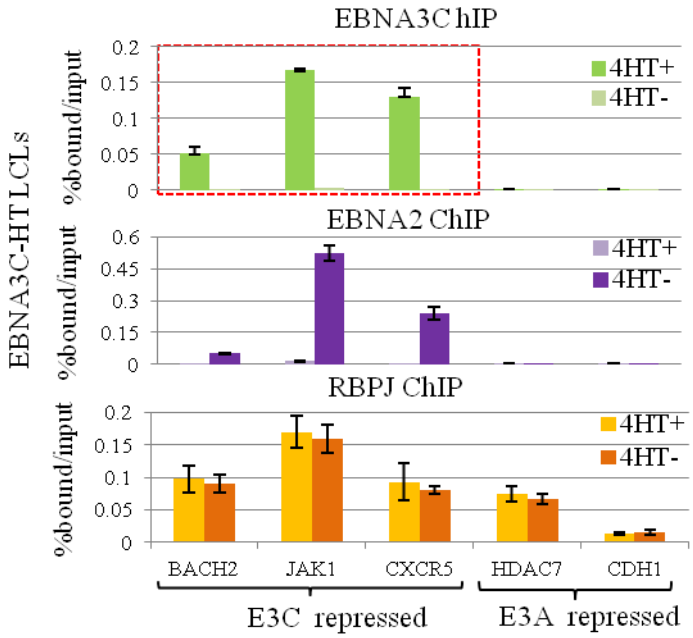

Figure III.6B

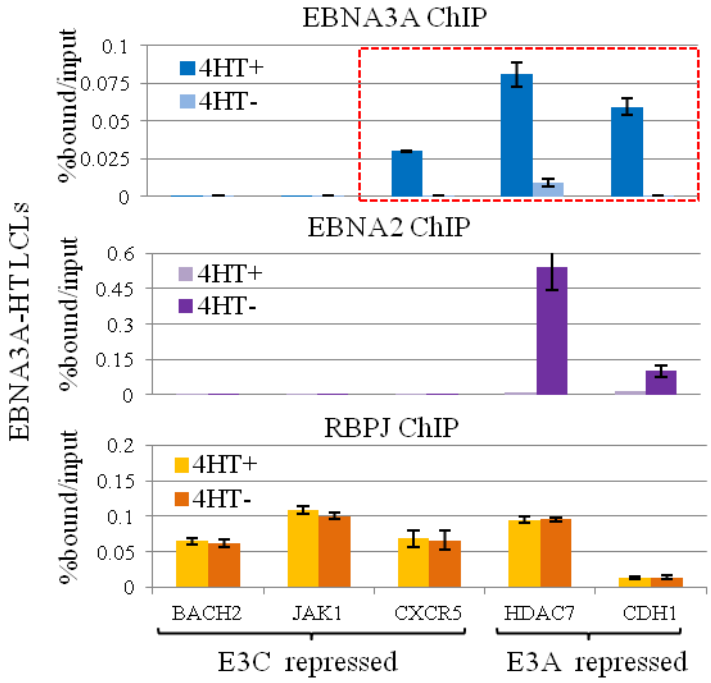

Figure III.6: Regulation of EBNA2 binding by EBNA3A or EBNA3C at specific RBPJ sites. A) EBNA3C, EBNA2 and RBPJ binding determined by ChIP-qPCR at the indicated loci in EBNA3C-HT LCLs cultured in the presence (4HT+) or absence (4HT-) of 4-hydroxytamoxifen for two weeks. Genomic loci included RBPJ binding sites near EBNA3C repressed genes (*BACH2, JAK1, CXCR5*) or EBNA3A repressed genes (*HDAC7* and *CDH1*) as indicated. The red dashed line indicates sites bound by EBNA3C from ChIP-seq data. All qPCR signals are reported as percentage of ChIPed DNA relative to input DNA. Results are shown as mean ± SEM of three independent experiments. B) Analogous experiment to that described in (A) using the EBNA3A-HT LCL. EBNA3A, EBNA2, and RBPJ binding were determined by ChIP-qPCR at the indicated sites in the presence or absence of 4-hydroxytamoxifen. The red dashed line indicates sites bound by EBNA3A from ChIP-seq data.

Figure III.7A

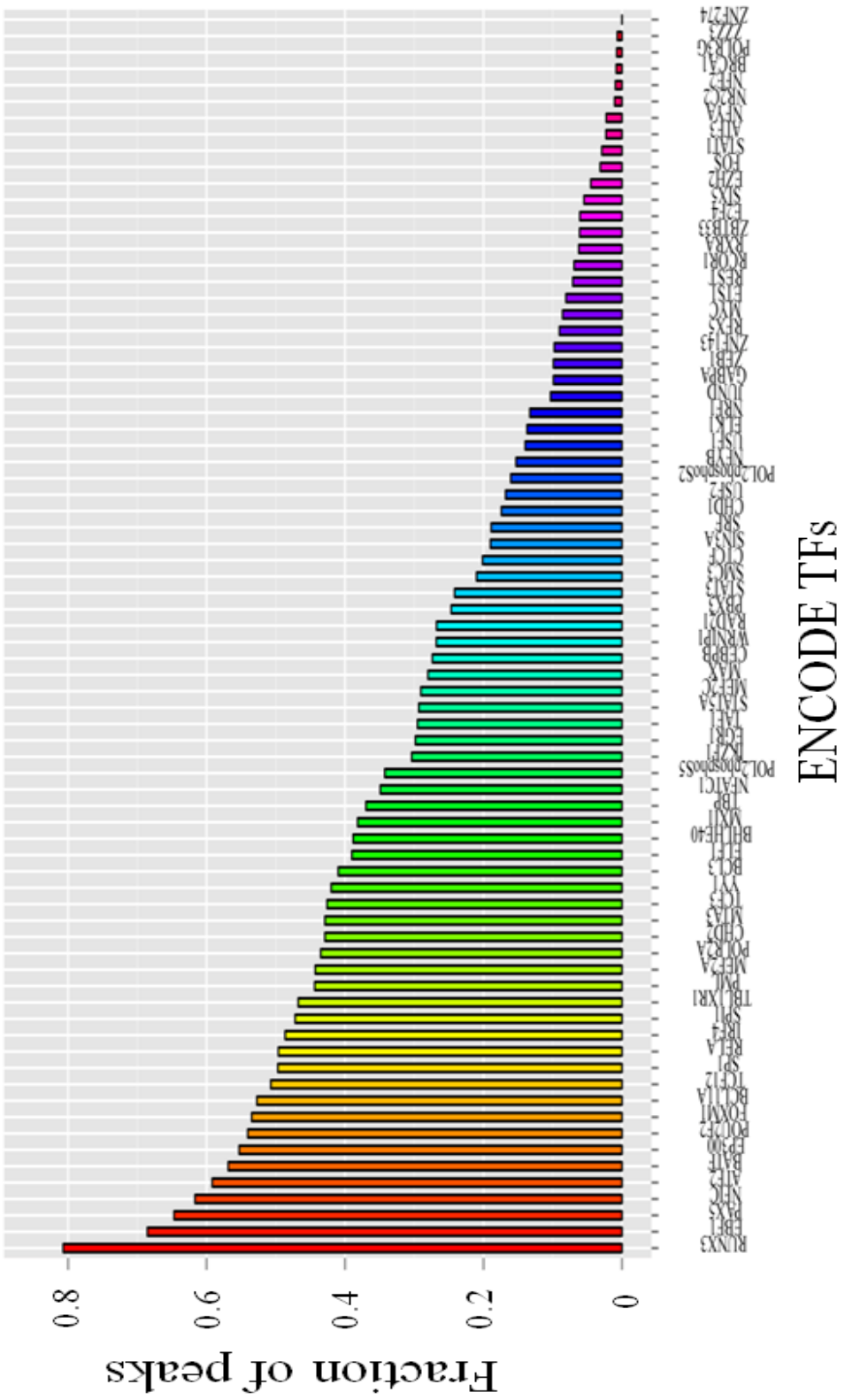

Figure III.7B

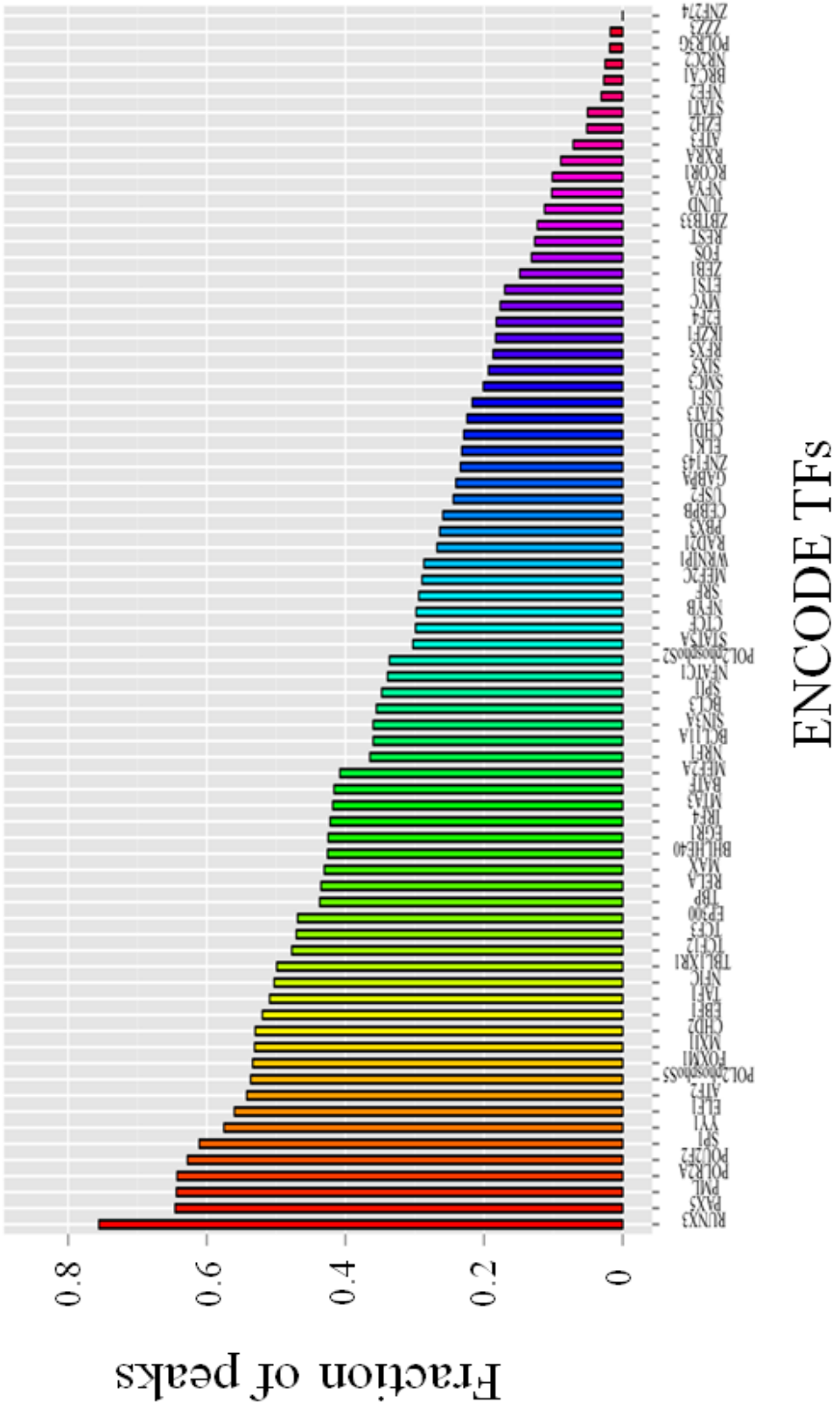

Figure III.7C

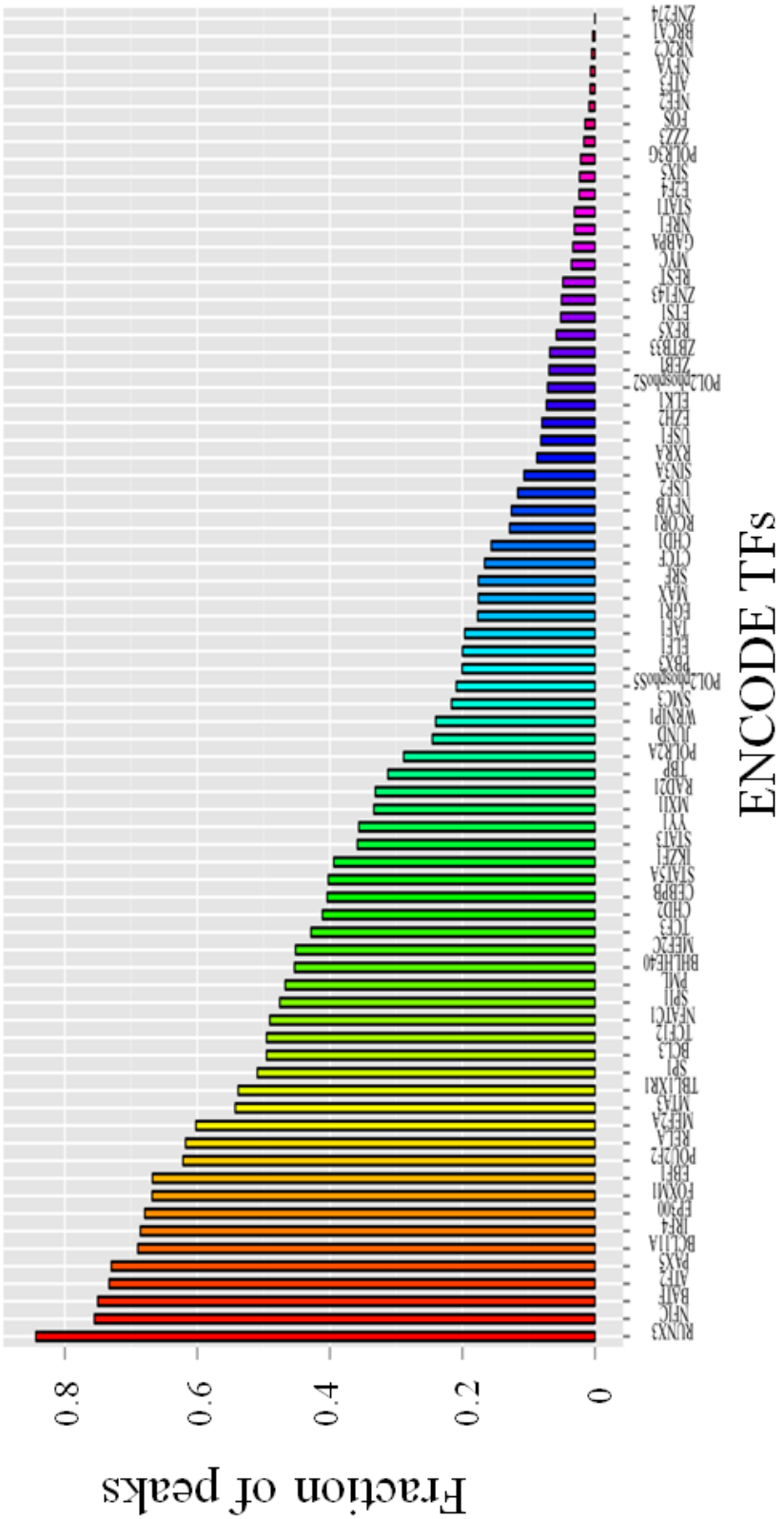

Figure 7D

EBNA3A

Motif sequence	P-value	Predicted TF
	3.2e-24	EGR1

EBNA3B

Motif sequence	P-value	Predicted TF
	5.9e-72	ETS family
	1.1e-29	–
	1.4e-20	PKNOX2
	3.0e-15	AP1 family
	5.0e-14	KLF4
	5.3e-13	RUNX

EBNA3C

Motif sequence	P-value	Predicted TF
	1.2e-30	–
	2.3e-24	AP1 family
	6.0e-21	EICE
	1.2e-20	IRF4
	4.0e-20	RUNX
	3.7e-12	ETS family

Figure III.7: Transcription factor co-binding and motif enrichment at EBNA3B bound sites. Bar plot showing the fraction of A) EBNA3A, B) EBNA3B and C) EBNA3C peaks co-associated with the indicated transcription factors (X-axis). Co-localization was defined as binding with 200 bp of EBNA3B bound sites and cell transcription factor binding locations were derived from ENCODE ChIP-seq data for 76 transcription factors in the GM12878 LCL. D) EBNA3A, EBNA3B and EBNA3C bound sites were analyzed for enriched motifs using MEME-ChIP. The motifs with the lowest p-values are indicated as well as any transcription factors predicted to recognize them.

Figure III.8

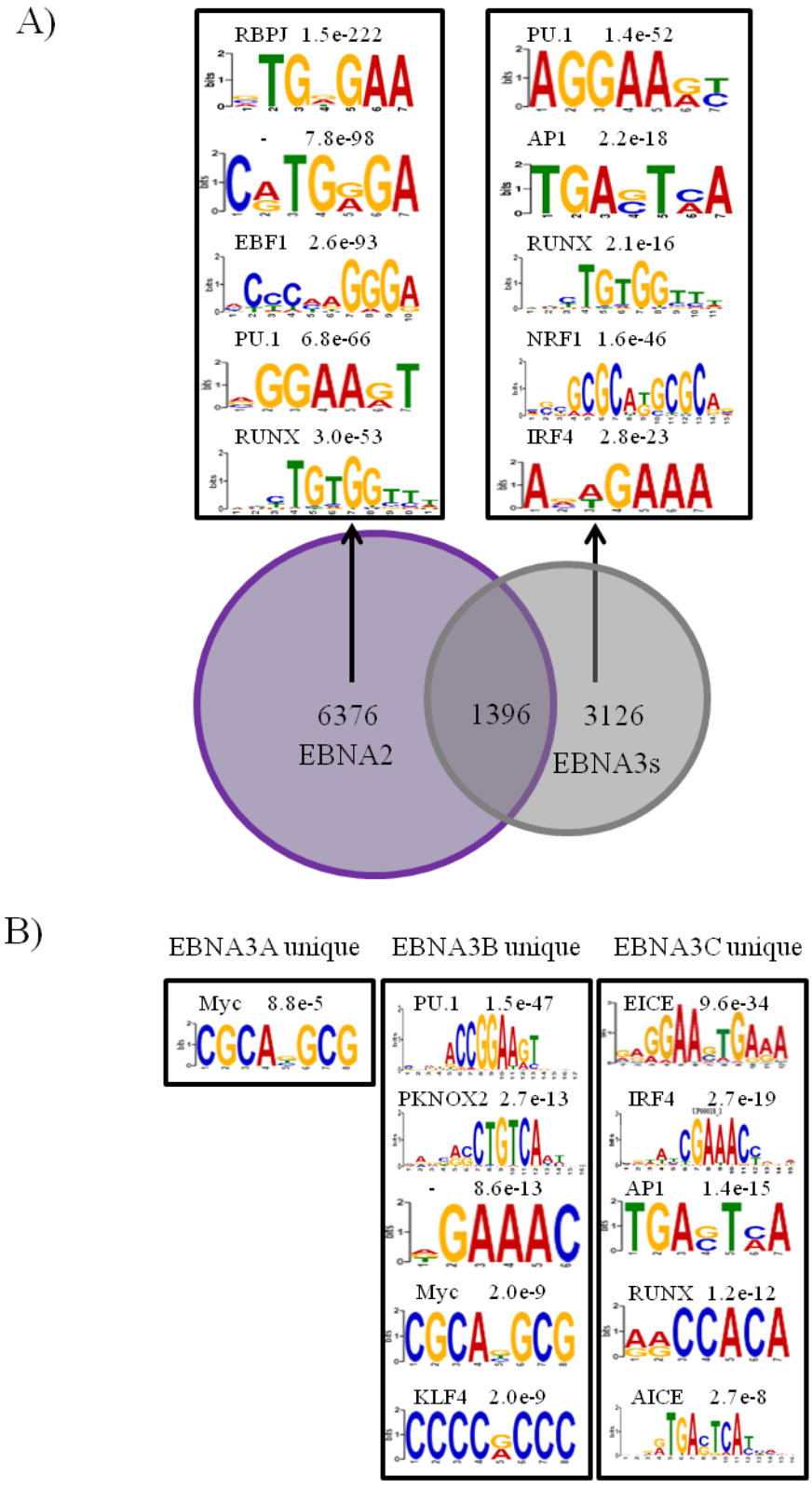
A)
RBPJ 1.5e-222
- 7.8e-98
EBF1 2.6e-93
PU.1 6.8e-66
RUNX 3.0e-53
PU.1 1.4e-52
AP1 2.2e-18
RUNX 2.1e-16
NRF1 1.6e-46
IRF4 2.8e-23
6376
EBNA2
1396
3126
EBNA3s
B)
EBNA3A unique
EBNA3B unique
EBNA3C unique
Myc 8.8e-5
PU.1 1.5e-47
PKNOX2 2.7e-13
- 8.6e-13
Myc 2.0e-9
KLF4 2.0e-9
EICE 9.6e-34
IRF4 2.7e-19
AP1 1.4e-15
RUNX 1.2e-12
AICE 2.7e-8

Figure III.8: Enriched motifs at sites bound uniquely by one EBNA protein.

A) Venn diagram summarizing the overlap of EBNA2 binding sites with sites bound by any EBNA3. Enriched motifs at sites bound only by EBNA2 (left box) or bound by any EBNA3, but not by EBNA2 (right box) are indicated with corresponding p-values and names of any matching transcription factors. B) Motifs enriched at sites bound uniquely by EBNA3A, EBNA3B and EBNA3C (but not by EBNA2 or another EBNA3) are indicated along with corresponding p-values and matching transcription factors.

Figure III.9

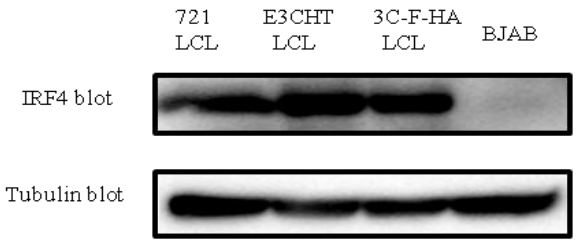

Figure III.9: Western blot for IRF4 expression levels in multiple B cell lines. Western blots for IRF4 (top panel) and tubulin (bottom panel) were done on whole cell lysates from the indicated B cell lines to identify candidate cell lines lacking detectible IRF4 expression. Each lane represents whole cell lysates from 10^6 cells.

Figure III.10

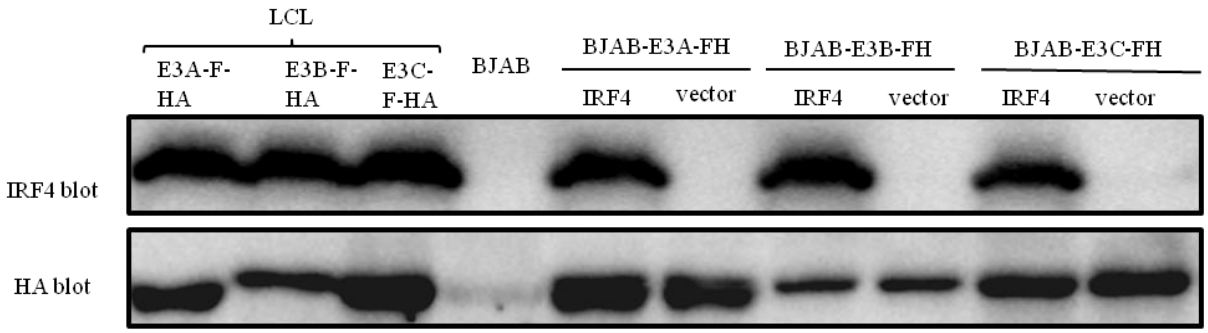

Figure III.10: Characterization of BJAB stably expressing flag-HA tagged EBNA3A, EBNA3B, or EBNA3C with or without IRF4. Western blots for IRF4 (top panel) and HA (bottom panel) were done in BJAB clones expressing EBNA3A-FHA, EBNA3B-FHA, EBNA3C-FHA with either IRF4 or vector control. For comparison LCLs expressing EBNA3A-FHA, EBNA3B-FHA, EBNA3C-FHA are shown (left 3 lanes). Each lane represents whole cell lysate from 10^6 cells.

Figure III.11

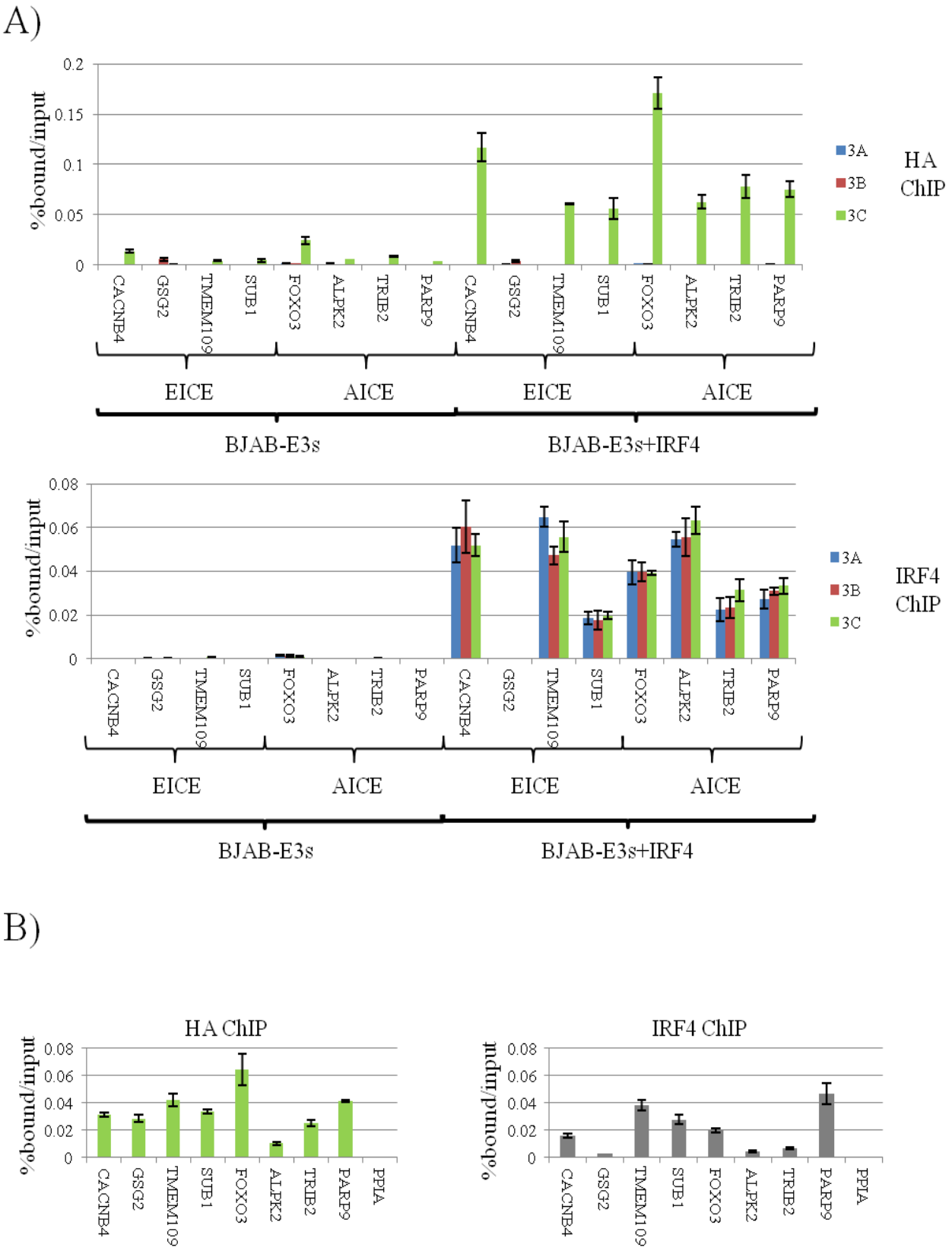

Figure III.11: IRF4 is essential for EBNA3C binding to specific sites in the human genome. A) Top panel: ChIP-qPCR experiment demonstrating extent of EBNA3A (blue), EBNA3B (red), or EBNA3C (green) binding in BJAB cells expressing either flagHA tagged EBNA3A, EBNA3B, or EBNA3C with or without stably co-expressed IRF4. Loci where chosen that exhibited EBNA3C and IRF4 co-binding in LCLs and conformed to ETS/IRF4 composite elements (EICE) or AP1/IRF4 composite elements (AICE), as indicated. Bottom panel: ChIP-qPCR demonstrating IRF4 binding at the same sites. B) ChIP-qPCR assay demonstrating extent of EBNA3C (left panel) and IRF4 (right panel) binding to the indicated EICE and AICE sites in EBNA3C-F-HA LCLs.

Figure III.12

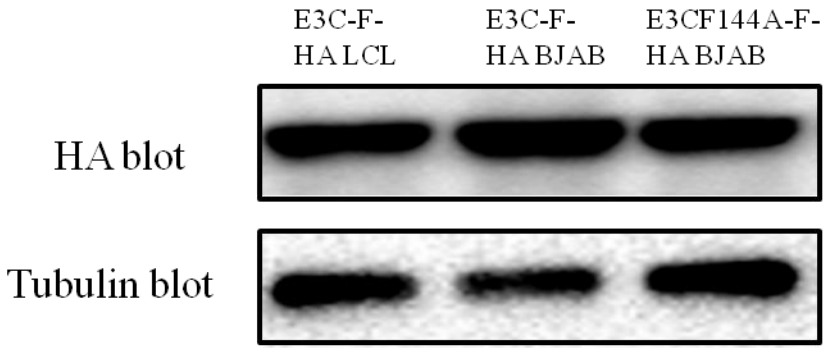

Figure III.12: Characterization of BJAB stably expressing flag-HA tagged wild type EBNA3C versus EBNA3C mutant. Western blots for HA (top panel) and tubulin (bottom panel) were done in E3C-F-HA LCL, BJAB clones expressing wild type EBNA3C (E3C-F-HA BJAB) and mutant EBNA3C (E3CF144A-F-HA BJAB). Each lane represents whole cell lysates from 10^6 cells.

Figure III.13

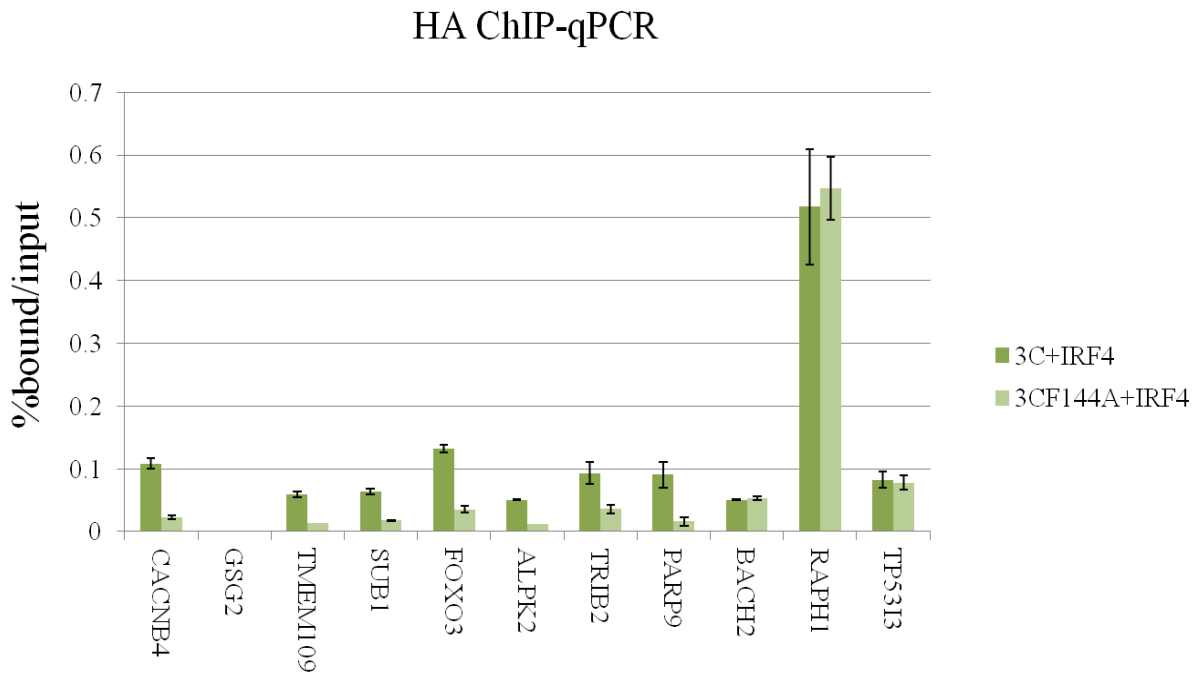

Figure III.13: IRF4 interaction is required for EBNA3C binding at EIAE and AICE sites in the human genome. Bar plot showing the ChIP-qPCR assay for the occupancies of wild type EBNA3C (dark green) and EBNA3C mutant that is deficient for IRF4 interaction (light green) in BJAB cells expressing IRF4. Binding was assessed at multiple sites that exhibited EBNA3C and IRF4 co-binding in LCLs and conformed to ETS/IRF4 composite elements (EICE) or AP1/IRF4 composite elements (AICE), and sites that are bound by EBNA3C without IRF4 co-bound as indicated. Results are shown as mean ± SEM of three independent experiments.

Figure III.14A

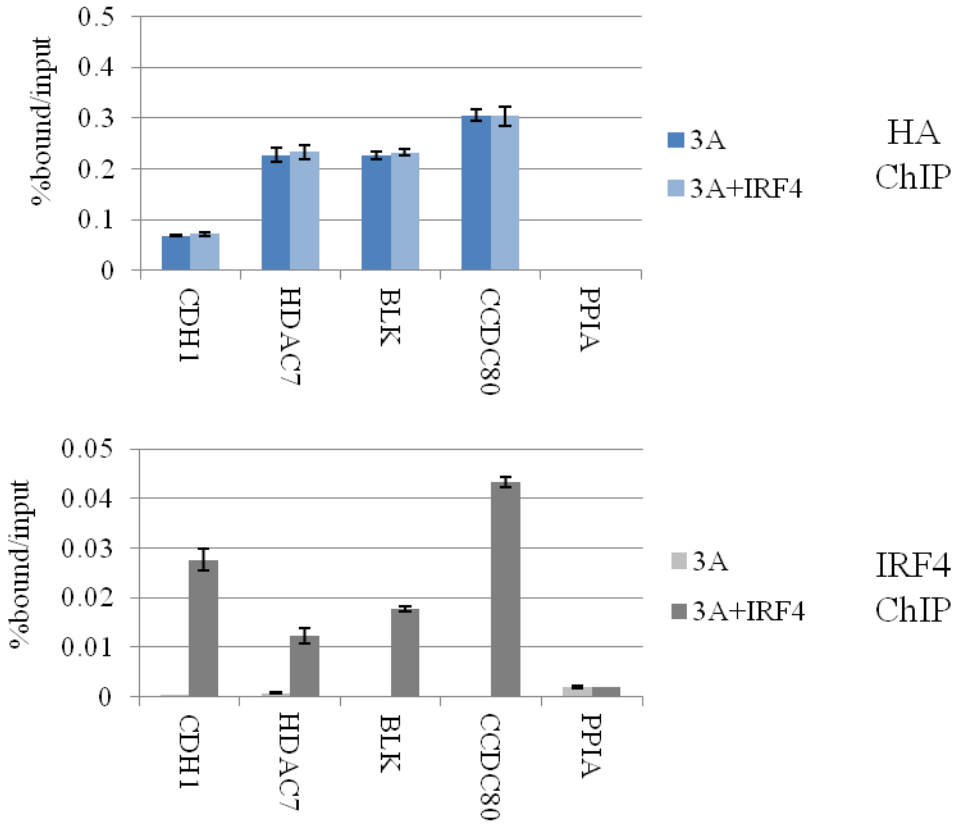

Figure III.14B

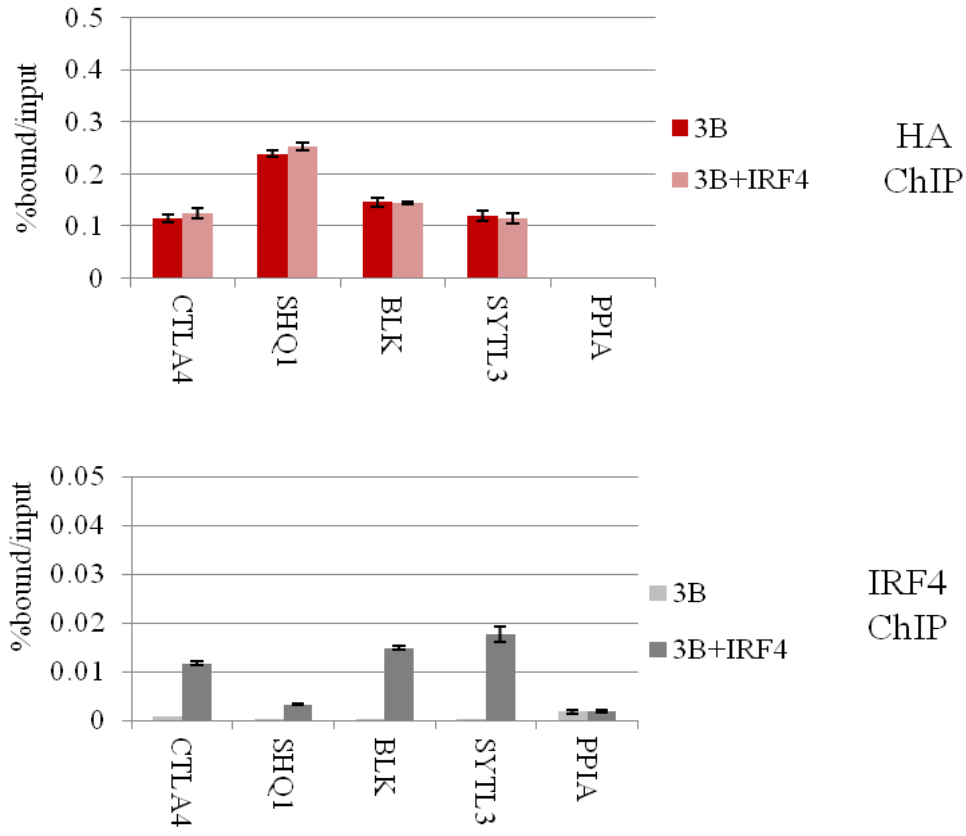

Figure III.14: IRF4 co-binding does not promote EBNA3A or EBNA3B at specific sites in the human genome. A) ChIP-qPCR assay for EBNA3A (HA, top panel) in BJAB cells expressing flag-HA tagged EBNA3A alone (blue) or with IRF4 (light blue). ChIP-qPCR assay for IRF4 (gray) from the same cells is shown in the bottom panel. Binding was assessed at multiple sites co-bound by EBNA3A and IRF4 in LCLs (*CDH1, HDAC7, BLK* and *CCDC80*). A site near the *PPIA* which is not bound by EBNAs or IRF4 was included as a negative control. B) ChIP-qPCR assay for EBNA3B (HA, top panel) in BJAB cells expressing flag-HA tagged EBNA3B alone (red) or with IRF4 (light red). ChIP-qPCR assay for IRF4 (gray) from the same cells is shown in the bottom panel. Representative EBNA3B/IRF4 co-bound sites based on LCL data were selected (*CTLA4, SHQ1, BLK* and *SYTL3*) as well as the *PPIA* negative control. All qPCR signals are reported as percent of DNA ChIPed relative to input. Results are shown as mean ± SEM of three independent experiments.

Figure III.15

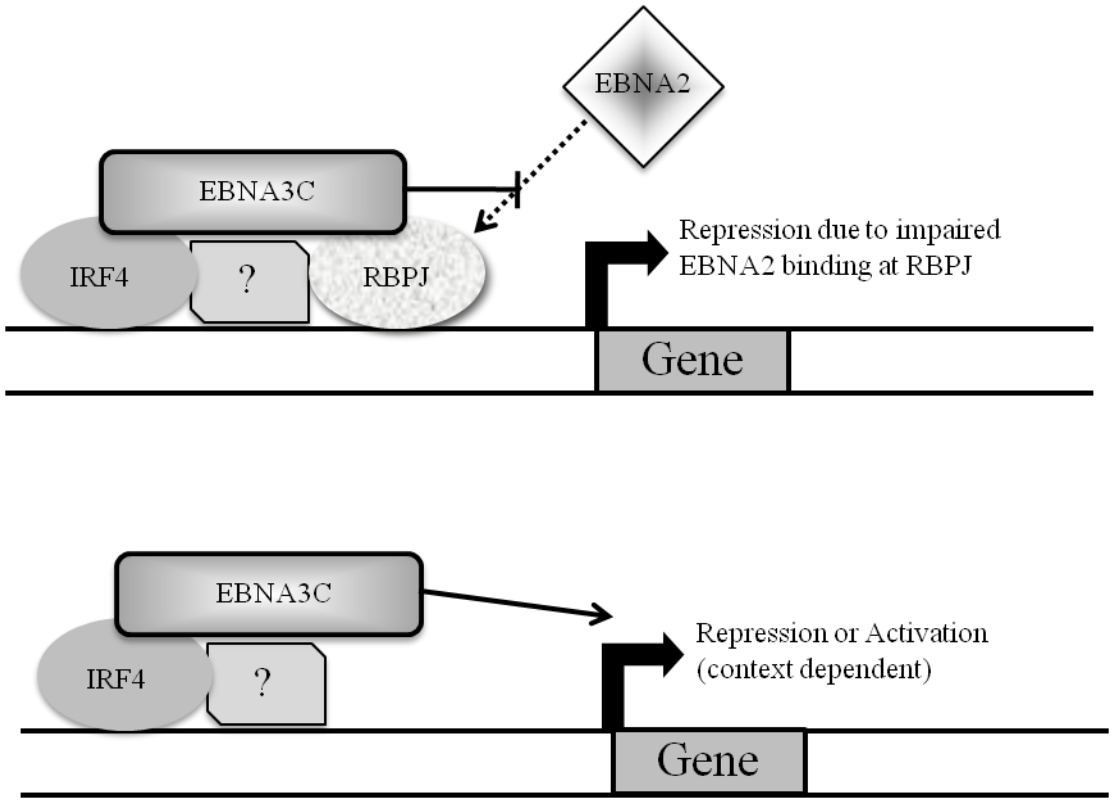

Figure III.15: Working model of EBNA3 binding and gene regulation. At RBPJ sites (top panel) EBNA3 binding limits EBNA2 access, resulting in cell gene repression. The specific sites bound by each EBNA3 are determined by interactions with other cell transcription factors (represented by the question mark), including IRF4 in the case of EBNA3C as depicted. At non-RBPJ sites (bottom panel), EBNA3 binding would not generally affect EBNA2 binding and produces activation or repression in a context dependent manner.

CHAPTER IV:

EBNA3C MEDIATED H3K27ME3 REGULATION IN LCLS

Introduction

EBNA3s regulate hundreds of host genes, including p16INK4a and BIM which may account for their growth promoting and anti-apoptotic effects, respectively. EBNA3A and EBNA3C cooperatively mediate the deposition of the H3K27me3 at the BIM and CDKN2A promoters to maintain their repression. The multiprotein complex PRC2 is the key regulator responsible for catalyzing this epigenetic modification. Studies in BLs and LCLs have identified other genes that are also repressed by EBNA3A and EBNA3C in the same fashion, including *ITGB1, ADAM28, ADAMDEC1, RASGRP1, NOTCH2, TOX and CXCL9* and *CXCL10* (112, 116, 159). The Kempkes group has done an analysis of genes regulated by EBNA3A wherein they compared the data on EBNA3A repressed genes with H3K27me3 ChIP-seq data from the ENCODE (112). They observed that about 70 % of genes repressed by EBNA3A carried the PcG-associated signature H3K27me3; 90 % of these genes were associated with PcG-mediated silencing in multiple cell types. This finding indicated that many EBNA3A repressed genes may have an inherent capacity to undergo PcG-mediated silencing by H3K27me3 deposition. A second important finding of this study is that, H3K27me3 marks spread across the *CXCL10/9* domain actually happened after transcriptional down-regulation of the genes due to loss of EBNA2 binding in response to EBNA3A expression. This raises the possibility that H3K27me3 deposition at EBNA3A repressed genes may be a consequence rather than the cause of transcriptional shut-down. However, whether this occurs at all EBNA3A repressed genes or any EBNA3C repressed genes is unknown.

Paschos *et al.* performed a detailed analyses of the chromatin around the *BIM* promoter in which they found that EBNA3A and EBNA3C co-expression trigger the recruitment of polycomb repressive complex 2 (PRC2) core subunits and H3K27me3 modification at this locus (154). They also claimed that there was an EBNA3C binding peak near the transcription start site of *BIM*. In addition, they found that EBV induces no consistent changes in the steady state expression of PRC2 components in BLs, but shRNAs against PRC2 and PRC1 subunits disrupted EBV repression of BIM. Therefore, they propose a model that EBNA3A and EBNA3C physically interact with PRC2 to recruit it to EBNA3A and EBNA3C bound sites for H3K27me3 deposition.

In mammalian cells, it remains unclear how the polycomb proteins are recruited to specific promoters. Unlike *Drosophila* which uses the sequence-specific DNA-binding protein Pleiohomeotic (Pho) to mediate PcG recruitment to PcG response elements (PREs) (191), no such sequences was found in mammalian cells. Many potential mechanisms have been proposed, *e.g.* preference for regions rich in CpG-islands (CGIs) (192); sequence-specific transcription factors such as YY1(193); non-coding RNA species that can interact with PRC2 and DNA (reviewed in (194)) and there may be as yet undefined factors involved in PRC2 recruitment [reviewed in (23,26,33–37)]. However, for the genes that are regulated by EBNA3 mediated epigenetic silencing, it remains to be investigated how H3K27me3 is deposited and maintained at their genomic regulatory elements.

In this Chapter I will discuss our findings regarding EBNA3A and EBNA3C effects on H3K27me3 modification and how they conflict with the current model. I will then describe our efforts to use H3K27me3 ChIP-seq experiments to identify locations that

undergo H3K27me3 level changes downstream of EBNA3C activity to shed light on this mystery.

Result

No significant binding of EBNA3A and EBNA3C was detected at *CDKN2A* and *BIM* loci.

To determine whether EBNA3A and EBNA3C directly bind to *CDKN2A* and *BIM* loci where the H3K27me3 changes occur, we first examined our EBNA3A and EBNA3C ChIP-seq datasets for binding peaks at these sites. Figure IV.1A shows a UCSC genome browser window depicting tracks for EBNA3 and RBPJ binding and H3K27me3 levels (GM12878, ENCODE database) at the *BIM* (chr2:111,860,000-111,890,000) and *CDKN2A* (chr9:21,960,000-22,020,000) loci. Based on this ChIP-seq data, there are no detectable EBNA3 binding peaks at locations reported to undergo H3K27me3 changes near the *INK4a* and *BIM* TSS in response to EBNA3A or EBNA3C inactivation (shown in the red box). To verify the ChIP-seq data, we performed ChIP-qPCR experiments at the above sites for EBNA3 protein binding using EBNA3-F-HA and wild type (untagged) LCLs. Again, there is no statistically significant enrichment in HA ChIP from the respective EBNA3-F-HA LCL relative to that observed in the wild type (untagged) LCL by a two sample t-test (Figure IV.1B). Thus, EBNA3A and EBNA3C binding is not detectible at either the *INK4a* or *BIM* genomic sites that undergo H3K27me3 change in response to EBNA3A and EBNA3C activity.

EBNA3 down-regulated genes show reduced H3K27me3 to a greater extent than EBNA3 bound genes in LCLs.

Having found no evidence that EBNA3A and EBNA3C bind to *INK4a* and *BIM* TSS where decreased H3K27me3 was seen upon EBNA3A and EBNA3C inactivation, we

decided to examine sites strongly bound by EBNA3s as well as promoter sites within EBNA3 regulated genes for evidence of H3K27me3 changes. H3K27me3 ChIP-qPCR experiments were performed using E3AHT cells (Figure IV.2A) cultured in medium supplied with 4HT (4HT+) or after withdrawal of 4HT for 14 (4HT- d14) and 21(4HT- d21) days. qPCR was used to examine H3K27me3 level change at genomic loci near genes known to be repressed by EBNA3A expression, including *INK4a*, *BIM*, *JAK1* and *RAPH1*; and genomic loci near genes bound by EBNA3A, including *RAPH1*, *MACC1*, *SYTL3*, *TP53I3* and *ROCK1*. *HNRPLL* genomic locus is neither bound nor repressed by EBNA3A. As expected, the H3K27me3 signal decreased at *INK4a* and *BIM* loci after EBNA3A was inactivated by 4HT withdrawal. Furthermore, the other two EBNA3A repressed genes *JAK1* and *RAPH1* also showed a decline in H3K27me3 signal upon 4HT withdrawal. However, there was no significant change of H3K27me3 signal at EBNA3A bound sites: *MACC1*, *SYTL3*, *TP53I3*. There was also no H3K27me3 signal change at *HNRPLL* which is neither bound nor repressed by EBNA3A.

We performed similar H3K27me3 ChIP-qPCR experiment using the E3CHT LCLs cultured in the presence of 4HT or after 14 to 21days of 4HT withdrawal (Figure IV.2B). Again, we observed a significant decrease of H3K27me3 signal at EBNA3C regulated genes including previously reported *INK4a* and *BIM*, as well as *JAK1* and *HNRPLL*. In contrast, there was no consistent change in H3K27me3 signal at genes near EBNA3C bound sites, including *MACC1*, *SYTL3* and *ROCK1*, with the exception of *RAPH1* which did undergo a decrease of H3K27me3 signal upon EBNA3C inactivation. Taken together, these results demonstrated that H3K27me3 level decrease to a greater extend at EBNA3A and EBNA3C

regulated genes than at EBNA3A and EBNA3C bound gene loci, suggesting their repressive effects may be indirect instead of physically recruiting PRC2 to deposit the H3K27me3 mark to their bound sites.

EBNA3A and EBNA3C do not consistently alter the global H3K27me3 levels or the expression of H3K27me3 methytransferase EZH2, or the H3K27me3 demethylase KDM6A and KDM6B.

Since the human (HPV) E7 oncoprotein induces KDM6B and thereby globally decreases H3K27me3 levels, we wondered whether EBNA3A or EBNA3C might act analogously to account for the change of H3K27me3 pattern. The steady state levels of H3K27me3, the methytransferase EZH2 that catalyze this modification, the demethylase KDM6A and KDM6B that remove this modification were therefore assessed by western blot in E3AHT and E3CHT LCLs cultured in the presence (4HT+) or absence (4HT-) of 4-hydroxytamoxifen for two weeks (Figure IV.3A). The western blot results for H3K27me3 and EZH2 did not show any significant change upon EBNA3A and EBNA3C inactivation. KDM6A and KDM6B expression was not reliably detectable using commercially available antibodies. We therefore attempted to detect their mRNA transcripts by RT-qPCR (Figure IV.3B). Using the same E3AHT and E3CHT LCL system, we measured the KDM6A and KDM6B mRNA levels with EZH2 mRNA (two splicing variants shown as EZH2 V1 and EZH2 V2) as control. After normalizing mRNA levels to GAPDH, we observed no significant change in KDM6A mRNA in response to EBNA3A and EBNA3C activity. The KDM6B mRNA was not reliably detected. EZH2 mRNA levels remained unchanged, consistent with the protein levels as assessed by western blot. Therefore, although

H3K27me3 signals were decreased at several EBNA3A and EBNA3C regulated gene loci, the global level of H3K27me3 is unchanged in the presence or absence of EBNA3A or EBNA3C activity and thus cannot account for the changes of this mark at specific sites. In addition, EBNA3A and EBNA3C did not seem to alter the steady state level of methytransferase EZH2 or the demethylases KDM6A and KDM6B in LCLs

ChIP-seq identifies genomic locations that undergo H3K27me3 level change upon EBNA3C inactivation

Having shown that H3K27me3 signal did not change globally or undergo significant change at EBNA3A and EBNA3C bound sites, we decided to determine where H3K27me3 changes do occur in response to EBNA3C inactivation. We chose to focus on EBNA3C because of the availability of a p16INKA/p14ARF double knockout LCL clone in our lab. This cell line cannot express functional p16INK4a or p14ARF and thus, does not exhibit the myriad of secondary effects that occur upon p16INK4a inactivation. In addition, this cell line contains an intact *INK4a* promoter, which allows us to confirm that EBNA3C mediating changes are occurring at this promoter as expected under experimental conditions despite disruption of the *CDKN2A* gene products. Using this mutant cell line, we performed four biological replicates of H3K27me3 ChIP-seq under permissive (4HT+) and non-permissive (4HT-) culture conditions.

ChIP samples were used to prepare libraries for Illumina sequencing, and the raw reads were aligned to the human hg19 genome using Bowtie (http://bowtie-bio.sourceforge.net/index.shtml) (176). Genomic sites that enriched for H3K27me3 signals were identified in ChIP-seq data set relative to input DNA using

mosaicsHMM pipeline. In contrast to ChIP-seq for transcription factors which typically generate sharp peaks with strong signal intensity, H3K27me3 ChIP-seq demonstrated broad enrichment across the entire gene region with the median width around 5-6Kb. By taking in peaks that are common in four replicates, we identified a total of 23805 genomic regions showing H3K27me3 signals in the 4HT+ condition and 17042 of such genomic regions in 4HT- condition. With the 23805 genomic regions, 15484 of them are only present in 4HT+ condition but not in the 4HT-, representing the locations that potentially undergo epigenetic silencing mediated by EBNA3C activity (Figure IV.4).

Based on the preliminary analysis, only 8 of 400 top EBNA3C bound sites (p-value and peak height in ChIP-seq) that undergo H3K27me3 level change within 10kb of peak region, whereas only one of the 8 sites shows direct overlap. However, when we compare the EBNA3C regulated genes (p16INK4a null LCL gene profiling data from Allday group (118)) to the regions that undergo H3K27me3 level change, we found that 20 of 113 EBNA3C repressed genes undergo H3K27me3 decrease when EBNA3C is inactivated; whereas 4 of 137 EBNA3C induced genes undergo H3K27me3 decrease when EBNA3C is inactivated. This finding is consistent with the H3K27me3 ChIP-qPCR data shown in figure IV. 2 that H3K27me3 decrease occurs more often near EBNA3C regulated genes instead of near genes bound by EBNA3C. Taken together, our results support the model that H3K27me3 level change appears to be an indirect effect of EBNA3C binding. However, the specific factors mediating these effects on H3K27me3 modification need to be further investigated.

Discussion

The products of *CDKN2A* gene locus p16INK4a and p14ARF are key mediators of oncogenic stress responses and potent barriers to the immortalization of cells in culture and the cancer development *in vivo*. It is therefore not surprising that p16INK4a and p14ARF are inactivated in various ways e.g., gene deletion, mutation, or promoter DNA methylation (140, 195, 196) in a wide variety of human cancers. The entire *INK4b-ARF-INK4a* locus appears to be coordinately regulated by polycomb protein complexes that generate repressive histone modifications (140, 196). It has been well established that EBNA3A and EBNA3C co-operatively repress p16INK4a via H3K27me3, which is induced early after EBV infection. Further, B cells lacking the ability to express p16INK4a do not require EBNA3C to be transformed by EBV into proliferating LCLs, suggesting p16INK4a is the main target for EBNA3C in maintaining LCL growth (118).

BIM is a strong inducer of apoptosis and a key regulator of lymphocyte survival. Inhibition of BIM induction enhances lymphomagenesis in mice and humans, and plays an crucial role in the pathogenesis of BL (147). It has also been shown that EBNA3A and EBNA3C co-operatively mediate repression of BIM transcription via H3K27me3 histone modification (154), potentially followed by DNA methylation of CpG islands flanking the BIM transcriptional initiation site is observed in BL cells (153). Because BIM is a key defense against dysregulated MYC, inhibition of the pro-apoptotic protein BIM by EBNA3A and 3C is likely to contribute to the progression of EBV positive BL (148).

The exact mechanism by which EBNA3A and EBNA3C mediate the epigenetic modification at p16INK4a and BIM promoters is still need poorly understood. The existing model proposed by Allday group is that EBNA3A and EBNA3C directly recruit PRC2 to

INK4a and *BIM* promoters thus, inducing H3K27me3 modification. However, our data challenge several predictions of this model. First, at the *INK4a* and *BIM* promoters where the most H3K27me3 changes occur, there is no significant binding of either EBNA3A or EBNA3C (Figure IV.1). Second, at sites strongly bound by EBNA3A and/or EBNA3C, there is no consistent alteration of H3K27me3 upon EBNA3A or EBNA3C inactivation (Figure IV.2 and Figure III.4). Instead, we observed reduced H3K27me3 signal near EBNA3A and EBNA3C regulated genes, suggesting that EBNA3A and EBNA3C mediated H3K27me3 regulation is more complicated than simple recruitment of PRC2 by chromatin associated EBNA3 proteins.

On the other hand, we do not observe any global change of H3K27me3 levels nor of its writer EZH2 or eraser KDM6A/6B when EBNA3A or EBNA3C was inactivated. Therefore, unlike HPV E7, EBV EBNA3s do not exert their effects on p16INK4a and BIM by globally altering the H3K27me3 levels. This suggests that EBNA3A and EBNA3C mediated H3K27me3 change is site specific. There is growing evidenc that EZH2 is phosphorylated at multiple threonine residues in order to regulate its stability and chromatin recruitment (197-200). For example, Cyclin-dependent kinases (CDK1/2) phosphorylate EZH2 at T350 which promotes the interaction between EZH2 and lncRNAs such as HOTAIR and Xist (197). Thus, EBNA3A and EBNA3C might indirectly regulate EZH2 targeting by modulating the CDK-mediated phosphorylation pathway, resulting in enhanced or reduced EZH2 recruitment at specific site on chromatin due to deregulated lncRNA interaction. Alternatively EBNA3A or EBNA3C may regulate expression of lncRNAs required for PRC2 recruitment.

Several histone demethylases have been identified to be present in complexes with transcription factors. For example, the H3K4me3 demethylase KDM5C/JARID1C associates with the REST repressive complex (201), which is responsible for repression of neuronal genes in non-neuronal tissues. The H3K4me1/2 demethylase KDM1 has been identified in various complexes with known DNA-binding proteins including the transcription initiation factor TFII-I (202), the E-cadherin promoter binding factors ZEB1/2 (203) and ZNF217 (204), as well as Androgen Receptor (AR) (205), suggesting that these DNA-binding proteins may play a role in histone demethylase recruitment or stabilization at particular genomic sites. Therefore, we can speculate that EBNA3A and EBNA3C might regulate the DNA-binding proteins involved in forming complexes with the histone demethylase KDM6A/6B, thus affecting their recruitment or stabilization at particular loci, leading to alterations in local H3K27me3 levels. In addition, it has also been suggested that transcription factors can modulate demethylase activity to affect the local histone modification status. For example, interaction of the *Drosophila* MYC homolog with the KDM5/LID/JARID1 abrogates its demethylase activity (206). Finally, as with EZH2, post-translation modifications may regulate demethylase activity. For example, KDM6A/UTX is specifically phosphorylated in the mouse developing brain (207). Although its biological relevance remains to be determined, this observation supports the possibility that demethylases are regulated by more than recruitment to specific genomic loci. EBNA3A and EBNA3C may therefore alter H3K27me3 levels at specific sites via many mechanisms other than PRC2 recruitment. An essential pre-requisite for

distinguishing among these potential mechanisms is to better define a larger subset of genomic loci at which H3K27me3 levels are regulated by EBNA3A and EBNA3C.

To identify the specific sites that undergo H3K27me3 level change in response to EBNA3C activity, we performed H3K27me3 ChIP-seq in the presence or absence of EBNA3C activity in LCLs deleted for p16INK4a and p14ARF. Because the H3K27me3 is a broad mark compared to the transcription factors, obtaining sufficient sequencing depth to reliably identify regions differentially modified between the two conditions has been a challenge. Using four biological replicates, we identified a total of 15484 locations that have H3K27me3 signal only when EBNA3C is active and lack this mark when EBNA3C is turned off. Therefore, these sites resemble the *INK4a* and *BIM* loci in their response to EBNA3C and are potentially interesting targets for further investigations. By comparing the EBNA3C bound sites and EBNA3C regulated gene loci to these15484 locations, we found our hypothesis still holds true that the vast majority of EBNA3C bound sites do not have H3K27me3 signals in their vicinity; however, a higher proportion of EBNA3C repressed genes (20/113) do than EBNA3C induced genes (4/137). These experiments, while still preliminary, further support our hypothesis that EBNA3s exert changes in the H3K27me3 histone modification through indirect mechanisms. In addition, in E3CHT LCLs that has been cultured in 4HT withdrawal medium for 30 days, more than 10 day are required to fully regain of H3K27me3 mark at the *INK4a* locus upon 4HT addition to the culture medium (115). This delay also suggests that an indirect process accounts for EBNA3A and EBNA3C induced epigenetic silencing.

Recent studies support a central role for long non-coding RNAs in PRC2 recruitment to repressed gene loci. Remarkably, examination of a comprehensive catalog of known human lncRNAs, about 20% of lncRNAs expressed in various cell types were observed to be bound by PRC2. Additional lncRNAs were bound by other chromatin-modifying complexes and affected cellular gene expression (208). This finding underscores the critical role of lncRNA in PRC2 targeting. Perhaps the best studied example is Xist (X Inactive Specific Transcript), a 3.2kb lncRNA can target PRC2 to the inactive regions of one of the X chromosomes in females (209). Another lncRNA, HOTAIR (HOX transcript antisense RNA), is a 2.2-kb lncRNA is involved in the repression of the *HOX* loci and promoting cancer metastasis (210, 211). In addition, other lncRNAs, such as HEIH, H19 and linc-UBC1 have been shown to interact with EZH2 and are involved in tumor growth and metastasis (212-214). Most relevant to EBNA3A and EBNA3C is ANRIL (antisense non-coding RNA in the *CDKN2A* locus), a 3.8 kb-long non-coding RNA reported to repress p15INK4b by recruiting PRC2 to this locus (215). ANRIL may also regulate p16INKa; however, we did not find evidence of ANRIL regulation by EBNA3C, making it an unlikely mediator of EBNA3C effects at the *CDKN2A* locus. Therefore, we are in the process of examining which lncRNAs are affected by EBNA3A and EBNA3C and whether H3K27me3 level changes downstream of EBNA3A and EBNA3C correlate with loci regulated by these lncRNAs.

Manipulation of the H3K27me3 modification catalyzed by PRC2 to reversibly repress key tumor suppressor genes in B cells allows EBV to transiently override these genes, without irreversibly inactivating them. In human cancers, these genes are frequently

deleted or epigenetically repressed; therefore understanding the complete molecular mechanism of how EBNA3s mediate this process may provide insights into more general mechanisms of carcinogenesis. Although the indirect pathway proposed herein “blunts” Occam’s razor, this more complex pathway also presents an opportunity to identify therapeutic targets that would not exist if the direct recruitment model were correct.

.

Figure IV.1

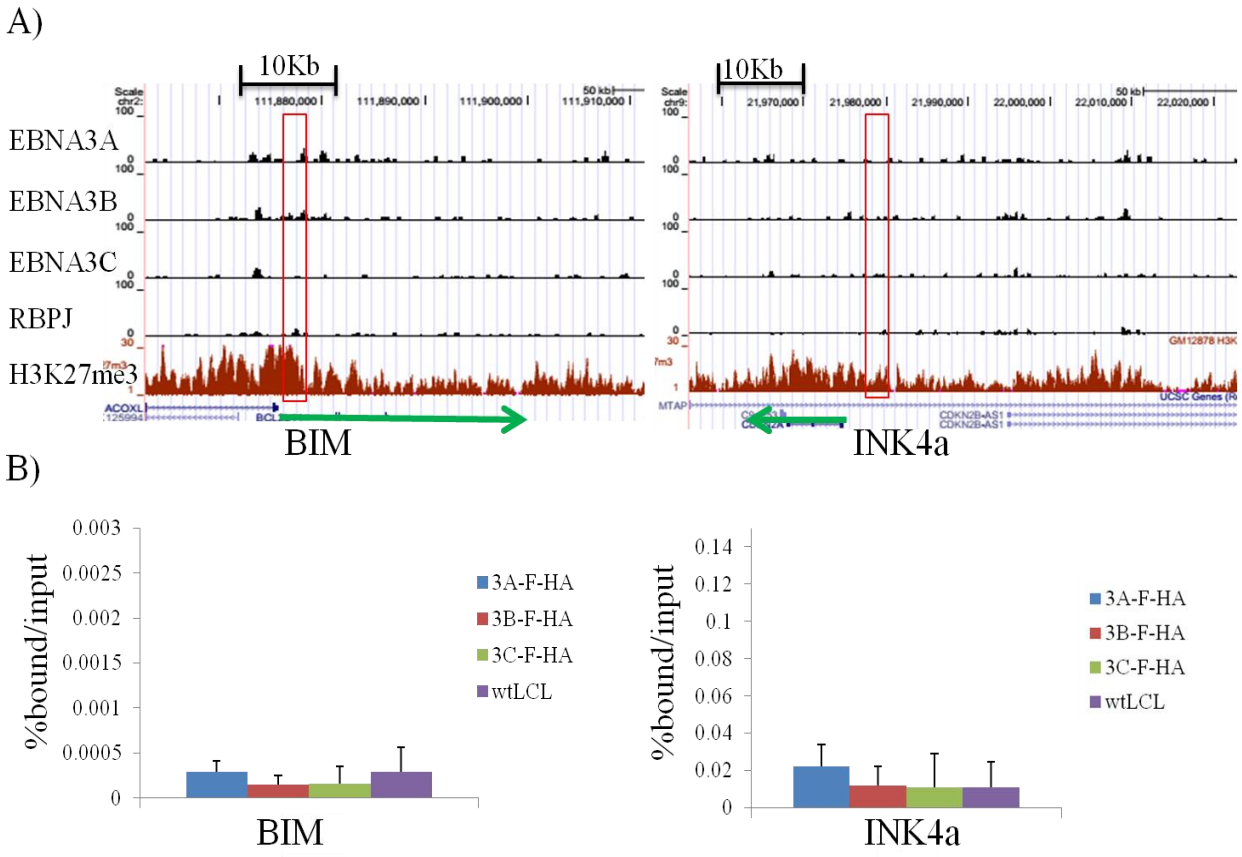

Figure IV.1 EBNA3 proteins binding and histone modification at *BIM* and *INK4a* loci.

A) Genome browser tracks showing EBNA3A, EBNA3B, EBNA3C, and RBPJ binding as well as H3K27me3 levels at the *BIM* and *INK4a* loci. The UCSC genome browser snapshots were taken at chr2:111,860,000-111,890,000 for *BIM* locus and chr9:21,960,000-22,020,000 *INK4a* locus respectively. The numbers at Y-axis were normalized signals (reads per kilobase per million mapped reads) from EBNA3s, RBPJ and H3K27me3 ChIP-seq datasets. Gene structures are shown at the bottom of the panel. The green arrows indicated the direction of transcription. The red boxes denoted to the genomic region previously reported to undergo H3K27me3 signal change upon EBNA3A and EBNA3C inactivation. B) Bar

plots showing ChIP-qPCR resultes at *BIM* and *INK4a* TSS regions with the red boxes indicated above. Y-axis indicating ennrichment of genomic DNA from ChIP of EBNA3A, EBNA3B, or EBNA3C relative to input. Each EBNA was specificaly ChIPed using HA antibody in either the EBNA3A-F-HA, EBNA3B- F-HA, EBNA3C-F-HA LCL with wild type (untagged) LCLs as a negative control. All qPCR signal are reported as percentage of ChIPed DNA relative to input DNA. Results are shown as mean ± SEM of three independent experiments.

Figure IV.2

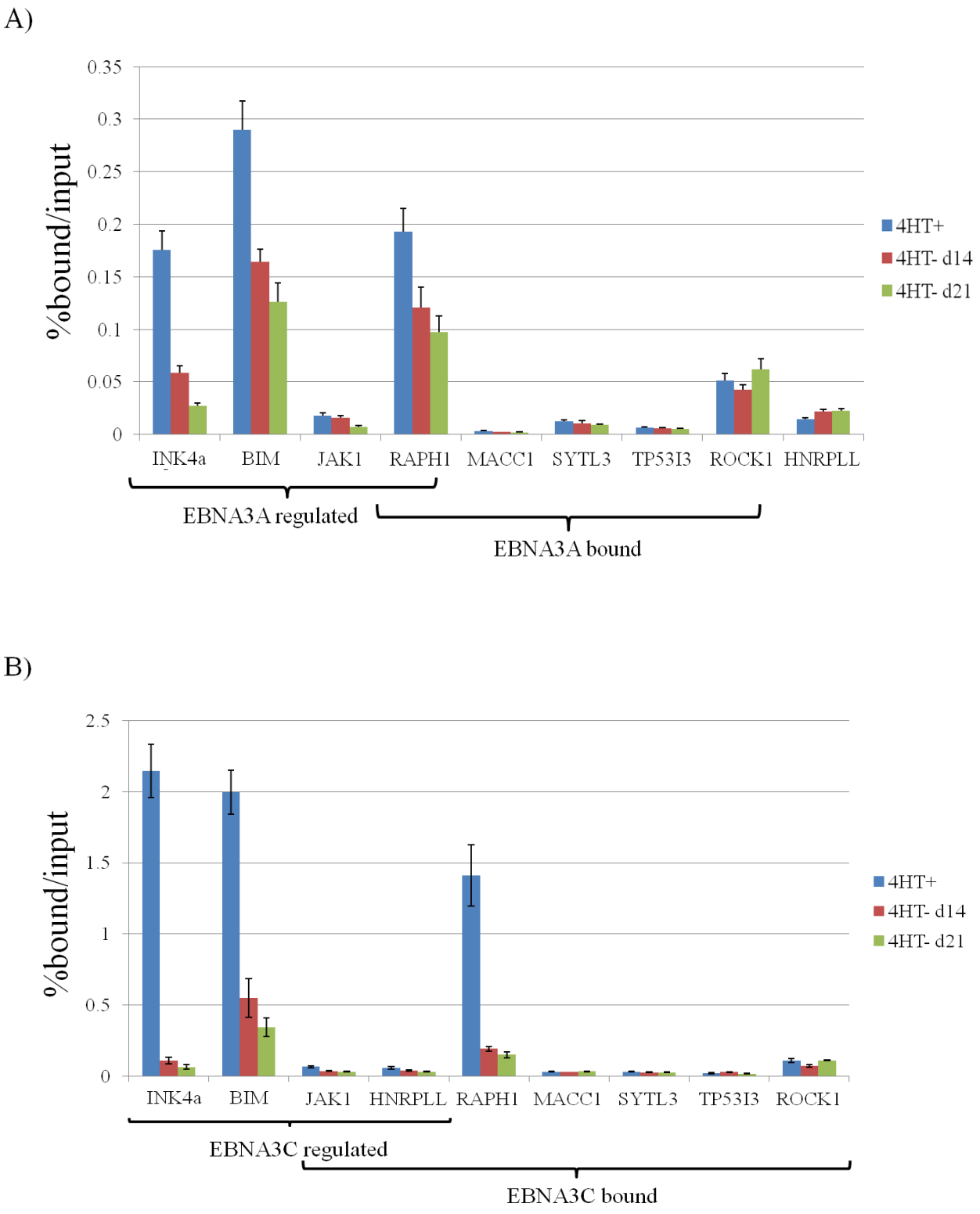
A)
%bound/input
0.35
0.3
0.25
0.2
0.15
0.1
0.05
0
INK4a
BIM
JAK1
RAPH1
MACC1
SYTL3
TP53I3
ROCK1
HNRPLL
4HT+
4HT- d14
4HT- d21
EBNA3A regulated
EBNA3A bound
B)
%bound/input
2.5
2
1.5
1
0.5
0
INK4a
BIM
JAK1
HNRPLL
RAPH1
MACC1
SYTL3
TP53I3
ROCK1
4HT+
4HT- d14
4HT- d21
EBNA3C regulated
EBNA3C bound

Figure IV.2 H3K27me3 levels at EBNA3 regulated and EBNA3 bound genomic loci, in LCLs, upon EBNA3A and EBNA3C inactivation. A) Bar plot showing H3K27me3 signal at the indicated loci in E3AHT LCLs cultured in the presence (4HT+) or absence (4HT-) of 4-hydroxytamoxifen for 14 to 21 days. Genomic loci included sites near EBNA3A repressed genes (*INK4a, BIM, JAK1, RAPH1*) or EBNA3Abound genes (*RAPH1, MACC1, SYTL3, TP53I3* and *ROCK1*) as indicated in the bracket underneath. All qPCR signals are reported as percentage of ChIPed DNA relative to input DNA. B) Analogous experiment to that described in (A) using the E3CHT LCL. H3K27me3 signal was determined by ChIP-qPCR at the indicated sites in the presence or absence of 4-hydroxytamoxifen. Genomic loci included sites near EBNA3C repressed genes (*INK4a, BIM, JAK1, HNRPLL*) or EBNA3Cbound genes (*JAK1, HNRPLL, RAPH1, MACC1, SYTL3, TP53I3* and *ROCK1*) as indicated in the bracket underneath. All results are shown as mean ± SEM of three independent experiments.

Figure IV.3

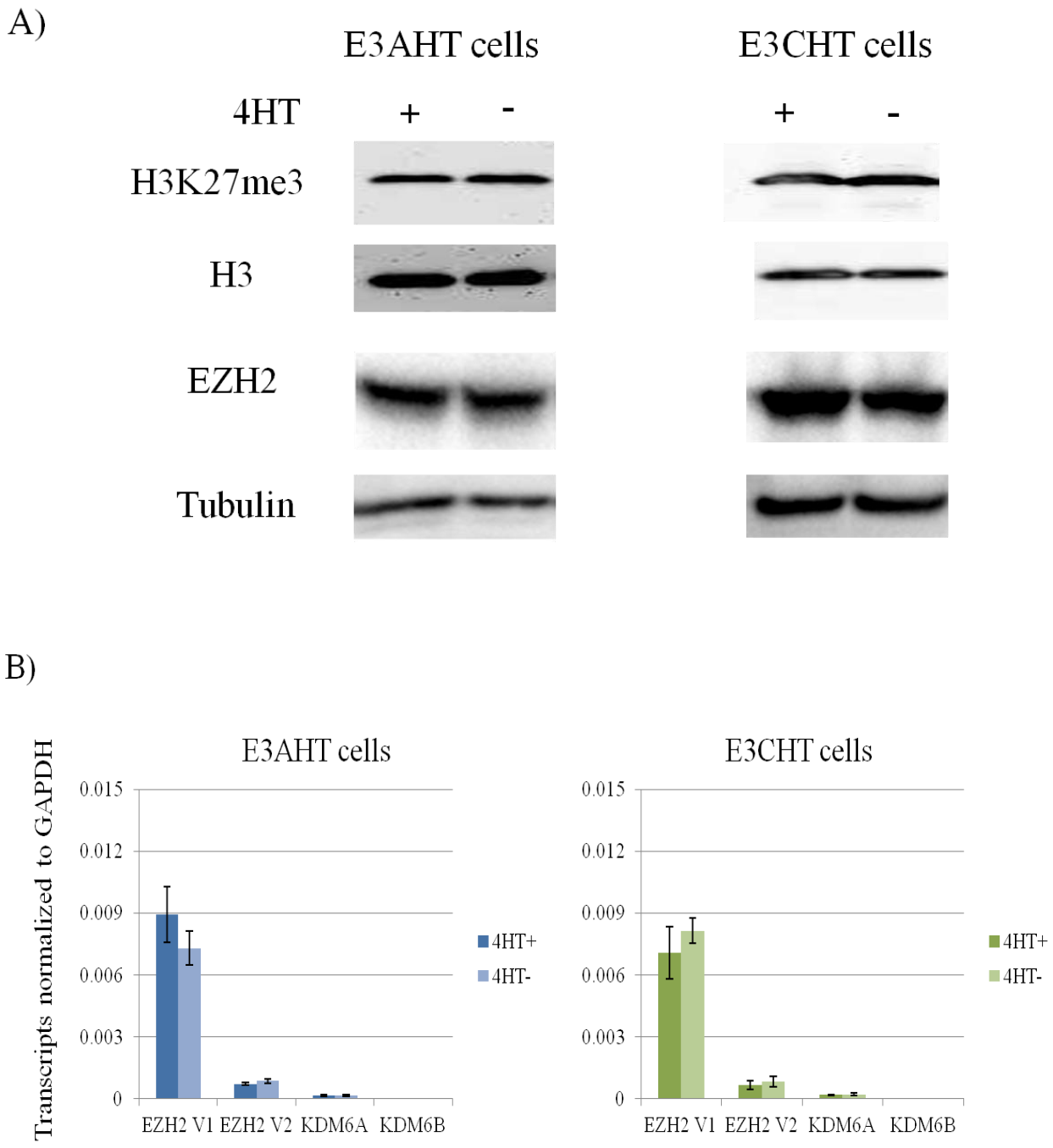

Figure IV.3 Steady-state levels of H3K27me3, EZH2, KDM6A and KDM6B in the presence and absence of EBNA3A or EBNA3C activity. A) Western blot showing the global H3K27me3 and EZH2 levels in E3AHT and E3CHT LCLs cultured in the presence

(4HT+) or absence (4HT-) of 4-hydroxytamoxifen for two weeks. Total Histone 3 (H3) and tubulin were used as loading controls. Each lane represents whole cell lysates from $2x10^5$ cells. B) Bar plot showing RT-qPCR results for EZH2 transcript variant 1 (EZH2 V1), EZH2 transcript variant 2 (EZH2 V2), KDM6A and KDM6B mRNA levels normalized to GAPDH in E3AHT and E3CHT LCLs cultured in the presence (4HT+) or absence (4HT-) of 4-hydroxytamoxifen for two weeks. All results are shown as mean ± SEM of three independent experiments.

Figure IV.4

Figure IV.4: H3K27me3 positive genomic regions in 4HT+ and 4HT- conditions detected by ChIP-seq experiments in LCLs deleted for p16INK4a and p14ARF. Venn diagram showing the number of genomic regions carrying H3K27me3 signals in the 4HT+ condition and 4HT- condition. Results represent peaks that are common in four biological replicates.

CHAPTER V:

DISCUSSION AND FUTURE DIRECTIONS

Contributions and implications in this dissertation

EBV nuclear antigens EBNA3A, EBNA3B and EBNA3C are a family of three nuclear proteins expressed in EBV transformed LCLs. The role EBNA3 proteins in EBV biology is less understood compared to the EBNA1 and EBNA2 EBV nuclear proteins. It has been well established that EBNA3A and EBNA3C are important for *in vitro* transformation of B cells into LCLs, and in recent years the transforming ability of EBNA3A and EBNA3C has been ascribed to their repression of the p16INK4a tumor suppressor (118, 138). In addition, because EBNA3A and EBNA3C inhibit p16INK4a transcription, they are believed to function as transcription factors that regulate host gene expression. However, the detailed molecular mechanisms by which EBNA3s mediate gene regulation are largely unknown.

Like EBNA2, the EBNA3 proteins bind to the cellular DNA binding protein RBPJ, a component of the Notch signaling pathway. It has been shown that binding of these viral proteins is mutually exclusive and competitive. Subsequent gene profiling studies in both BLs and LCLs have demonstrated that EBNA3 proteins regulate partially overlapping sets of genes. An important unanswered question is how these EBNAs exert their unique effects through interactions with a shared transcription factor. To address this, we performed ChIP-seq of each EBNA3 in LCLs and analyzed this data concurrently with previously published EBNA2 and RBPJ ChIP-seq data from LCLs.

We found that EBNA3A, EBNAB and EBNA3C bind to distinct genomic sites with only limited overlap. In contrast to EBNA2 which has over 80% bound sites co-localize with RBPJ, only a minority of EBNA3s binding sites co-localize with RBPJ.

When EBNA3 bound sites do co-localize with RBPJ, frequently EBNA2 is observed, suggesting the primary role of RBPJ co-localization is to limit EBNA2 access. Our data suggests this may actually be an underestimate as EBNA3 binding may abrogate EBNA2 binding at these sites. We demonstrated this observation using LCLs conditional for EBNA3A or EBNA3C activity and further found that EBNA3A and EBNA3C regulate EBNA2 binding at specific RBPJ sites. Our results demonstrated that differences in the genomic sites bound by each EBNA3 protein determine which EBNA2 bound sites they regulate and ultimately lead to differences in gene regulation. These EBNA3s functions may be critical *in vivo* to prevent uncontrolled EBNA2 activity, which could be detrimental to host cells.

By examining transcription factor co-localization and motif enrichment at unique EBNA3 bound sites, we identified IRF4 as specifically enriched at EBNA3C bound sites. More importantly, using BJAB cells ectopically expressing physiologic levels of IRF4, EBNA3C binding at ETS/IRF4 (EICE) and AP1/IRF4 (AICE) sites was greatly enhanced, whereas IRF4 expression did not affect EBNA3A or EBNA3B binding at these sites. Although a prior study by has observed EBNA3C co-localization with BATF/IRF4/SPI1/RUNX3 sites and that EBNA3C binding signals were stronger at IRF4 co-bound sites than sites without IRF4 binding (110), our results provide the first concrete evidence that IRF4 specifically contributes to EBNA3C binding. Our results support the notion that EBV exploits transcription factors critical for B cell development to achieve immortalization of host cells.

EBNA3A and EBNA3C co-operatively regulate two tumor suppressors p16INK4a and BIM, and this repression correlates with increased levels of the H3K27me3 repressive mark. Subsequent studies also identified several other genes that undergo H3K27me3 level change in response to EBNA3A and EBNA3C activity, suggesting a role for EBNA3 proteins in mediating epigenetic silencing of host genes. H3K27me3 is catalyzed by PRC2 which contains the methyltransferase EZH2; and is removed by histone demethylase KDM6A and KDM6B. A straightforward model has been proposed to explain these observations in which EBNA3A and EBNA3C mediate H3K27me3 regulation by physically interacting with PRC2 and recruiting it to their bound sites (154). However, our studies have contradicted fundamental predictions of this model. We found that EBNA3A and EBNA3C did not bind to *INK4a* and *BIM* promoter regions where the greatest H3K27me3 changes are observed. In addition, we found that H3K27me3 level changes induced by EBNA3A and EBNA3C occur primarily at genes regulated by these EBV proteins, not at EBNA3A and EBNA3C bound sites. We also showed that EBNA3A and EBNA3C do not affect the global level of H3K27me3, nor do they affect the EZH2 and KDM6A/6B expression. Taken together, these suggest the old model is inadequate and we proposed that EBNA3A and EBNA3C mediate H3K27me3 changes at specific sites via indirect mechanisms.

We performed H3K27me3 ChIP-seq study in LCLs to identify the locations that undergo H3K27me3 level changes in response to EBNA3C activity. This study allowed us to identify thousands of locations with the H3K27me3 modification when EBNA3C is active, but lost this mark when EBNA3C is inactivated. Due to the complexity of this dataset and the intrinsic challenges to analyze H3K27me3 distribution, which is a very

broad histone mark, these results remain preliminary and efforts to fully elucidate the pathways through which EBNA3C mediates H3K27me3 deposition and maintenance in LCLs are ongoing.

In conclusion, we believe our findings contribute significantly to our current understanding of the role played by EBNA3 proteins in the LCL transformation process. Our findings suggest that each EBNA3 (EBNA3A, EBNA3B, or EBNA3C) is able to regulate EBNA2 binding at distinct RBPJ genomic sites, and explain how these proteins can exert different effects through a common interacting partner. We further demonstrate that IRF4 interaction with EBNA3C is one determinant of its distinct genomic binding profile. We propose a model where interactions of other EBNA3 proteins with specific cell transcription factors determine their ability to regulate distinct subsets of cell genes to fulfill their unique role in LCL transformation. Finally, we suggest that EBNA3A and EBNA3C repress gene expression by altering H3K27me3 levels via an indirect mechanism. Mapping the genome-wide locations that undergo H3K27me3 level change downstream of EBNA3C activity will facilitate identification of the molecular mechanisms underlying this effect, e.g. by regulating lncRNAs or specific transcription factors that are involved in the recruitment or stability of PRC2 and KDM6A/6B on chromatin.

Future directions

EBNA3 regulation of EBNA2 binding

Based on our current studies, we maintain that the degree to which EBNA2, EBNA3A and EBNA3C compete for RBPJ bound sites is underestimated by static ChIP-seq

experiments. To fully define the extent of this competition, EBNA2 ChIP-seq could be done in LCLs conditional for EBNA3A and EBNA3C activity respectively. This will allow us to identify genomic sites that have enhanced EBNA2 binding when EBNA3A or EBN3C is inactive. In addition, by analyzing the motifs and transcription factors co-occupancies at these locations, we expect to find the factors that contribute to EBNA3A and EBNA3C competition with EBNA2 for binding to specific genomic sites. We can also examine whether this competition leads to critical gene regulation by EBNA2 and EBNA3s; and whether EBNA3 competition for RBPJ affects the ability of Notch to signal in LCLs.

Mechanisms of EBNA3s gene regulation

Our knowledge of how EBNA3s regulate a variety of host genes is still very limited. Is it not clear how EBNA3 binding is connected to the genes they regulate. Chromatin conformation capture has been used to show that chromatin looping brings the intergenic element that binds EBNA3s into close proximity with the *ADAM28* and *ADAMDEC1* promoters (113). Whereas at *CtBP2* locus, EBNA3A prevents enhancer–promoter looping which is consistent with EBNA3A playing a central role in the repression of this locus. Both our ChIP-seq data and previously published studies have demonstrated that EBNA3s bound sites are over-represented at enhancer regions, suggesting the importance of long-range regulation in EBNA3s function. Therefore, the exact mechanism of how EBNA3s modulate the long-range enhancer-promoter interactions is an intriguing aspect to investigate in the future.

The accurate assignment of enhancer and corresponding promoters is almost impossible if only examines the linear distances between binding sites and the genes being

regulated. The nuclear architecture of chromosome territories and topological association domains (TADs) (216) has been shown to be critical in transcriptional regulation. TADs are mega-base size chromatin interaction domains and are thought to represent functional domains of gene regulation (217). A recent study characterized a class of EBV super-enhancers and has provided important clues as to how EBV nuclear proteins may cooperate with cellular transcription factors to regulate genes (218). This study found that approximately 86% of EBNA2 super-enhancers and their associated gene pairs occurred within the same TAD. In addition, MYC and BCL2 expression is driven by EBV super-enhancers, indicating that long-range interactions might be a common way for EBNA proteins to co-coordinately regulate key oncogenes as well as host transcriptome. Therefore, further characterization of EBV super-enhancer and the topological associated domains structure in EBV infected B cells will help us dissect the complexity of EBV mediated gene regulation and transformation.

Our current understanding of how the EBNA3s regulate key tumor suppressors like p16INK4a and BIM is far from complete. Although it is clear that EBNA3A and EBNA3C cooperatively maintain the deposition of H3K27me3 at *INK4a* and *BIM* loci, exactly how this cooperation is achieved to mediate PRC2 recruitment to specific sites is unclear. We are analyzing our H3K27me3 ChIP-seq data concomitantly with RNA-seq data done in EBNA3C activity on and off conditions in an effort to discover intermediates used by EBNA3s to regulate host genes via epigenetic modifications of chromatin. On the other hand, we are cognizant of the suggestion that H3K27me3 deposition may be a consequence rather than the mechanism of some EBNA3 effects.

Moreover, it still needs to be fully addressed what determines the requirement for both EBNA3A and EBNA3C and what are their relative contributions. Our data have suggested that EBNA3A and EBNA3C each compete for RBPJ binding at specific sites. This suggests, for example, that p16INK4a repression involves at least two RPBJ bound sites mediating cooperative EBNA3 effects. However, given the large number of EBNA3 bound sites that lack RBPJ co-binding, it is likely that there are RBPJ-independent effects of the EBNA3s via interaction with other transcription factors. We are currently determining which protein-protein interactions are required for EBNA3C regulation of genes using a complementation assay with EBNA3C mutants coupled with RNA-seq.

EBNA3 binding specificity

Our ChIP-seq studies for EBNA3s have identified thousands of genomic sites bound by each EBNA3 protein. However, the full details of what determines binding at particular loci are incomplete. We have demonstrated that IRF4 is a key factor contributing to EBNA3C binding at AICE and EICE sites. However, there are IRF4 bound sites that lack EBNA3C binding and vice versa, suggesting a role for additional transcription factors in EBNA3C recruitment. It is likely that EBNA3A and EBNA3B recruitment are similarly complex. Another caveat of this study is that the experiments were performed in a BJAB background because IRF4 is required for LCL growth (182). However, there are two alternative experiments could be done in the future to circumvent this problem. First, we can generate LCLs carrying an inducible shRNA against IRF4 thus it could be controlled by drug and turned off in the short term. In this way, we can test whether in LCL background IRF4 still specifically promotes EBNA3C binding instead of EBNA3A and EBNA3B.

Second, we have the EBNA3C mutant that is deficient for IRF4 binding (EBNA3C_F144A) and is unable to promote EBNA3C binding to AICE and EICE sites in BJAB cells. These experiments could be repeated using the E3CHT LCL in which the 4HT minus state is transcomplemented with the pCEP-EBNA3C_F144A-FHA expression plasmid. In addition, this transcomplementation assay could also be used to determine whether an IRF4 interaction with EBNA3C is required for p16INK4a suppression and LCL growth. Our lab had published the data using this type of transcomplementation assay showing that EBNA3A mutants impaired for RBPJ or WDR48 association were unable to maintain LCL growth whereas EBNA3A CtBP1 binding mutant resulted in modestly impaired growth (98). Therefore, it will be interesting to know to what extend the EBNA3C IRF4 binding mutant can cause a LCL growth defect, and whether this is due to other mechanisms in addition to the inability of EBNA3C to interact with IRF4. Finally, if there is a growth defect that prevents adequate study of EBNA3C_F144A, the transcomplementation assay could be repeated in p16INK4a/p14ARF KO 3CHT LCLs that have been generated in our lab by CRISPR-Cas9 technique. This will allow us to overcome the growth defect caused by p16INK4a or p14ARF induction thus to only look at the genes regulated downstream of IRF4 binding. Taken together, we believe the above experiments will facilitate our understanding of how the key B cell differentiation factor IRF4 is involved in EBNA3C function.

Our transcription factor co-association study and motif searching also identified candidates that may help determine EBNA3A and EBNA3B binding specificity. For example the MYC binding motif was enriched at EBNA3A unique sites and the PU.1

binding motif is enriched at EBNA3B binding sites. Further analysis and experiments are needed to address how these known or novel factors determine EBNA3A and EBNA3B genomic binding and other functions.

Another interesting observation that EBNA2 from type I EBV, which has superior transforming ability compared to type II EBV is due to a single amino acid mutation at S442D; and this caused a increased binding of type I EBNA2 at ETS/IRF4 sites (171). Therefore, delineating whether the "novel" binding sites observed with type I EBNA2 are due to an enhanced ability to compete with EBNA3C for binding at ETS/IRF4 sites will provide further information on the role of ETS/IRF4 (EICE) composite elements in EBV biology.

EBNA3 function *in vivo*

Another long-term goal is to determine the function of EBNA3s during B cell infection *in vivo*. Only PTLD and a subset of DLBCLs (219) express the full latency III EBV latent proteins; while the Wp-restricted BLs express EBNA3s, but lack EBNA2 expression (220). These studies are important because *in vitro* models may not fully capture critical *in vivo* phenomena. For example, EBNA3B is dispensable for *in vitro* transformation, but may function as a tumor suppressor *in vivo* as its deletion is associated with more aggressive, immune-evading monomorphic DLBCL-like tumors in humanized mice (78). Loss of EBNA3B expression resulted in decreased expression of the T cell-chemoattractant CXCL10 that led to reduced T cell recruitment *in vitro* and T cell-mediated killing *in vivo*. However, for EBNA3A and EBNA3C this kind of *in vivo* study is still lacking. Further experiments using humanized mouse model will contribute to our understanding of this

question. Furthermore, the role of the EBNA3s in other malignancies remains to be clearly defined. It is possible the EBNA3s may contribute to the onset of malignancies that later exit the type III latency due to their immunogenicity and additional cellular mutations that compensate their functions. As discussed previously, the EBNA3s may continue to epigenetic silencing through inheritable imprinting, exemplified by BIM and p16INK4a, which are usually methylated in latency I EBV-positive BLs; and are frequently mutated or deleted in EBV-negative BLs. In conclusion, exploring the *in vivo* functions of EBNA3s will greatly enhance our understanding on the mechanisms of EBV associated tumorigenesis, thus contribute to the identification of potential therapeutic interventions and vaccines.

REFERENCES

1. **Young LS, Rickinson AB.** 2004. Epstein-Barr virus: 40 years on. Nat Rev Cancer **4:**757-768.
2. **Epstein MA, Achong BG, Barr YM.** 1964. Virus Particles in Cultured Lymphoblasts from Burkitt's Lymphoma. Lancet **1:**702-703.
3. **Babcock GJ, Decker LL, Volk M, Thorley-Lawson DA.** 1998. EBV persistence in memory B cells in vivo. Immunity **9:**395-404.
4. **Khan G, Miyashita EM, Yang B, Babcock GJ, Thorley-Lawson DA.** 1996. Is EBV persistence in vivo a model for B cell homeostasis? Immunity **5:**173-179.
5. **Thorley-Lawson DA.** 2001. Epstein-Barr virus: exploiting the immune system. Nat Rev Immunol **1:**75-82.
6. **Thorley-Lawson DA, Hawkins JB, Tracy SI, Shapiro M.** 2013. The pathogenesis of Epstein-Barr virus persistent infection. Curr Opin Virol **3:**227-232.
7. **Khan G, Hashim MJ.** 2014. Global burden of deaths from Epstein-Barr virus attributable malignancies 1990-2010. Infect Agent Cancer **9:**38.
8. **Longnecker R KE, Cohen J.** 2013. Epstein-Barr Virus. Fields Virology **2:**1898-1959.
9. **Henle W, Diehl V, Kohn G, Zur Hausen H, Henle G.** 1967. Herpes-type virus and chromosome marker in normal leukocytes after growth with irradiated Burkitt cells. Science **157:**1064-1065.
10. **Consortium EP.** 2012. An integrated encyclopedia of DNA elements in the human genome. Nature **489:**57-74.
11. **International HapMap C.** 2003. The International HapMap Project. Nature **426:**789-796.
12. **Thorley-Lawson DA, Allday MJ.** 2008. The curious case of the tumour virus: 50 years of Burkitt's lymphoma. Nat Rev Microbiol **6:**913-924.
13. **Mosialos G, Birkenbach M, Yalamanchili R, VanArsdale T, Ware C, Kieff E.** 1995. The Epstein-Barr virus transforming protein LMP1 engages signaling proteins for the tumor necrosis factor receptor family. Cell **80:**389-399.
14. **Floettmann JE, Rowe M.** 1997. Epstein-Barr virus latent membrane protein-1 (LMP1) C-terminus activation region 2 (CTAR2) maps to the far C-terminus and requires oligomerisation for NF-kappaB activation. Oncogene **15:**1851-1858.
15. **Izumi KM, Kieff ED.** 1997. The Epstein-Barr virus oncogene product latent membrane protein 1 engages the tumor necrosis factor receptor-associated death domain protein to mediate B lymphocyte growth transformation and activate NF-kappaB. Proc Natl Acad Sci U S A **94:**12592-12597.
16. **Kieser A, Kilger E, Gires O, Ueffing M, Kolch W, Hammerschmidt W.** 1997. Epstein-Barr virus latent membrane protein-1 triggers AP-1 activity via the c-Jun N-terminal kinase cascade. EMBO J **16:**6478-6485.
17. **Hatzivassiliou E, Miller WE, Raab-Traub N, Kieff E, Mosialos G.** 1998. A fusion of the EBV latent membrane protein-1 (LMP1) transmembrane domains to the CD40 cytoplasmic domain is similar to LMP1 in constitutive activation of epidermal growth factor receptor expression, nuclear factor-kappa B, and stress-activated protein kinase. J Immunol **160:**1116-1121.

18. **Kilger E, Kieser A, Baumann M, Hammerschmidt W.** 1998. Epstein-Barr virus-mediated B-cell proliferation is dependent upon latent membrane protein 1, which simulates an activated CD40 receptor. EMBO J **17:**1700-1709.
19. **Gires O, Kohlhuber F, Kilger E, Baumann M, Kieser A, Kaiser C, Zeidler R, Scheffer B, Ueffing M, Hammerschmidt W.** 1999. Latent membrane protein 1 of Epstein-Barr virus interacts with JAK3 and activates STAT proteins. EMBO J **18:**3064-3073.
20. **Mancao C, Hammerschmidt W.** 2007. Epstein-Barr virus latent membrane protein 2A is a B-cell receptor mimic and essential for B-cell survival. Blood **110:**3715-3721.
21. **Longnecker R, Druker B, Roberts TM, Kieff E.** 1991. An Epstein-Barr virus protein associated with cell growth transformation interacts with a tyrosine kinase. J Virol **65:**3681-3692.
22. **Longnecker R, Miller CL, Miao XQ, Marchini A, Kieff E.** 1992. The only domain which distinguishes Epstein-Barr virus latent membrane protein 2A (LMP2A) from LMP2B is dispensable for lymphocyte infection and growth transformation in vitro; LMP2A is therefore nonessential. J Virol **66:**6461-6469.
23. **Miller CL, Lee JH, Kieff E, Longnecker R.** 1994. An integral membrane protein (LMP2) blocks reactivation of Epstein-Barr virus from latency following surface immunoglobulin crosslinking. Proc Natl Acad Sci U S A **91:**772-776.
24. **Rovedo M, Longnecker R.** 2007. Epstein-barr virus latent membrane protein 2B (LMP2B) modulates LMP2A activity. J Virol **81:**84-94.
25. **Rechsteiner MP, Berger C, Zauner L, Sigrist JA, Weber M, Longnecker R, Bernasconi M, Nadal D.** 2008. Latent membrane protein 2B regulates susceptibility to induction of lytic Epstein-Barr virus infection. J Virol **82:**1739-1747.
26. **Baer R, Bankier AT, Biggin MD, Deininger PL, Farrell PJ, Gibson TJ, Hatfull G, Hudson GS, Satchwell SC, Seguin C, et al.** 1984. DNA sequence and expression of the B95-8 Epstein-Barr virus genome. Nature **310:**207-211.
27. **Cai X, Schafer A, Lu S, Bilello JP, Desrosiers RC, Edwards R, Raab-Traub N, Cullen BR.** 2006. Epstein-Barr virus microRNAs are evolutionarily conserved and differentially expressed. PLoS Pathog **2:**e23.
28. **Zhu JY, Pfuhl T, Motsch N, Barth S, Nicholls J, Grasser F, Meister G.** 2009. Identification of novel Epstein-Barr virus microRNA genes from nasopharyngeal carcinomas. J Virol **83:**3333-3341.
29. **Imig J, Motsch N, Zhu JY, Barth S, Okoniewski M, Reineke T, Tinguely M, Faggioni A, Trivedi P, Meister G, Renner C, Grasser FA.** 2011. microRNA profiling in Epstein-Barr virus-associated B-cell lymphoma. Nucleic Acids Res **39:**1880-1893.
30. **Kuzembayeva M, Hayes M, Sugden B.** 2014. Multiple functions are mediated by the miRNAs of Epstein-Barr virus. Curr Opin Virol **7:**61-65.
31. **Marquitz AR, Mathur A, Chugh PE, Dittmer DP, Raab-Traub N.** 2014. Expression profile of microRNAs in Epstein-Barr virus-infected AGS gastric carcinoma cells. J Virol **88:**1389-1393.
32. **Rymo L.** 1979. Identification of transcribed regions of Epstein-Barr virus DNA in Burkitt lymphoma-derived cells. J Virol **32:**8-18.

33. **Lerner MR, Andrews NC, Miller G, Steitz JA.** 1981. Two small RNAs encoded by Epstein-Barr virus and complexed with protein are precipitated by antibodies from patients with systemic lupus erythematosus. Proc Natl Acad Sci U S A **78:**805-809.
34. **Swaminathan S, Tomkinson B, Kieff E.** 1991. Recombinant Epstein-Barr virus with small RNA (EBER) genes deleted transforms lymphocytes and replicates in vitro. Proc Natl Acad Sci U S A **88:**1546-1550.
35. **Komano J, Maruo S, Kurozumi K, Oda T, Takada K.** 1999. Oncogenic role of Epstein-Barr virus-encoded RNAs in Burkitt's lymphoma cell line Akata. J Virol **73:**9827-9831.
36. **Ruf IK, Rhyne PW, Yang C, Cleveland JL, Sample JT.** 2000. Epstein-Barr virus small RNAs potentiate tumorigenicity of Burkitt lymphoma cells independently of an effect on apoptosis. J Virol **74:**10223-10228.
37. **Yajima M, Kanda T, Takada K.** 2005. Critical role of Epstein-Barr Virus (EBV)-encoded RNA in efficient EBV-induced B-lymphocyte growth transformation. J Virol **79:**4298-4307.
38. **Repellin CE, Tsimbouri PM, Philbey AW, Wilson JB.** 2010. Lymphoid hyperplasia and lymphoma in transgenic mice expressing the small non-coding RNA, EBER1 of Epstein-Barr virus. PLoS One **5:**e9092.
39. **Gregorovic G, Bosshard R, Karstegl CE, White RE, Pattle S, Chiang AK, Dittrich-Breiholz O, Kracht M, Russ R, Farrell PJ.** 2011. Cellular gene expression that correlates with EBER expression in Epstein-Barr Virus-infected lymphoblastoid cell lines. J Virol **85:**3535-3545.
40. **Rawlins DR, Milman G, Hayward SD, Hayward GS.** 1985. Sequence-specific DNA binding of the Epstein-Barr virus nuclear antigen (EBNA-1) to clustered sites in the plasmid maintenance region. Cell **42:**859-868.
41. **Yates JL, Warren N, Sugden B.** 1985. Stable replication of plasmids derived from Epstein-Barr virus in various mammalian cells. Nature **313:**812-815.
42. **Sears J, Ujihara M, Wong S, Ott C, Middeldorp J, Aiyar A.** 2004. The amino terminus of Epstein-Barr Virus (EBV) nuclear antigen 1 contains AT hooks that facilitate the replication and partitioning of latent EBV genomes by tethering them to cellular chromosomes. J Virol **78:**11487-11505.
43. **Frappier L.** 2015. Ebna1. Curr Top Microbiol Immunol **391:**3-34.
44. **Wilson JB, Bell JL, Levine AJ.** 1996. Expression of Epstein-Barr virus nuclear antigen-1 induces B cell neoplasia in transgenic mice. EMBO J **15:**3117-3126.
45. **Tsimbouri P, Drotar ME, Coy JL, Wilson JB.** 2002. bcl-xL and RAG genes are induced and the response to IL-2 enhanced in EmuEBNA-1 transgenic mouse lymphocytes. Oncogene **21:**5182-5187.
46. **Kang MS, Lu H, Yasui T, Sharpe A, Warren H, Cahir-McFarland E, Bronson R, Hung SC, Kieff E.** 2005. Epstein-Barr virus nuclear antigen 1 does not induce lymphoma in transgenic FVB mice. Proc Natl Acad Sci U S A **102:**820-825.
47. **Kang MS, Soni V, Bronson R, Kieff E.** 2008. Epstein-Barr virus nuclear antigen 1 does not cause lymphoma in C57BL/6J mice. J Virol **82:**4180-4183.

48. **Cohen JI, Wang F, Mannick J, Kieff E.** 1989. Epstein-Barr virus nuclear protein 2 is a key determinant of lymphocyte transformation. Proc Natl Acad Sci U S A **86:**9558-9562.
49. **Wang F, Tsang SF, Kurilla MG, Cohen JI, Kieff E.** 1990. Epstein-Barr virus nuclear antigen 2 transactivates latent membrane protein LMP1. J Virol **64:**3407-3416.
50. **Kempkes B, Pawlita M, Zimber-Strobl U, Eissner G, Laux G, Bornkamm GW.** 1995. Epstein-Barr virus nuclear antigen 2-estrogen receptor fusion proteins transactivate viral and cellular genes and interact with RBP-J kappa in a conditional fashion. Virology **214:**675-679.
51. **Kaiser C, Laux G, Eick D, Jochner N, Bornkamm GW, Kempkes B.** 1999. The proto-oncogene c-myc is a direct target gene of Epstein-Barr virus nuclear antigen 2. J Virol **73:**4481-4484.
52. **Sample J, Hummel M, Braun D, Birkenbach M, Kieff E.** 1986. Nucleotide sequences of mRNAs encoding Epstein-Barr virus nuclear proteins: a probable transcriptional initiation site. Proc Natl Acad Sci U S A **83:**5096-5100.
53. **Speck SH, Pfitzner A, Strominger JL.** 1986. An Epstein-Barr virus transcript from a latently infected, growth-transformed B-cell line encodes a highly repetitive polypeptide. Proc Natl Acad Sci U S A **83:**9298-9302.
54. **Alfieri C, Birkenbach M, Kieff E.** 1991. Early events in Epstein-Barr virus infection of human B lymphocytes. Virology **181:**595-608.
55. **Harada S, Kieff E.** 1997. Epstein-Barr virus nuclear protein LP stimulates EBNA-2 acidic domain-mediated transcriptional activation. J Virol **71:**6611-6618.
56. **Peng R, Tan J, Ling PD.** 2000. Conserved regions in the Epstein-Barr virus leader protein define distinct domains required for nuclear localization and transcriptional cooperation with EBNA2. J Virol **74:**9953-9963.
57. **McCann EM, Kelly GL, Rickinson AB, Bell AI.** 2001. Genetic analysis of the Epstein-Barr virus-coded leader protein EBNA-LP as a co-activator of EBNA2 function. J Gen Virol **82:**3067-3079.
58. **Yokoyama A, Tanaka M, Matsuda G, Kato K, Kanamori M, Kawasaki H, Hirano H, Kitabayashi I, Ohki M, Hirai K, Kawaguchi Y.** 2001. Identification of major phosphorylation sites of Epstein-Barr virus nuclear antigen leader protein (EBNA-LP): ability of EBNA-LP to induce latent membrane protein 1 cooperatively with EBNA-2 is regulated by phosphorylation. J Virol **75:**5119-5128.
59. **Mannick JB, Cohen JI, Birkenbach M, Marchini A, Kieff E.** 1991. The Epstein-Barr virus nuclear protein encoded by the leader of the EBNA RNAs is important in B-lymphocyte transformation. J Virol **65:**6826-6837.
60. **Jiang H, Cho YG, Wang F.** 2000. Structural, functional, and genetic comparisons of Epstein-Barr virus nuclear antigen 3A, 3B, and 3C homologues encoded by the rhesus lymphocryptovirus. J Virol **74:**5921-5932.
61. **Rivailler P, Cho YG, Wang F.** 2002. Complete genomic sequence of an Epstein-Barr virus-related herpesvirus naturally infecting a new world primate: a defining point in the evolution of oncogenic lymphocryptoviruses. J Virol **76:**12055-12068.

62. **Zhao B, Dalbies-Tran R, Jiang H, Ruf IK, Sample JT, Wang F, Sample CE.** 2003. Transcriptional regulatory properties of Epstein-Barr virus nuclear antigen 3C are conserved in simian lymphocryptoviruses. J Virol **77:**5639-5648.
63. **Joab I, Rowe DT, Bodescot M, Nicolas JC, Farrell PJ, Perricaudet M.** 1987. Mapping of the gene coding for Epstein-Barr virus-determined nuclear antigen EBNA3 and its transient overexpression in a human cell line by using an adenovirus expression vector. J Virol **61:**3340-3344.
64. **Petti L, Kieff E.** 1988. A sixth Epstein-Barr virus nuclear protein (EBNA3B) is expressed in latently infected growth-transformed lymphocytes. J Virol **62:**2173-2178.
65. **Petti L, Sample C, Kieff E.** 1990. Subnuclear localization and phosphorylation of Epstein-Barr virus latent infection nuclear proteins. Virology **176:**563-574.
66. **Le Roux A, Berebbi M, Moukaddem M, Perricaudet M, Joab I.** 1993. Identification of a short amino acid sequence essential for efficient nuclear targeting of the Epstein-Barr virus nuclear antigen 3A. J Virol **67:**1716-1720.
67. **Sample C, Parker B.** 1994. Biochemical characterization of Epstein-Barr virus nuclear antigen 3A and 3C proteins. Virology **205:**534-539.
68. **Krauer K, Buck M, Flanagan J, Belzer D, Sculley T.** 2004. Identification of the nuclear localization signals within the Epstein-Barr virus EBNA-6 protein. J Gen Virol **85:**165-172.
69. **Buck M, Burgess A, Stirzaker R, Krauer K, Sculley T.** 2006. Epstein-Barr virus nuclear antigen 3A contains six nuclear-localization signals. J Gen Virol **87:**2879-2884.
70. **Burgess A, Buck M, Krauer K, Sculley T.** 2006. Nuclear localization of the Epstein-Barr virus EBNA3B protein. J Gen Virol **87:**789-793.
71. **Bain M, Watson RJ, Farrell PJ, Allday MJ.** 1996. Epstein-Barr virus nuclear antigen 3C is a powerful repressor of transcription when tethered to DNA. J Virol **70:**2481-2489.
72. **Bourillot PY, Waltzer L, Sergeant A, Manet E.** 1998. Transcriptional repression by the Epstein-Barr virus EBNA3A protein tethered to DNA does not require RBP-Jkappa. J Gen Virol **79 (Pt 2):**363-370.
73. **Cludts I, Farrell PJ.** 1998. Multiple functions within the Epstein-Barr virus EBNA-3A protein. J Virol **72:**1862-1869.
74. **Tomkinson B, Kieff E.** 1992. Use of second-site homologous recombination to demonstrate that Epstein-Barr virus nuclear protein 3B is not important for lymphocyte infection or growth transformation in vitro. J Virol **66:**2893-2903.
75. **Tomkinson B, Robertson E, Kieff E.** 1993. Epstein-Barr virus nuclear proteins EBNA-3A and EBNA-3C are essential for B-lymphocyte growth transformation. J Virol **67:**2014-2025.
76. **Maruo S, Johannsen E, Illanes D, Cooper A, Kieff E.** 2003. Epstein-Barr Virus nuclear protein EBNA3A is critical for maintaining lymphoblastoid cell line growth. J Virol **77:**10437-10447.
77. **Maruo S, Wu Y, Ishikawa S, Kanda T, Iwakiri D, Takada K.** 2006. Epstein-Barr virus nuclear protein EBNA3C is required for cell cycle progression and growth maintenance of lymphoblastoid cells. Proc Natl Acad Sci U S A **103:**19500-19505.

78. **White RE, Ramer PC, Naresh KN, Meixlsperger S, Pinaud L, Rooney C, Savoldo B, Coutinho R, Bodor C, Gribben J, Ibrahim HA, Bower M, Nourse JP, Gandhi MK, Middeldorp J, Cader FZ, Murray P, Munz C, Allday MJ.** 2012. EBNA3B-deficient EBV promotes B cell lymphomagenesis in humanized mice and is found in human tumors. J Clin Invest **122:**1487-1502.
79. **Grossman SR, Johannsen E, Tong X, Yalamanchili R, Kieff E.** 1994. The Epstein-Barr virus nuclear antigen 2 transactivator is directed to response elements by the J kappa recombination signal binding protein. Proc Natl Acad Sci U S A **91:**7568-7572.
80. **Zimber-Strobl U, Strobl LJ, Meitinger C, Hinrichs R, Sakai T, Furukawa T, Honjo T, Bornkamm GW.** 1994. Epstein-Barr virus nuclear antigen 2 exerts its transactivating function through interaction with recombination signal binding protein RBP-J kappa, the homologue of Drosophila Suppressor of Hairless. EMBO J **13:**4973-4982.
81. **Lai EC.** 2002. Keeping a good pathway down: transcriptional repression of Notch pathway target genes by CSL proteins. EMBO Rep **3:**840-845.
82. **Artavanis-Tsakonas S, Rand MD, Lake RJ.** 1999. Notch signaling: cell fate control and signal integration in development. Science **284:**770-776.
83. **Weinmaster G.** 1997. The ins and outs of notch signaling. Mol Cell Neurosci **9:**91-102.
84. **Wang F, Gregory CD, Rowe M, Rickinson AB, Wang D, Birkenbach M, Kikutani H, Kishimoto T, Kieff E.** 1987. Epstein-Barr virus nuclear antigen 2 specifically induces expression of the B-cell activation antigen CD23. Proc Natl Acad Sci U S A **84:**3452-3456.
85. **Henkel T, Ling PD, Hayward SD, Peterson MG.** 1994. Mediation of Epstein-Barr virus EBNA2 transactivation by recombination signal-binding protein J kappa. Science **265:**92-95.
86. **Waltzer L, Logeat F, Brou C, Israel A, Sergeant A, Manet E.** 1994. The human J kappa recombination signal sequence binding protein (RBP-J kappa) targets the Epstein-Barr virus EBNA2 protein to its DNA responsive elements. EMBO J **13:**5633-5638.
87. **Woisetschlaeger M, Jin XW, Yandava CN, Furmanski LA, Strominger JL, Speck SH.** 1991. Role for the Epstein-Barr virus nuclear antigen 2 in viral promoter switching during initial stages of infection. Proc Natl Acad Sci U S A **88:**3942-3946.
88. **Hofelmayr H, Strobl LJ, Stein C, Laux G, Marschall G, Bornkamm GW, Zimber-Strobl U.** 1999. Activated mouse Notch1 transactivates Epstein-Barr virus nuclear antigen 2-regulated viral promoters. J Virol **73:**2770-2780.
89. **Strobl LJ, Hofelmayr H, Marschall G, Brielmeier M, Bornkamm GW, Zimber-Strobl U.** 2000. Activated Notch1 modulates gene expression in B cells similarly to Epstein-Barr viral nuclear antigen 2. J Virol **74:**1727-1735.
90. **Gordadze AV, Peng R, Tan J, Liu G, Sutton R, Kempkes B, Bornkamm GW, Ling PD.** 2001. Notch1IC partially replaces EBNA2 function in B cells immortalized by Epstein-Barr virus. J Virol **75:**5899-5912.

91. **Hofelmayr H, Strobl LJ, Marschall G, Bornkamm GW, Zimber-Strobl U.** 2001. Activated Notch1 can transiently substitute for EBNA2 in the maintenance of proliferation of LMP1-expressing immortalized B cells. J Virol **75:**2033-2040.
92. **Rowe M, Raithatha S, Shannon-Lowe C.** 2014. Counteracting effects of cellular Notch and Epstein-Barr virus EBNA2: implications for stromal effects on virus-host interactions. J Virol **88:**12065-12076.
93. **Robertson ES, Lin J, Kieff E.** 1996. The amino-terminal domains of Epstein-Barr virus nuclear proteins 3A, 3B, and 3C interact with RBPJ(kappa). J Virol **70:**3068-3074.
94. **Zhao B, Marshall DR, Sample CE.** 1996. A conserved domain of the Epstein-Barr virus nuclear antigens 3A and 3C binds to a discrete domain of Jkappa. J Virol **70:**4228-4236.
95. **Dalbies-Tran R, Stigger-Rosser E, Dotson T, Sample CE.** 2001. Amino acids of Epstein-Barr virus nuclear antigen 3A essential for repression of Jkappa-mediated transcription and their evolutionary conservation. J Virol **75:**90-99.
96. **Maruo S, Johannsen E, Illanes D, Cooper A, Zhao B, Kieff E.** 2005. Epstein-Barr virus nuclear protein 3A domains essential for growth of lymphoblasts: transcriptional regulation through RBP-Jkappa/CBF1 is critical. J Virol **79:**10171-10179.
97. **Calderwood MA, Lee S, Holthaus AM, Blacklow SC, Kieff E, Johannsen E.** 2011. Epstein-Barr virus nuclear protein 3C binds to the N-terminal (NTD) and beta trefoil domains (BTD) of RBP/CSL; only the NTD interaction is essential for lymphoblastoid cell growth. Virology **414:**19-25.
98. **Ohashi M, Holthaus AM, Calderwood MA, Lai CY, Krastins B, Sarracino D, Johannsen E.** 2015. The EBNA3 family of Epstein-Barr virus nuclear proteins associates with the USP46/USP12 deubiquitination complexes to regulate lymphoblastoid cell line growth. PLoS Pathog **11:**e1004822.
99. **Waltzer L, Perricaudet M, Sergeant A, Manet E.** 1996. Epstein-Barr virus EBNA3A and EBNA3C proteins both repress RBP-J kappa-EBNA2-activated transcription by inhibiting the binding of RBP-J kappa to DNA. J Virol **70:**5909-5915.
100. **Le Roux A, Kerdiles B, Walls D, Dedieu JF, Perricaudet M.** 1994. The Epstein-Barr virus determined nuclear antigens EBNA-3A, -3B, and -3C repress EBNA-2-mediated transactivation of the viral terminal protein 1 gene promoter. Virology **205:**596-602.
101. **Robertson ES, Grossman S, Johannsen E, Miller C, Lin J, Tomkinson B, Kieff E.** 1995. Epstein-Barr virus nuclear protein 3C modulates transcription through interaction with the sequence-specific DNA-binding protein J kappa. J Virol **69:**3108-3116.
102. **Radkov SA, Bain M, Farrell PJ, West M, Rowe M, Allday MJ.** 1997. Epstein-Barr virus EBNA3C represses Cp, the major promoter for EBNA expression, but has no effect on the promoter of the cell gene CD21. J Virol **71:**8552-8562.
103. **Cooper A, Johannsen E, Maruo S, Cahir-McFarland E, Illanes D, Davidson D, Kieff E.** 2003. EBNA3A association with RBP-Jkappa down-regulates c-myc and Epstein-Barr virus-transformed lymphoblast growth. J Virol **77:**999-1010.

104. **Zhao B, Sample CE.** 2000. Epstein-barr virus nuclear antigen 3C activates the latent membrane protein 1 promoter in the presence of Epstein-Barr virus nuclear antigen 2 through sequences encompassing an spi-1/Spi-B binding site. J Virol **74:**5151-5160.
105. **Lin J, Johannsen E, Robertson E, Kieff E.** 2002. Epstein-Barr virus nuclear antigen 3C putative repression domain mediates coactivation of the LMP1 promoter with EBNA-2. J Virol **76:**232-242.
106. **Rosendorff A, Illanes D, David G, Lin J, Kieff E, Johannsen E.** 2004. EBNA3C coactivation with EBNA2 requires a SUMO homology domain. J Virol **78:**367-377.
107. **Jimenez-Ramirez C, Brooks AJ, Forshell LP, Yakimchuk K, Zhao B, Fulgham TZ, Sample CE.** 2006. Epstein-Barr virus EBNA-3C is targeted to and regulates expression from the bidirectional LMP-1/2B promoter. J Virol **80:**11200-11208.
108. **Lee S, Sakakibara S, Maruo S, Zhao B, Calderwood MA, Holthaus AM, Lai CY, Takada K, Kieff E, Johannsen E.** 2009. Epstein-Barr virus nuclear protein 3C domains necessary for lymphoblastoid cell growth: interaction with RBP-Jkappa regulates TCL1. J Virol **83:**12368-12377.
109. **Maruo S, Wu Y, Ito T, Kanda T, Kieff ED, Takada K.** 2009. Epstein-Barr virus nuclear protein EBNA3C residues critical for maintaining lymphoblastoid cell growth. Proc Natl Acad Sci U S A **106:**4419-4424.
110. **Jiang S, Willox B, Zhou H, Holthaus AM, Wang A, Shi TT, Maruo S, Kharchenko PV, Johannsen EC, Kieff E, Zhao B.** 2014. Epstein-Barr virus nuclear antigen 3C binds to BATF/IRF4 or SPI1/IRF4 composite sites and recruits Sin3A to repress CDKN2A. Proc Natl Acad Sci U S A **111:**421-426.
111. **Schmidt SC, Jiang S, Zhou H, Willox B, Holthaus AM, Kharchenko PV, Johannsen EC, Kieff E, Zhao B.** 2015. Epstein-Barr virus nuclear antigen 3A partially coincides with EBNA3C genome-wide and is tethered to DNA through BATF complexes. Proc Natl Acad Sci U S A **112:**554-559.
112. **Harth-Hertle ML, Scholz BA, Erhard F, Glaser LV, Dolken L, Zimmer R, Kempkes B.** 2013. Inactivation of intergenic enhancers by EBNA3A initiates and maintains polycomb signatures across a chromatin domain encoding CXCL10 and CXCL9. PLoS Pathog **9:**e1003638.
113. **McClellan MJ, Wood CD, Ojeniyi O, Cooper TJ, Kanhere A, Arvey A, Webb HM, Palermo RD, Harth-Hertle ML, Kempkes B, Jenner RG, West MJ.** 2013. Modulation of enhancer looping and differential gene targeting by Epstein-Barr virus transcription factors directs cellular reprogramming. PLoS Pathog **9:**e1003636.
114. **Hertle ML, Popp C, Petermann S, Maier S, Kremmer E, Lang R, Mages J, Kempkes B.** 2009. Differential gene expression patterns of EBV infected EBNA-3A positive and negative human B lymphocytes. PLoS Pathog **5:**e1000506.
115. **Skalska L, White RE, Franz M, Ruhmann M, Allday MJ.** 2010. Epigenetic repression of p16(INK4A) by latent Epstein-Barr virus requires the interaction of EBNA3A and EBNA3C with CtBP. PLoS Pathog **6:**e1000951.
116. **White RE, Groves IJ, Turro E, Yee J, Kremmer E, Allday MJ.** 2010. Extensive co-operation between the Epstein-Barr virus EBNA3 proteins in the manipulation of host gene expression and epigenetic chromatin modification. PLoS One **5:**e13979.

117. **McClellan MJ, Khasnis S, Wood CD, Palermo RD, Schlick SN, Kanhere AS, Jenner RG, West MJ.** 2012. Downregulation of integrin receptor-signaling genes by Epstein-Barr virus EBNA 3C via promoter-proximal and -distal binding elements. J Virol **86:**5165-5178.
118. **Skalska L, White RE, Parker GA, Turro E, Sinclair AJ, Paschos K, Allday MJ.** 2013. Induction of p16(INK4a) is the major barrier to proliferation when Epstein-Barr virus (EBV) transforms primary B cells into lymphoblastoid cell lines. PLoS Pathog **9:**e1003187.
119. **Zhao B, Mar JC, Maruo S, Lee S, Gewurz BE, Johannsen E, Holton K, Rubio R, Takada K, Quackenbush J, Kieff E.** 2011. Epstein-Barr virus nuclear antigen 3C regulated genes in lymphoblastoid cell lines. Proc Natl Acad Sci U S A **108:**337-342.
120. **Cotter MA, 2nd, Robertson ES.** 2000. Modulation of histone acetyltransferase activity through interaction of epstein-barr nuclear antigen 3C with prothymosin alpha. Mol Cell Biol **20:**5722-5735.
121. **Subramanian C, Hasan S, Rowe M, Hottiger M, Orre R, Robertson ES.** 2002. Epstein-Barr virus nuclear antigen 3C and prothymosin alpha interact with the p300 transcriptional coactivator at the CH1 and CH3/HAT domains and cooperate in regulation of transcription and histone acetylation. J Virol **76:**4699-4708.
122. **Radkov SA, Touitou R, Brehm A, Rowe M, West M, Kouzarides T, Allday MJ.** 1999. Epstein-Barr virus nuclear antigen 3C interacts with histone deacetylase to repress transcription. J Virol **73:**5688-5697.
123. **Touitou R, Hickabottom M, Parker G, Crook T, Allday MJ.** 2001. Physical and functional interactions between the corepressor CtBP and the Epstein-Barr virus nuclear antigen EBNA3C. J Virol **75:**7749-7755.
124. **Knight JS, Lan K, Subramanian C, Robertson ES.** 2003. Epstein-Barr virus nuclear antigen 3C recruits histone deacetylase activity and associates with the corepressors mSin3A and NCoR in human B-cell lines. J Virol **77:**4261-4272.
125. **Knight JS, Robertson ES.** 2004. Epstein-Barr virus nuclear antigen 3C regulates cyclin A/p27 complexes and enhances cyclin A-dependent kinase activity. J Virol **78:**1981-1991.
126. **Knight JS, Sharma N, Kalman DE, Robertson ES.** 2004. A cyclin-binding motif within the amino-terminal homology domain of EBNA3C binds cyclin A and modulates cyclin A-dependent kinase activity in Epstein-Barr virus-infected cells. J Virol **78:**12857-12867.
127. **Knight JS, Sharma N, Robertson ES.** 2005. Epstein-Barr virus latent antigen 3C can mediate the degradation of the retinoblastoma protein through an SCF cellular ubiquitin ligase. Proc Natl Acad Sci U S A **102:**18562-18566.
128. **Knight JS, Sharma N, Robertson ES.** 2005. SCFSkp2 complex targeted by Epstein-Barr virus essential nuclear antigen. Mol Cell Biol **25:**1749-1763.
129. **Choudhuri T, Verma SC, Lan K, Murakami M, Robertson ES.** 2007. The ATM/ATR signaling effector Chk2 is targeted by Epstein-Barr virus nuclear antigen 3C to release the G2/M cell cycle block. J Virol **81:**6718-6730.

130. **Saha A, Murakami M, Kumar P, Bajaj B, Sims K, Robertson ES.** 2009. Epstein-Barr virus nuclear antigen 3C augments Mdm2-mediated p53 ubiquitination and degradation by deubiquitinating Mdm2. J Virol **83:**4652-4669.
131. **Yi F, Saha A, Murakami M, Kumar P, Knight JS, Cai Q, Choudhuri T, Robertson ES.** 2009. Epstein-Barr virus nuclear antigen 3C targets p53 and modulates its transcriptional and apoptotic activities. Virology **388:**236-247.
132. **Saha A, Bamidele A, Murakami M, Robertson ES.** 2011. EBNA3C attenuates the function of p53 through interaction with inhibitor of growth family proteins 4 and 5. J Virol **85:**2079-2088.
133. **Saha A, Lu J, Morizur L, Upadhyay SK, Aj MP, Robertson ES.** 2012. E2F1 mediated apoptosis induced by the DNA damage response is blocked by EBV nuclear antigen 3C in lymphoblastoid cells. PLoS Pathog **8:**e1002573.
134. **Jha HC, Lu J, Saha A, Cai Q, Banerjee S, Prasad MA, Robertson ES.** 2013. EBNA3C-mediated regulation of aurora kinase B contributes to Epstein-Barr virus-induced B-cell proliferation through modulation of the activities of the retinoblastoma protein and apoptotic caspases. J Virol **87:**12121-12138.
135. **Parker GA, Crook T, Bain M, Sara EA, Farrell PJ, Allday MJ.** 1996. Epstein-Barr virus nuclear antigen (EBNA)3C is an immortalizing oncoprotein with similar properties to adenovirus E1A and papillomavirus E7. Oncogene **13:**2541-2549.
136. **Serrano M, Lin AW, McCurrach ME, Beach D, Lowe SW.** 1997. Oncogenic ras provokes premature cell senescence associated with accumulation of p53 and p16INK4a. Cell **88:**593-602.
137. **Parker GA, Touitou R, Allday MJ.** 2000. Epstein-Barr virus EBNA3C can disrupt multiple cell cycle checkpoints and induce nuclear division divorced from cytokinesis. Oncogene **19:**700-709.
138. **Maruo S, Zhao B, Johannsen E, Kieff E, Zou J, Takada K.** 2011. Epstein-Barr virus nuclear antigens 3C and 3A maintain lymphoblastoid cell growth by repressing p16INK4A and p14ARF expression. Proc Natl Acad Sci U S A **108:**1919-1924.
139. **Brookes S, Rowe J, Ruas M, Llanos S, Clark PA, Lomax M, James MC, Vatcheva R, Bates S, Vousden KH, Parry D, Gruis N, Smit N, Bergman W, Peters G.** 2002. INK4a-deficient human diploid fibroblasts are resistant to RAS-induced senescence. EMBO J **21:**2936-2945.
140. **Gil J, Peters G.** 2006. Regulation of the INK4b-ARF-INK4a tumour suppressor locus: all for one or one for all. Nat Rev Mol Cell Biol **7:**667-677.
141. **Vousden KH, Prives C.** 2009. Blinded by the Light: The Growing Complexity of p53. Cell **137:**413-431.
142. **Sherr CJ.** 2012. Ink4-Arf locus in cancer and aging. Wiley Interdiscip Rev Dev Biol **1:**731-741.
143. **Strasser A.** 2005. The role of BH3-only proteins in the immune system. Nat Rev Immunol **5:**189-200.
144. **Fischer SF, Bouillet P, O'Donnell K, Light A, Tarlinton DM, Strasser A.** 2007. Proapoptotic BH3-only protein Bim is essential for developmentally programmed death of germinal center-derived memory B cells and antibody-forming cells. Blood **110:**3978-3984.

145. **Egle A, Harris AW, Bouillet P, Cory S.** 2004. Bim is a suppressor of Myc-induced mouse B cell leukemia. Proc Natl Acad Sci U S A **101:**6164-6169.
146. **Hemann MT, Bric A, Teruya-Feldstein J, Herbst A, Nilsson JA, Cordon-Cardo C, Cleveland JL, Tansey WP, Lowe SW.** 2005. Evasion of the p53 tumour surveillance network by tumour-derived MYC mutants. Nature **436:**807-811.
147. **Dang CV, O'Donnell K A, Juopperi T.** 2005. The great MYC escape in tumorigenesis. Cancer Cell **8:**177-178.
148. **Anderton E, Yee J, Smith P, Crook T, White RE, Allday MJ.** 2008. Two Epstein-Barr virus (EBV) oncoproteins cooperate to repress expression of the proapoptotic tumour-suppressor Bim: clues to the pathogenesis of Burkitt's lymphoma. Oncogene **27:**421-433.
149. **Kelly GL, Long HM, Stylianou J, Thomas WA, Leese A, Bell AI, Bornkamm GW, Mautner J, Rickinson AB, Rowe M.** 2009. An Epstein-Barr virus anti-apoptotic protein constitutively expressed in transformed cells and implicated in burkitt lymphomagenesis: the Wp/BHRF1 link. PLoS Pathog **5:**e1000341.
150. **Watanabe A, Maruo S, Ito T, Ito M, Katsumura KR, Takada K.** 2010. Epstein-Barr virus-encoded Bcl-2 homologue functions as a survival factor in Wp-restricted Burkitt lymphoma cell line P3HR-1. J Virol **84:**2893-2901.
151. **Vereide DT, Sugden B.** 2011. Lymphomas differ in their dependence on Epstein-Barr virus. Blood **117:**1977-1985.
152. **Yee J, White RE, Anderton E, Allday MJ.** 2011. Latent Epstein-Barr virus can inhibit apoptosis in B cells by blocking the induction of NOXA expression. PLoS One **6:**e28506.
153. **Paschos K, Smith P, Anderton E, Middeldorp JM, White RE, Allday MJ.** 2009. Epstein-barr virus latency in B cells leads to epigenetic repression and CpG methylation of the tumour suppressor gene Bim. PLoS Pathog **5:**e1000492.
154. **Paschos K, Parker GA, Watanatanasup E, White RE, Allday MJ.** 2012. BIM promoter directly targeted by EBNA3C in polycomb-mediated repression by EBV. Nucleic Acids Res **40:**7233-7246.
155. **Margueron R, Reinberg D.** 2011. The Polycomb complex PRC2 and its mark in life. Nature **469:**343-349.
156. **Agger K, Cloos PA, Rudkjaer L, Williams K, Andersen G, Christensen J, Helin K.** 2009. The H3K27me3 demethylase JMJD3 contributes to the activation of the INK4A-ARF locus in response to oncogene- and stress-induced senescence. Genes Dev **23:**1171-1176.
157. **Barradas M, Anderton E, Acosta JC, Li S, Banito A, Rodriguez-Niedenfuhr M, Maertens G, Banck M, Zhou MM, Walsh MJ, Peters G, Gil J.** 2009. Histone demethylase JMJD3 contributes to epigenetic control of INK4a/ARF by oncogenic RAS. Genes Dev **23:**1177-1182.
158. **Wang JK, Tsai MC, Poulin G, Adler AS, Chen S, Liu H, Shi Y, Chang HY.** 2010. The histone demethylase UTX enables RB-dependent cell fate control. Genes Dev **24:**327-332.

159. **McLaughlin-Drubin ME, Crum CP, Munger K.** 2011. Human papillomavirus E7 oncoprotein induces KDM6A and KDM6B histone demethylase expression and causes epigenetic reprogramming. Proc Natl Acad Sci U S A **108:**2130-2135.
160. **Anderton JA, Bose S, Vockerodt M, Vrzalikova K, Wei W, Kuo M, Helin K, Christensen J, Rowe M, Murray PG, Woodman CB.** 2011. The H3K27me3 demethylase, KDM6B, is induced by Epstein-Barr virus and over-expressed in Hodgkin's Lymphoma. Oncogene **30:**2037-2043.
161. **Sciammas R, Shaffer AL, Schatz JH, Zhao H, Staudt LM, Singh H.** 2006. Graded expression of interferon regulatory factor-4 coordinates isotype switching with plasma cell differentiation. Immunity **25:**225-236.
162. **Menezes J, Leibold W, Klein G, Clements G.** 1975. Establishment and characterization of an Epstein-Barr virus (EBC)-negative lymphoblastoid B cell line (BJA-B) from an exceptional, EBV-genome-negative African Burkitt's lymphoma. Biomedicine **22:**276-284.
163. **Lebkowski JS, Clancy S, Calos MP.** 1985. Simian virus 40 replication in adenovirus-transformed human cells antagonizes gene expression. Nature **317:**169-171.
164. **Maunders MJ, Petti L, Rowe M.** 1994. Precipitation of the Epstein-Barr virus protein EBNA 2 by an EBNA 3c-specific monoclonal antibody. J Gen Virol **75 (Pt 4):**769-778.
165. **Rozenblatt-Rosen O, Deo RC, Padi M, Adelmant G, Calderwood MA, Rolland T, Grace M, Dricot A, Askenazi M, Tavares M, Pevzner SJ, Abderazzaq F, Byrdsong D, Carvunis AR, Chen AA, Cheng J, Correll M, Duarte M, Fan C, Feltkamp MC, Ficarro SB, Franchi R, Garg BK, Gulbahce N, Hao T, Holthaus AM, James R, Korkhin A, Litovchick L, Mar JC, Pak TR, Rabello S, Rubio R, Shen Y, Singh S, Spangle JM, Tasan M, Wanamaker S, Webber JT, Roecklein-Canfield J, Johannsen E, Barabasi AL, Beroukhim R, Kieff E, Cusick ME, Hill DE, Munger K, Marto JA, Quackenbush J, Roth FP, et al.** 2012. Interpreting cancer genomes using systematic host network perturbations by tumour virus proteins. Nature **487:**491-495.
166. **Zhao B, Zou J, Wang H, Johannsen E, Peng CW, Quackenbush J, Mar JC, Morton CC, Freedman ML, Blacklow SC, Aster JC, Bernstein BE, Kieff E.** 2011. Epstein-Barr virus exploits intrinsic B-lymphocyte transcription programs to achieve immortal cell growth. Proc Natl Acad Sci U S A **108:**14902-14907.
167. **Kuan PF, Chung D, Pan G, Thomson JA, Stewart R, Keles S.** 2011. A Statistical Framework for the Analysis of ChIP-Seq Data. J Am Stat Assoc **106:**891-903.
168. **Machanick P, Bailey TL.** 2011. MEME-ChIP: motif analysis of large DNA datasets. Bioinformatics **27:**1696-1697.
169. **Johannsen E, Kaye K.** 2015. Epstein-Barr Virus (Infectious Mononucleosis, Epstein-Barr Virus-Associated Malignant Diseases, and Other Diseases), p 1754-1771. *In* Bennett J, Dolin R, Blaser M (ed), Mandell, Douglas, and Bennett's Principles and Practice of Infectious Diseases, vol 2. Elsevier Saunders, Philadelphia.
170. **Longnecker R, Kieff E, Cohen J.** 2013. Epstein-Barr Virus, p 1898-1959. *In* Knipe D, Howley P, Cohen J, Griffin D, Lamb R, Martin M, Racaniello V, Roizman B (ed),

Fields Virology, 6 ed, vol 2. Wolters Kluwer/Lippincott Williams & Wilkins, Philadelphia.

171. **Tzellos S, Correia PB, Karstegl CE, Cancian L, Cano-Flanagan J, McClellan MJ, West MJ, Farrell PJ.** 2014. A single amino acid in EBNA-2 determines superior B lymphoblastoid cell line growth maintenance by Epstein-Barr virus type 1 EBNA-2. J Virol **88:**8743-8753.
172. **Chen A, Zhao B, Kieff E, Aster JC, Wang F.** 2006. EBNA-3B- and EBNA-3C-regulated cellular genes in Epstein-Barr virus-immortalized lymphoblastoid cell lines. J Virol **80:**10139-10150.
173. **Bazot Q, Paschos K, Skalska L, Kalchschmidt JS, Parker GA, Allday MJ.** 2015. Epstein-Barr Virus Proteins EBNA3A and EBNA3C Together Induce Expression of the Oncogenic MicroRNA Cluster miR-221/miR-222 and Ablate Expression of Its Target p57KIP2. PLoS Pathog **11:**e1005031.
174. **Nikitin PA, Yan CM, Forte E, Bocedi A, Tourigny JP, White RE, Allday MJ, Patel A, Dave SS, Kim W, Hu K, Guo J, Tainter D, Rusyn E, Luftig MA.** 2010. An ATM/Chk2-mediated DNA damage-responsive signaling pathway suppresses Epstein-Barr virus transformation of primary human B cells. Cell Host Microbe **8:**510-522.
175. **Tursiella ML, Bowman ER, Wanzeck KC, Throm RE, Liao J, Zhu J, Sample CE.** 2014. Epstein-Barr virus nuclear antigen 3A promotes cellular proliferation by repression of the cyclin-dependent kinase inhibitor p21WAF1/CIP1. PLoS Pathog **10:**e1004415.
176. **Langmead B, Trapnell C, Pop M, Salzberg SL.** 2009. Ultrafast and memory-efficient alignment of short DNA sequences to the human genome. Genome Biol **10:**R25.
177. **Thurman RE, Rynes E, Humbert R, Vierstra J, Maurano MT, Haugen E, Sheffield NC, Stergachis AB, Wang H, Vernot B, Garg K, John S, Sandstrom R, Bates D, Boatman L, Canfield TK, Diegel M, Dunn D, Ebersol AK, Frum T, Giste E, Johnson AK, Johnson EM, Kutyavin T, Lajoie B, Lee BK, Lee K, London D, Lotakis D, Neph S, Neri F, Nguyen ED, Qu H, Reynolds AP, Roach V, Safi A, Sanchez ME, Sanyal A, Shafer A, Simon JM, Song L, Vong S, Weaver M, Yan Y, Zhang Z, Zhang Z, Lenhard B, Tewari M, Dorschner MO, Hansen RS, et al.** 2012. The accessible chromatin landscape of the human genome. Nature **489:**75-82.
178. **Natarajan A, Yardimci GG, Sheffield NC, Crawford GE, Ohler U.** 2012. Predicting cell-type-specific gene expression from regions of open chromatin. Genome Res **22:**1711-1722.
179. **Schneider R, Grosschedl R.** 2007. Dynamics and interplay of nuclear architecture, genome organization, and gene expression. Genes Dev **21:**3027-3043.
180. **Ernst J, Kheradpour P, Mikkelsen TS, Shoresh N, Ward LD, Epstein CB, Zhang X, Wang L, Issner R, Coyne M, Ku M, Durham T, Kellis M, Bernstein BE.** 2011. Mapping and analysis of chromatin state dynamics in nine human cell types. Nature **473:**43-49.

181. **Johannsen E, Miller CL, Grossman SR, Kieff E.** 1996. EBNA-2 and EBNA-3C extensively and mutually exclusively associate with RBPJkappa in Epstein-Barr virus-transformed B lymphocytes. J Virol **70:**4179-4183.
182. **Xu D, Zhao L, Del Valle L, Miklossy J, Zhang L.** 2008. Interferon regulatory factor 4 is involved in Epstein-Barr virus-mediated transformation of human B lymphocytes. J Virol **82:**6251-6258.
183. **Banerjee S, Lu J, Cai Q, Saha A, Jha HC, Dzeng RK, Robertson ES.** 2013. The EBV Latent Antigen 3C Inhibits Apoptosis through Targeted Regulation of Interferon Regulatory Factors 4 and 8. PLoS Pathog **9:**e1003314.
184. **Calderwood MA, Venkatesan K, Xing L, Chase MR, Vazquez A, Holthaus AM, Ewence AE, Li N, Hirozane-Kishikawa T, Hill DE, Vidal M, Kieff E, Johannsen E.** 2007. Epstein-Barr virus and virus human protein interaction maps. Proc Natl Acad Sci U S A **104:**7606-7611.
185. **Lenz G, Staudt LM.** 2010. Aggressive lymphomas. N Engl J Med **362:**1417-1429.
186. **De Silva NS, Simonetti G, Heise N, Klein U.** 2012. The diverse roles of IRF4 in late germinal center B-cell differentiation. Immunol Rev **247:**73-92.
187. **Wang L, Yao ZQ, Moorman JP, Xu Y, Ning S.** 2014. Gene expression profiling identifies IRF4-associated molecular signatures in hematological malignancies. PLoS One **9:**e106788.
188. **Simonetti G, Carette A, Silva K, Wang H, De Silva NS, Heise N, Siebel CW, Shlomchik MJ, Klein U.** 2013. IRF4 controls the positioning of mature B cells in the lymphoid microenvironments by regulating NOTCH2 expression and activity. J Exp Med **210:**2887-2902.
189. **Martin F, Kearney JF.** 2000. B-cell subsets and the mature preimmune repertoire. Marginal zone and B1 B cells as part of a "natural immune memory". Immunol Rev **175:**70-79.
190. **Tanigaki K, Han H, Yamamoto N, Tashiro K, Ikegawa M, Kuroda K, Suzuki A, Nakano T, Honjo T.** 2002. Notch-RBP-J signaling is involved in cell fate determination of marginal zone B cells. Nat Immunol **3:**443-450.
191. **Simon J, Chiang A, Bender W, Shimell MJ, O'Connor M.** 1993. Elements of the Drosophila bithorax complex that mediate repression by Polycomb group products. Dev Biol **158:**131-144.
192. **Ku M, Koche RP, Rheinbay E, Mendenhall EM, Endoh M, Mikkelsen TS, Presser A, Nusbaum C, Xie X, Chi AS, Adli M, Kasif S, Ptaszek LM, Cowan CA, Lander ES, Koseki H, Bernstein BE.** 2008. Genomewide analysis of PRC1 and PRC2 occupancy identifies two classes of bivalent domains. PLoS Genet **4:**e1000242.
193. **Atchison L, Ghias A, Wilkinson F, Bonini N, Atchison ML.** 2003. Transcription factor YY1 functions as a PcG protein in vivo. EMBO J **22:**1347-1358.
194. **Davidovich C, Cech TR.** 2015. The recruitment of chromatin modifiers by long noncoding RNAs: lessons from PRC2. RNA **21:**2007-2022.
195. **Kim WY, Sharpless NE.** 2006. The regulation of INK4/ARF in cancer and aging. Cell **127:**265-275.
196. **Popov N, Gil J.** 2010. Epigenetic regulation of the INK4b-ARF-INK4a locus: in sickness and in health. Epigenetics **5:**685-690.

197. **Chen S, Bohrer LR, Rai AN, Pan Y, Gan L, Zhou X, Bagchi A, Simon JA, Huang H.** 2010. Cyclin-dependent kinases regulate epigenetic gene silencing through phosphorylation of EZH2. Nat Cell Biol **12:**1108-1114.
198. **Kaneko S, Li G, Son J, Xu CF, Margueron R, Neubert TA, Reinberg D.** 2010. Phosphorylation of the PRC2 component Ezh2 is cell cycle-regulated and up-regulates its binding to ncRNA. Genes Dev **24:**2615-2620.
199. **Wei Y, Chen YH, Li LY, Lang J, Yeh SP, Shi B, Yang CC, Yang JY, Lin CY, Lai CC, Hung MC.** 2011. CDK1-dependent phosphorylation of EZH2 suppresses methylation of H3K27 and promotes osteogenic differentiation of human mesenchymal stem cells. Nat Cell Biol **13:**87-94.
200. **Lee JM, Lee JS, Kim H, Kim K, Park H, Kim JY, Lee SH, Kim IS, Kim J, Lee M, Chung CH, Seo SB, Yoon JB, Ko E, Noh DY, Kim KI, Kim KK, Baek SH.** 2012. EZH2 generates a methyl degron that is recognized by the DCAF1/DDB1/CUL4 E3 ubiquitin ligase complex. Mol Cell **48:**572-586.
201. **Tahiliani M, Mei P, Fang R, Leonor T, Rutenberg M, Shimizu F, Li J, Rao A, Shi Y.** 2007. The histone H3K4 demethylase SMCX links REST target genes to X-linked mental retardation. Nature **447:**601-605.
202. **Hakimi MA, Dong Y, Lane WS, Speicher DW, Shiekhattar R.** 2003. A candidate X-linked mental retardation gene is a component of a new family of histone deacetylase-containing complexes. J Biol Chem **278:**7234-7239.
203. **Shi Y, Sawada J, Sui G, Affar el B, Whetstine JR, Lan F, Ogawa H, Luke MP, Nakatani Y, Shi Y.** 2003. Coordinated histone modifications mediated by a CtBP co-repressor complex. Nature **422:**735-738.
204. **Cowger JJ, Zhao Q, Isovic M, Torchia J.** 2007. Biochemical characterization of the zinc-finger protein 217 transcriptional repressor complex: identification of a ZNF217 consensus recognition sequence. Oncogene **26:**3378-3386.
205. **Metzger E, Wissmann M, Yin N, Muller JM, Schneider R, Peters AH, Gunther T, Buettner R, Schule R.** 2005. LSD1 demethylates repressive histone marks to promote androgen-receptor-dependent transcription. Nature **437:**436-439.
206. **Secombe J, Li L, Carlos L, Eisenman RN.** 2007. The Trithorax group protein Lid is a trimethyl histone H3K4 demethylase required for dMyc-induced cell growth. Genes Dev **21:**537-551.
207. **Ballif BA, Villen J, Beausoleil SA, Schwartz D, Gygi SP.** 2004. Phosphoproteomic analysis of the developing mouse brain. Mol Cell Proteomics **3:**1093-1101.
208. **Khalil AM, Guttman M, Huarte M, Garber M, Raj A, Rivea Morales D, Thomas K, Presser A, Bernstein BE, van Oudenaarden A, Regev A, Lander ES, Rinn JL.** 2009. Many human large intergenic noncoding RNAs associate with chromatin-modifying complexes and affect gene expression. Proc Natl Acad Sci U S A **106:**11667-11672.
209. **Engreitz JM, Pandya-Jones A, McDonel P, Shishkin A, Sirokman K, Surka C, Kadri S, Xing J, Goren A, Lander ES, Plath K, Guttman M.** 2013. The Xist lncRNA exploits three-dimensional genome architecture to spread across the X chromosome. Science **341:**1237973.

210. **Rinn JL, Kertesz M, Wang JK, Squazzo SL, Xu X, Brugmann SA, Goodnough LH, Helms JA, Farnham PJ, Segal E, Chang HY.** 2007. Functional demarcation of active and silent chromatin domains in human HOX loci by noncoding RNAs. Cell **129:**1311-1323.
211. **Tsai MC, Manor O, Wan Y, Mosammaparast N, Wang JK, Lan F, Shi Y, Segal E, Chang HY.** 2010. Long noncoding RNA as modular scaffold of histone modification complexes. Science **329:**689-693.
212. **Yang F, Zhang L, Huo XS, Yuan JH, Xu D, Yuan SX, Zhu N, Zhou WP, Yang GS, Wang YZ, Shang JL, Gao CF, Zhang FR, Wang F, Sun SH.** 2011. Long noncoding RNA high expression in hepatocellular carcinoma facilitates tumor growth through enhancer of zeste homolog 2 in humans. Hepatology **54:**1679-1689.
213. **He W, Cai Q, Sun F, Zhong G, Wang P, Liu H, Luo J, Yu H, Huang J, Lin T.** 2013. linc-UBC1 physically associates with polycomb repressive complex 2 (PRC2) and acts as a negative prognostic factor for lymph node metastasis and survival in bladder cancer. Biochim Biophys Acta **1832:**1528-1537.
214. **Luo M, Li Z, Wang W, Zeng Y, Liu Z, Qiu J.** 2013. Long non-coding RNA H19 increases bladder cancer metastasis by associating with EZH2 and inhibiting E-cadherin expression. Cancer Lett **333:**213-221.
215. **Kotake Y, Nakagawa T, Kitagawa K, Suzuki S, Liu N, Kitagawa M, Xiong Y.** 2011. Long non-coding RNA ANRIL is required for the PRC2 recruitment to and silencing of p15(INK4B) tumor suppressor gene. Oncogene **30:**1956-1962.
216. **Lieberman-Aiden E, van Berkum NL, Williams L, Imakaev M, Ragoczy T, Telling A, Amit I, Lajoie BR, Sabo PJ, Dorschner MO, Sandstrom R, Bernstein B, Bender MA, Groudine M, Gnirke A, Stamatoyannopoulos J, Mirny LA, Lander ES, Dekker J.** 2009. Comprehensive mapping of long-range interactions reveals folding principles of the human genome. Science **326:**289-293.
217. **Dowen JM, Fan ZP, Hnisz D, Ren G, Abraham BJ, Zhang LN, Weintraub AS, Schuijers J, Lee TI, Zhao K, Young RA.** 2014. Control of cell identity genes occurs in insulated neighborhoods in mammalian chromosomes. Cell **159:**374-387.
218. **Zhou H, Schmidt SC, Jiang S, Willox B, Bernhardt K, Liang J, Johannsen EC, Kharchenko P, Gewurz BE, Kieff E, Zhao B.** 2015. Epstein-Barr virus oncoprotein super-enhancers control B cell growth. Cell Host Microbe **17:**205-216.
219. **Nguyen-Van D, Keane C, Han E, Jones K, Nourse JP, Vari F, Ross N, Crooks P, Ramuz O, Green M, Griffith L, Trappe R, Grigg A, Mollee P, Gandhi MK.** 2011. Epstein-Barr virus-positive diffuse large B-cell lymphoma of the elderly expresses EBNA3A with conserved CD8 T-cell epitopes. Am J Blood Res **1:**146-159.
220. **Kelly G, Bell A, Rickinson A.** 2002. Epstein-Barr virus-associated Burkitt lymphomagenesis selects for downregulation of the nuclear antigen EBNA2. Nat Med **8:**1098-1104.